POLITECNICO
MILANO 1863

SCUOLA DI INGEGNERIA INDUSTRIALE
E DELL'INFORMAZIONE

Mechanical characterization of bio-composites

TESI DI LAUREA MAGISTRALE IN
MECHANICAL ENGINEERING

Author: **Rachele Massetti**

Student ID: 10507663
Advisor: Giampiero Mastinu
Co-advisor: Chiara Pernechele
Academic Year: 2024-2025

Abstract

The current geopolitical situation and the growing interest in environmental issues brought great interest in the search for new materials that, in addition to having excellent mechanical performance, comply with sustainability requirements.

This has led to the birth of numerous research and experimentation projects around the world on innovative composite materials characterized by bio-based matrices and/or fibers.

The goal of always obtaining new matrices and reinforcements of natural origin, which have more controllable mechanical characteristics and can be produced in a simple and economical way, has become predominant for many companies.

The push in this direction has not been driven only by the regulations imposed by States and international agreements, but also by an ethical question, and by a choice of image, as the creation of green products brings benefits to the reputation of the company itself.

The following work, carried out entirely within the research laboratories of *Dallara Automobili*, fits into this context by providing an overview of the current state of knowledge in the field of bio-based composites, then focusing on the complete mechanical characterization of a series of green materials.

Out of the five materials supplied by *Angeloni Group*, two are made with long carbon fibers and impregnated with a resin of natural origin. The remaining are reinforced with short fiber obtained from recycled weaving of long fibers.

The tests carried out have led to a series of considerations on the effect of the use of bio-based resin on the mechanical properties of the materials and on their possible applications in countless sectors, including the automotive sector.

Key-words: bio composites; sustainability; mechanical characterization; automotive;

Abstract in lingua italiana

L'attuale situazione geopolitica e il crescente interesse verso le problematiche ambientali ha creato grande interesse attorno alla ricerca di nuovi materiali che oltre ad avere delle ottime prestazioni meccaniche, rispettano quelle che sono le prescrizioni di sostenibilità.

Questo ha portato alla nascita in tutto il mondo di numerosi progetti di ricerca e sperimentazione su materiali compositi innovativi caratterizzati da matrice e/o fibre di origine bio.

L'obbiettivo di ottenere sempre nuove matrici e rinforzi di origine naturale, che presentino delle caratteristiche meccaniche più controllabili e che si possano produrre in maniera semplice ed economica, è diventato preponderante per molte aziende.

La spinta in questa direzione non è stata guidata solo dalle regolamentazioni imposte dagli Stati e dagli accordi internazionali, ma anche da una questione etica, e da una scelta di immagine, in quanto la realizzazione di prodotti green porta benefici alla reputazione dell'impresa stessa.

Il seguente lavoro, svolto interamente all'interno dei laboratori di ricerca di *Dallara Automobili*, si inserisce in questo contesto fornendo una panoramica sullo stato attuale delle conoscenze in materia di compositi bio, focalizzandosi poi sulla completa caratterizzazione meccanica di una serie di materiali green.

Dei cinque materiali forniti da *Angeloni Group*, due sono realizzati con un fibre lunghe di carbonio e impregnati con una resina di origine naturale. I restanti sono rinforzati con fibra corta ottenuta da riciclo di tessitura di fibre lunghe.

I test realizzati hanno portato ad una serie di considerazioni sull'effetto dell'utilizzo della resina di origine bio sulle proprietà meccaniche dei materiali e sulle loro possibili applicazioni in innumerevoli settori, tra cui quello automotive.

Parole chiave: materiali compositi bio; sostenibilità; caratterizzazione meccanica; automotive;

Contents

Introduction

In recent years, the demand for products that are increasingly high performing in terms of mechanics and weight, along with the growing interest in environmental issues, has brought to the forefront new types of materials that can meet this demand. It is precisely in this context that the use of bio composites has become essential.

Bio composite materials are products of completely or partially natural origin, obtained by combining different raw materials with the aim of achieving a final product that is eco-sustainable and high performing.

They represent an evolution of standard composite materials, which are created based on the same principle but are synthetically produced. [1]

They can result from the combination of a natural matrix and synthetic fibers, or vice versa, and in some cases, both the matrix and fibers are of natural origin.

Natural fibers can be obtained from plants, animals, or mineral sources. Examples of plant-based fibers include fibers made from flax, wood, sisal, kenaf, hemp, jute, henequen, cotton, agave, and other fibers obtained from the leaves or shells of certain fruit plants, such as those derived from pineapple leaves and coconut shells.

As for animal-based fibers, there are fibers obtained from the processing of wool and animal hair. Among mineral-based fibers, we can mention asbestos, ferrous brucite (a magnesium oxide), and those obtained from wollastonite (a calcium metasilicate). [3][9]

Speaking of bio-based resins, they are characterized by precursors obtained from natural sources such as vegetable oils: soybean oil, linseed oil, rapeseed oil, palm oil, coconut oil, and castor oil, or through the fermentation of carbohydrates and agricultural by-products.

There are also examples of bio-resins obtained from starch extracted from potatoes, corn, and sugar cane. [4]

Choosing to use a composite material means choosing a high-performance natural material that, thanks to the increased attention towards issues related to renewability, good resource management, and climate change, is becoming increasingly popular among builders and customers in various fields.

These new materials of natural origin find their place in the market as substitutes for plastics, whose potential health hazards are becoming increasingly evident thanks to numerous research studies and scientific publications on the topic.

Their use not only ensures economic returns related to reduced production costs but also decreases emissions during both production and disposal phases. Additionally, the materials needed for their production are available in large quantities.

On the other hand, several issues are associated with their use; they possess lower tensile strength, variable raw material costs, and poor thermal stability.

Public and private investments and research into green materials are therefore working to resolve these issues to make them increasingly appealing on the market.

All these benefits, combined with ever-increasing mechanical properties and the growing international push for emission reduction, are spreading their use more broadly.

It is estimated that the current market for bio composites is about $30,86 billion and that their market share, with a CAGR of 18,75%, is expected to increase to $171,75 billion by 2033.

Currently, the largest market in this sector is the Asia-Pacific region, valued at $11,95 billion. Following are the American and European markets, with approximately 26% and 23% shares of the global market, respectively.[2][15]

The ever-growing demand for sustainable materials, due to increased awareness of health issues related to plastic use and stricter regulations, will drive a strong market growth in the coming years.

In Europe, the promotion of these materials is part of the European Green Deal, a broader package of initiatives aimed at achieving climate neutrality by 2050. Similarly, the United States, Japan, and many other nations are moving in this direction. [17][18]

Bio composite production experienced a reduction during the COVID-19 period, but it is evident that their use will spread increasingly in the coming years.

These new materials are an excellent solution for constructing eco-friendly products and buildings, making them gradually preferred over materials of the past.

With excellent mechanical properties and their lightness, they are also finding growing use in sectors such as aerospace, automotive, defense, and many others.

The last few decades have been entirely dominated by petrochemical polymers, as the growth of oil-based chemistry revolutionized plastic production both economically and efficiently. For this reason, bio composites are perceived as new materials in the collective imagination. However, they have actually been around for a long time.

Over the centuries, humanity has used easily accessible and workable materials such as clay, flint, or horn to solve technical problems or achieve artistic effects.

The first known use of natural composites is attributed to the Mesopotamians, who glued strips of wood at different angles to create plywood as early as 3400 B.C.

Between 2181 and 2055 B.C., the Egyptians used cartonnage and layers of linen or papyrus soaked in plaster to make burial masks.

Around 1500 B.C., Egyptian and Mesopotamian builders and artisans used straw to reinforce mud bricks, ceramics, and boats.

In 1200 A.D., the Mongols invented the first composite bows made from a combination of wood, bamboo, bovine tendons, horns, and silk bound with natural pine resin. These small, powerful, and extremely accurate bows were the most feared weapons on earth until the invention of firearms in the 14th century. [23][21]

The rapid development and constant changes in social structures during the 18th and 19th centuries led to an increase in imitations and surrogate materials that allowed common people access to objects that were previously reserved for the wealthy.

During this period, a mixture of linseed oil and powdered cork on a fabric base (linoleum) was used for the first time as flooring and as a substitute for simple wooden floors.

Caucho (or natural rubber) was discovered in the 18th century as a polymeric material extracted from the latex of certain plants. However, this material alone does not have good properties and therefore cannot be used as it is; today, it is used only after a vulcanization process.

In 1908, Swiss chemical engineer Brandenberger invented cellophane, a thin, transparent film made of cellulose regenerated through a specific process. This material is still used today for packaging and food wrapping.[20]

This phase of modified natural material derivatives, composed of casein, cellulose, natural rubber, etc., was followed by the discovery of Bakelite as the first synthetic product.

Bakelite was developed by Belgian-born New York chemist Leo Baekeland in 1907.

A thermosetting phenol-formaldehyde resin formed by the condensation reaction of phenol with formaldehyde, Bakelite was one of the first plastics made from synthetic components. Its non-conductive and heat-resistant properties made the composite widely used in industrial and consumer applications, including electrical insulators, radio and telephone casings, kitchenware, jewelry, pipe stems, and children's toys.

In 1993, in recognition of Bakelite's importance as the first synthetic plastic, the American Chemical Society designated it a National Historic Chemical Landmark.

Bakelite thus marked the starting point for the development of various synthetic thermoplastic materials starting in the 1920s and 1930s. Before this, all materials were entirely of natural origin.

The first reports regarding the synthesis of biopolymers date back to 1925 when French microbiologist Maurice Lemoigne described polyhydroxybutyrate (PHB), which gave rise to bioplastic materials primarily used for medical applications and later for packaging.

During World War II, under the supervision and funding of the American government, there was a dramatic increase in the production of synthetic plastics as they were used for wartime applications.

There is evidence of the first experimentation with bio-based composite materials in the modern age as early as 1941-42. That year, Henry Ford presented the "Soybean Car," the first prototype automobile made using flax and soybean fibers to produce plastic-like materials. The resulting car was 450 kg, lighter than a steel car, but due to a series of technical and economic limitations, it was not mass-produced.

In the 1950s, amylomaize was successfully obtained, and the first commercial applications of bioplastics began to be explored.

However, research in this direction was halted by the large availability of petroleum-based products at advantageous prices, which at the time could be used without any restrictions and on which the production of automotive components has relied until today.

In the 1970s, the environmental movement began pushing for the resumption of research into biomaterials, leading to the founding of the first bioplastics company, Marlborough Biopolymers, in 1983.

In the 2000s, research and successful attempts in bio-resin production multiplied, leading to a wide range of production methods for these resins.[23]

Even today, bioplastics represent only a small part of global plastic production, as the few manufacturing companies face intense competition from the traditional petroleum industry. However, some actions taken at the European level for environmental protection are trying to steer the market toward greater sustainability.

Bio composites are finding applications in various sectors, with automotive and construction standing out, but they can also be found in aerospace, toy manufacturing, musical instruments, sports equipment, and many others.

In the automotive sector, they are used for manufacturing bumpers, door interior panels, headrests, seat padding, cup holders, trunk covers, and all non-structural components.

In the construction sector, they are used for producing windows, doors, frames, ceilings, flooring, and tiles. They are also employed in some load-bearing applications such as floors, beams, pipes, tanks, and in the repair of some structural components. Due to their good thermal and acoustic properties, they are used as insulating and sound-absorbing materials.

An example of their use in the aeronautical field is the construction of aircraft interior panels. Thanks to the BME CLEAN SKY 027 project, resins derived from sugars obtained from sources not competing with food production were synthesized, and to meet mechanical requirements, natural fibers (jute, flax, hemp) were incorporated and treated to reduce flammability. [16]

In the musical field, due to their excellent vibration response, silk fiber composites are used in the construction of violins, cellos, guitars, and percussion instruments.[14]

Flax fiber, thanks to its lightness, flexibility, stiffness, natural appearance, and especially its internal damping and vibration control properties, is used in many high-performance sports applications.

The vibration damping properties allow flax fiber composites to absorb shocks well and reduce fatigue, making them very favorable for use in manufacturing sports equipment for skiing, cycling, golf, rowing, and much more. [9]

As an example of their application in the sports filed, LOOK created the 765, a bicycle with a frame made of a combination of carbon fibers and flax fibers.

Lonely Mountain Skis produces a series of freeride skis made of flax and carbon fibers, characterized by high stiffness and very low weight.

Flax fiber is also starting to be used in the construction of technical fabrics for sports.[12]

The automotive sector is where bio composites are having the most success, having gained a foothold in recent years, with their applications multiplying very quickly.

Mercedes-Benz uses jute-based bio composites for interior panels, flax fiber composites for shelves and trunk covers, and sisal fiber composites for rear panel shelves.

The use of bio composites has led to a weight reduction of about 10% and an energy consumption reduction of up to 80% compared to synthetic composites.

Toyota uses kenaf fibers in tire covers, soy foam for vehicle seats, and has announced that between 2008 and 2015, it replaced 20% of the plastics used inside its vehicles with bio-based materials.

Volkswagen uses bio composites for door panels, outer flap linings, door inserts, and parcel shelf trays.

BMW uses flax, kenaf, and hemp fibers for seat backs, acoustic insulation panels, and dashboards.

In the Fiat models Punto, Brava, Marea, and Alfa Romeo 146, flax, sisal, hemp, cotton, and coconut fibers are used for floor panels, seat cushions, door linings, and headrests.

Additionally, Ford Motors has used wood fiber, wheat straw, coconut fiber, soy, and rice straw for cargo floorboards, backrest foams, headrests, and headliners in models like the Ford Flex, Ford Focus BEV, and Freestar. In its growing commitment to promoting sustainability, the company has also announced the use of rice hulls to replace talc in truck wiring, recycled cotton fiber for carpet insulation, soy-based composite seat cushions, and recycled plastics for underbody shields and covers.

General Motors, another American automaker, uses cotton for acoustic insulation and kenaf in ceiling linings of its vehicles. The Chevrolet Impala features a PP (polypropylene) composite reinforced with flax fibers for the rear shelf. They have also used wood reinforcements for the seatbacks of the Cadillac DTS and the cargo area floor of the Chevrolet Trailblazer.

Audi uses wood, flax, and sisal natural fibers in models A2, A3, A4, A6, A8, Roadster, Coupe, and Q7 for seatbacks, side and rear door panels, and tire linings.

These are just a few examples of the many automotive companies that have chosen to use bio-based composite materials in their vehicles.[6][7][19][22]

The trend shows a continuous increase in the use of these materials, chosen not only for environmental reasons and their good mechanical properties but also because their use is becoming a true fashion capable of achieving great success with the end customer.

However, the use of these innovative materials still implies some challenges. Bio-composite materials, while having many positive aspects, still have inferior mechanical characteristics compared to their synthetic counterparts.

It has been observed that they have a lower elastic modulus, reduced breaking stress, and a higher degree of deformation at break compared to standard materials. They are also characterized by poor thermal stability and are easily flammable.

The production process of natural fibers presents some challenges, as long fibers tend to break during processing, and due to their poor thermal stability, the processing temperature range is very narrow.

Natural fibers have mechanical characteristics that are difficult to predict because they depend on the geographical origin of the fibers, the age of the plant from which they were obtained, the amount of rainfall during the plant's growth period, and the soaking technique used for their production.

The external variables influencing the mechanical behavior of natural fibers are numerous and difficult to control, which is a significant issue if they needed to be used in high-precision production processes.

Additionally, there is difficulty in bonding and thus in load transfer between the matrix and the natural fibers because the fibers are hydrophilic while the matrix behaves hydrophobically.

Untreated composite materials exhibit poor resistance to humid environments, water, and all atmospheric agents.

Public and private funding aimed at solving these problems has been increasing in recent years, thanks to growing interest in environmental issues.

The main research projects focus not only on finding new ways to produce natural fibers and resins but also on identifying production processes or treatments that can resolve all the mentioned problems.

Thanks to these initiatives, a series of pre-embedding fiber treatments and expedients to improve resin chemistry during impregnation have been discovered.

To increase moisture resistance and improve adhesion between the two composite components, a series of surface treatments for fibers have been successfully tested, such as dewaxing, alkaline treatment, vinyl grafting, cyanoethylation, acetylation, and others.

The alkaline treatment, in particular, is used to increase the roughness of the contact surface between the fibers and the matrix.

To improve load transfer between the matrix and the fibers, various surface treatments have been performed, such as solvent extraction, corona discharge treatment, plasma discharge treatment, laser treatments, gamma ray treatments, UV bombardment, and bacterial modification.

To reduce the moisture absorption of cellulose fibers, hydrothermal treatments have been devised to render the cellulose crystalline, thereby reducing its absorption. Among these treatments there is Duralin, aimed at waterproofing the fibers through the acetylation of the natural fiber, where the acetyl group is inserted into the fiber in place of the hydroxyl groups that cause its hydrophilic nature.[8]

Research is also being developed, of great interest for the application of these materials in the automotive field, aimed at reducing the flammability of composite materials.

Bio fibers are subject to thermal degradation and combustion when exposed to intense heat. The trend is such that a higher concentration of cellulose increases the flammability of natural fibers, while a higher composition of lignin delays flame formation. There are various ways to incorporate flame retardants into treated natural fibers, such as impregnation in a retardant solution and the inclusion of flame-

retardant additives in the interfacial coupling system. Recently, flame-resistant fibers have also been studied, made with the application of nano-coatings. [13]

Ford Motor Company has sponsored the "Lightweight Sustainable Thermoplastic Composites" project in collaboration with the University of Waterloo in Canada. This project aims to study the use of natural fibers as fillers in polyamide. Specifically, the fibers focused on are those obtained from the eucalyptus plant, treated with UV rays to improve their thermal stability. [10]

Another noteworthy project is ReInvent, born from the commitment of a group of European researchers with the aim of decarbonizing the food, paper, steel, and plastics sectors.

This team of researchers has aimed to improve the performance of bio-based resins through the use of nano-composite foams.

To create the nano-fillers necessary for these foams, various natural sources have been proposed, such as hazelnut shells and waste containing lignocellulosic fibers. In fact, among other topics surrounding the spread of bio-composite materials, there is the issue of exploiting fertile land for non-food-related production.

It is not advisable to use agricultural crops exclusively for the production of raw materials aimed at synthesizing composites or for biofuel production. This would have a significant environmental impact concerning land and irrigation water usage, and thus on human food needs, as it would reduce the available fertile land which would instead be used for non-edible products. Therefore, the use of natural waste seems the best choice for the production of these materials. [11]

ESA is working with the University of the Côte d'Azur on a project running until 2025, which aims to study 100% bio-based composite materials for space applications. In particular, the use of biomass derived from vegetable oils from wood waste or marine algae has been studied.

One of the driving forces behind research in this direction is the European Union, which through REACH (Registration, Evaluation, Authorization and Restriction of Chemicals) is seeking to reduce the use of bisphenol. Bisphenol is a fundamental element for the production of thermosetting resins. However, it has been proven that this element has genetic modification and hormonal alteration effects on the human body, and for this reason, it has already been banned from food packaging and will face further restrictions in the future. [5]

Research is also focusing on finding good alternatives where both the resin and the fibers are of natural origin, and mixtures that make the bio-resins recyclable so that second-generation composite materials can be produced.

This study, carried out in collaboration with *Dallara Automobili* and *Angeloni Group S.r.l.*, fits coherently into the current context described above, of growing interest and constant push towards the study and use of natural composite materials.

The aim of this work is to achieve the mechanical characterization of a series of bio-composite materials, composed of carbon fibers immersed in a bio-resin matrix.

Specifically, two long-fiber materials and three short-fiber materials obtained through recycling carbon fiber waste from other production processes will be studied.

Once the mechanical characteristics are obtained, and potential problems are assessed, possible applications will be hypothesized.

1.→Bio Composites

A composite material is defined as a system made up of two or more phases, whose properties and performance are designed to be superior to those of the individual materials acting independently. Typically, one of the phases is discontinuous, stiffer, and stronger and is called the "reinforcement," while the less stiff and weaker phase is continuous and is called the "matrix." Sometimes, due to chemical interactions or other effects, there is an additional phase, called the "interface," between the reinforcement and the matrix.

The phases of a composite have "different" roles depending on the type and application of the composite. In low- or medium-performance composite materials, the reinforcement, usually short fiber or particles, provides some stiffening but only strengthens the material locally. The matrix, on the other hand, is the main component for bearing loads and determines the mechanical properties of the material.

In high-performance structural composites, the reinforcement is usually made of continuous fibers and forms the skeleton of the material, determining stiffness and strength in the fiber direction. The matrix phase provides protection and support for the fibers and transfers local stresses from one fiber to another. The interface, though small in size, can play an important role in controlling the failure mechanism, fracture resistance, and, most importantly, the stress-strain behavior of the material.

Thanks to growing interest and commitment to environmental issues, bio composite materials have been developed and are gaining significant attention. Bio composites can be defined as materials in which at least one of the components is derived from natural sources: either fossil-derived polymers reinforced with natural fibers, biopolymers reinforced with synthetic fibers (e.g., glass, carbon), or biopolymers reinforced with natural fibers.

Natural fibers represent a sustainable alternative to metallic and synthetic fibers as they are eco-friendly, lightweight, biodegradable, available in large quantities, and renewable. These fibers have lower density compared to steel fibers or synthetic fibers such as glass, aramid, and carbon. The recycling and disposal technologies for bio composites are simpler and more efficient.

Polymers reinforced with natural fibers have good relative mechanical properties, such as tensile modulus and flexural modulus, are resistant to corrosion and fatigue, and offer better surface finish in molded parts compared to synthetic composites. However, they are characterized by slightly lower and disperse mechanical properties

than their synthetic counterparts, high flammability, lower workability and low moisture resistance.

Due to the hydrophilic nature of the fibers, there are compatibility issues with the matrix, which tends to exhibit hydrophobic behavior. Moreover, it is difficult to find reliable values for their mechanical properties, as they are influenced by many factors such as the geographic origin, the age of the plant from which they were obtained, and the retting technique used for their production, among others. They also exhibit low thermal stability, making them difficult to process at high temperatures, and natural fibers are often subject to breakage during the manufacturing process.

Current research is focused on finding possible solutions to these problems, with promising results, to make these materials even more competitive in the market. Despite some challenges, composites reinforced with natural fibers are increasingly being used in automotive applications, such as body parts.

There is a wide range of natural fibers. The most interesting fibers for composite reinforcements come from plants, particularly from the bark, leaves, and wood. Bark fibers, such as flax, hemp, jute, and kenaf, are the most commonly used as reinforcements because they are the longest and offer the highest strength and stiffness.

Flax and hemp are the most interesting in Europe because they are native to the region. Flax is widely used in high-performance applications, such as in motorsport. Kenaf fiber is derived from *Hibiscus cannabinus* (similar to jute) and is mainly produced in the Po Valley, with its cultivation not requiring pesticides. Hemp can be used to produce fibers with properties similar to those of glass fibers. Most hemp is produced in China, South Korea, Chile, Spain, and France.

Flax, thanks to its low density and very high stiffness, allows for components with high impact resistance and good vibration damping properties. It was also becoming popular for its aesthetic appeal, making it striking for car interiors. Jute fiber production, however, requires large amounts of water, both for cultivation and resting.

The plants can grow up to 4 meters in height, making it possible to obtain very long fibers. Jute is produced in the Near East, India, Bangladesh, Nepal, and Pakistan. Another type of fiber gaining popularity is henequen, obtained from the agave plant. From this plant, short fibers are produced, giving composite materials characteristics similar to those conferred by glass fiber.

The possibilities for producing natural fibers are becoming increasingly diverse, such as those obtained from pineapple leaves, sisal plants, and many others. As shown in

the following diagram, fibers are not only obtained from plant sources but also from animal and mineral sources.[32][33][36]

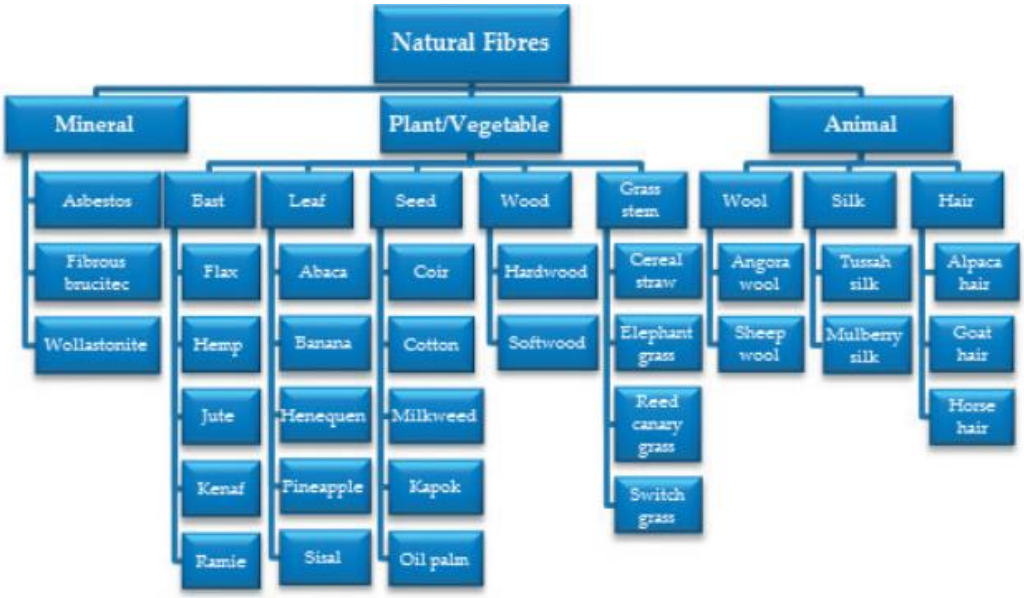

Figure1.1: Natural fibers typologies

Regarding the matrix of composite materials, the production of plastics is very complex and involves various processing stages.

The resource used to produce synthetic resins is virgin naphtha, a product of petroleum distillation, or it can be derived from natural gas. From virgin naphtha, through a process called cracking (or reforming, which involves the splitting of hydrocarbons), a chain of molecules is broken down, and different simple molecules, called monomers, are obtained. The transformation of resins, through the physic-chemical process of polymerization, causes the monomers to bond together, giving rise to compounds with different characteristics, known as polymers, each of which has distinct properties, structure, and size based on the different types of base monomers. The produced resins, depending on the nature or type of bonding of the monomers they consist of, are divided into thermoplastics, if they can be reprocessed, and thermosetting resins, which can only be processed once.

At this point, to create plastic material, synthetic resins need to be combined with additives—substances that impart particular characteristics to the material, improving its appearance and mechanical strength. The resulting mixtures are then transformed into granules, powders, or pastes, depending on industrial requirements. [31]

There are two main types of resin used in the production of composite materials: thermosetting and thermoplastic resins. Thermosetting resins are currently the most widely used, but with the expansion of composite materials, thermoplastic resins are gaining increasing attention.

Thermosetting resins are hardened through a polymerization process using heat to form highly cross-linked polymers with rigid, insoluble, or infusible bonds that do not melt when exposed to heat. On the other hand, thermoplastics are chains or branches of monomers that soften when heated and solidify when cooled, a reversible process with no chemical bonds involved.

Thermosetting resins, such as epoxy resins or polyester-based resins, are popular for composite material production because their low viscosity helps achieve good penetration into the fiber network. This allows for the use of more fibers and increases the strength of the final composite material.

The process for a thermosetting resin begins, in the pultrusion phase, by immersing the fibers in the resin. The fibers are then pulled into a mold where heat is applied. This initiates the polymerization reaction, which converts the low-molecular-weight liquid resin into a solid three-dimensional network structure, locking the fibers into the newly formed network.

Since most polymerization reactions are exothermic, once the reaction starts, it propagates easily, making the production of thermosets easily scalable. Once set, the three-dimensional structure locks the fiber in place and imparts strength and rigidity to the composite.[30]

The matrix production process is therefore far from being considered sustainable, which is why, in order to make composite materials truly green, natural origin matrices, such as cellulose-based plastics, corn-based plastics, and those derived from starch and soy, are being developed.

The cost of these new green materials is lower than that of synthetic materials, and their life cycle from production to disposal has a reduced environmental impact.

The three most commonly used domestic oils for industrial bio-resin production are soybean, linseed, and rapeseed oils, in addition to the less popular palm, coconut, and castor oils.

New approaches in the research and development of these vegetable oils exploit the natural physical or chemical properties of these substances to create high-performance materials that can complement, and in some cases replace, existing materials produced by the petrochemical industry. [34][35][36]

In the diagram below, a possible division between those of natural origin and those of synthetic origin, along with the respective resin families used for the creation of bio-composite materials, can be observed. [35]

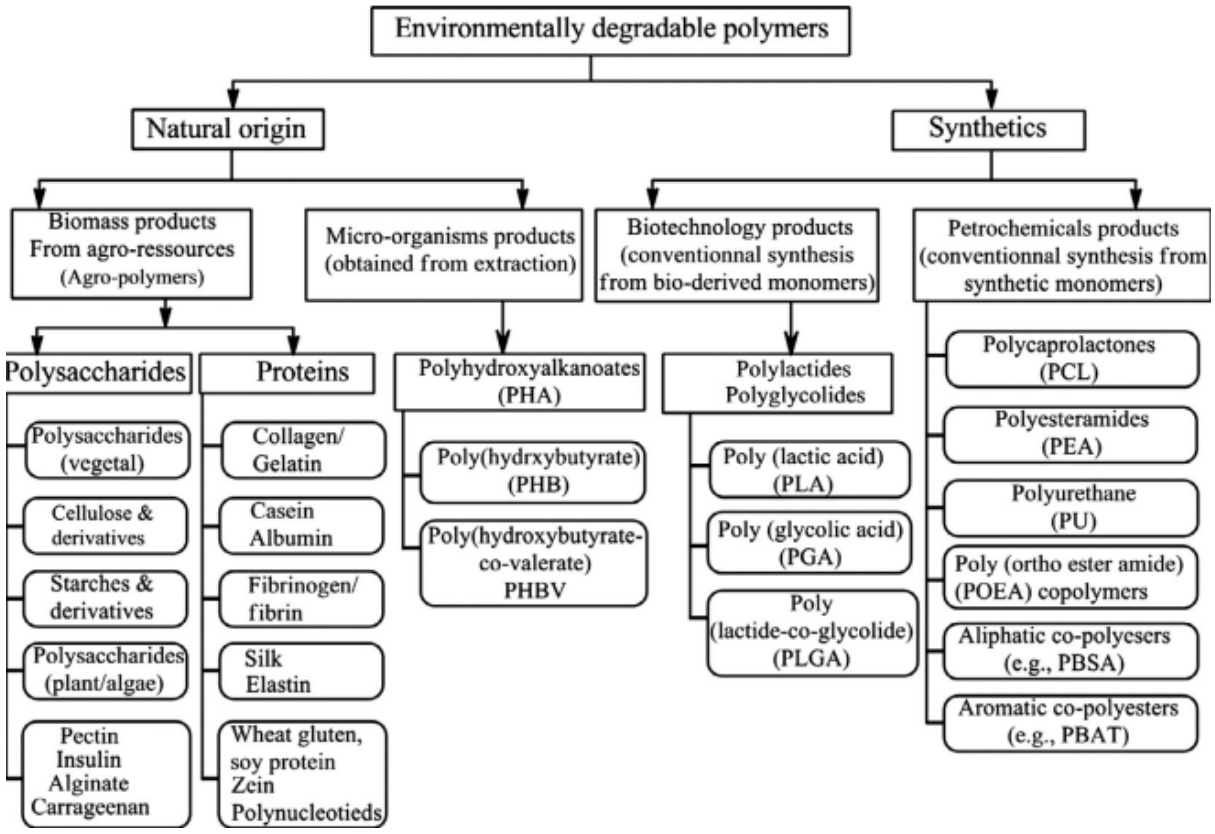

Figure1.2: Biopolymers typologies

Another feasible option for the production of bio-composites is the use of natural resin in combination with recycled fibers. [36]

The high mechanical properties of carbon fibers stem from the specific crystalline structure of graphite. The higher the crystalline structure, the greater the material's properties.

A graphite crystal has a structure composed of overlapping layers of planes made up of carbon atoms. The bonds between atoms within the same plane are strong (covalent bonds), while the bonds between atoms in different planes are relatively weak (Van der Waals bonds). It is clear that crystals are highly anisotropic structures, and it is the task of the manufacturing process to arrange the crystalline structure in the desired direction.

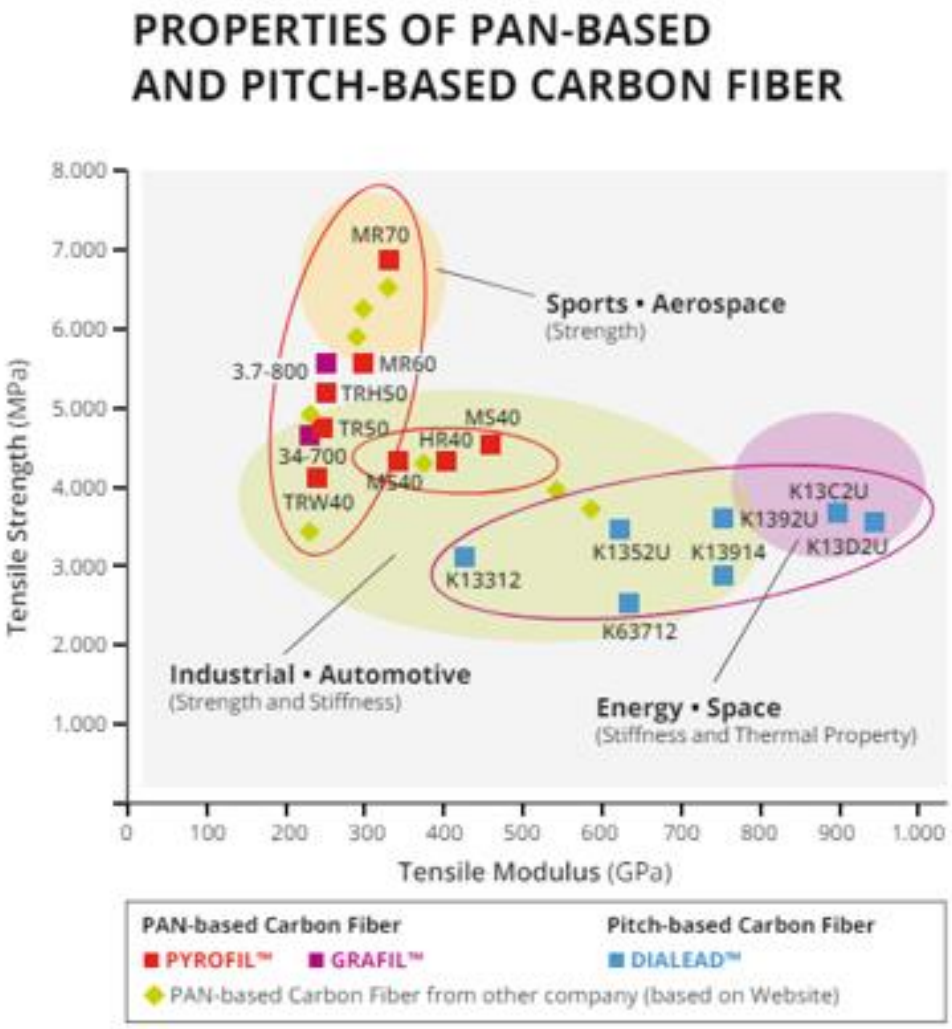

Figure1.3: Carbon fibers properties

Carbon fibers can be classified into two main families: fibers with variable tensile strength and a more or less constant elastic modulus, and fibers with a variable elastic modulus that can be very high and a more or less constant tensile strength for all fibers in this category.

Specifically, the first family of fibers described above is called the T series. This series can further be divided into fibers with a standard tensile strength value and fiber with a low tensile strength value.

The second family is called the K series and is characterized by fibers with high elastic modulus values and low tensile strength values.[25][27]

We can then identify four families of materials depending on the origin of the fiber.

The PYROFIL and GRAFIL fibers are polyacrylonitrile (PAN) based fibers, which is a polymer obtained from the polymerization of acrylonitrile.

They are characterized by excellent strength and stiffness, dimensional stability, and are produced on a large scale in the United States.

Thanks to their characteristics, these two types of materials have evolved as high-performance materials where high strength is required. They are indeed characterized by high and stable strength, excellent processability allowing for increased productivity, and can be used in applications involving high levels of deformation.

Then there are DIALEAD fibers, which are derived from pitch. These fibers have a high carbon content, which allows for high stability in composite materials.

They have a vertically oriented structure due to the graphite structure, which gives these fibers lightness, high rigidity, excellent thermal conductivity, and a low thermal expansion coefficient, making them ideal for good fiber-matrix coupling.

These properties make DIALEAD fibers particularly suitable for aerospace, sports, and many other industrial applications. [26]

Fibers can be produced in two modes: twisted and untwisted. They can also be produced in different sizes depending on the fiber considered. In general, for small fibers, each individual tow consists of 1000-6000 filaments, which are used to make woven fabrics and prepregs.

Standard sizes of larger tows range from 12.000 to 24.000 or 36.000 filaments per tow.

Carbon fibers can be woven in various ways, resulting in different characteristics both aesthetically and in terms of mechanical properties.

Plain weaves feature a simple pattern with a symmetrical appearance and a small checkerboard motif, which varies in width depending on the thickness of the material's tows.

In this weave, the fibers (tow) are interlaced in an over/under pattern. The tight spacing between the interlacing significantly contributes to the stability of the plain weave fabric.

The stability of the fabric corresponds to its ability to maintain the weaving angle and fiber orientation. Due to its significant stability, plain weave is not particularly suited for layups with intricate contours.

Additionally, it lacks the flexibility shown by many other waves. Plain weave fabrics are generally suitable for two-dimensional curves, tubes, and flat sheets.

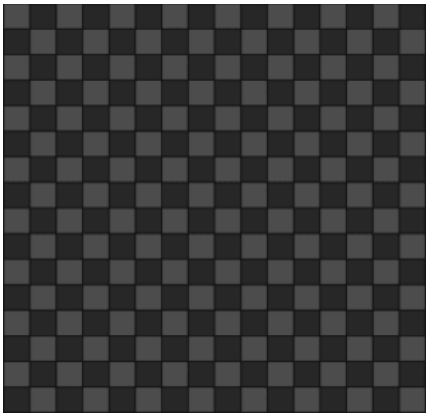

Figure1.4: Plain fabric

Twill weave is more flexible and capable of conforming to complex contours. Twill fabrics can be 2x2, 3x3, and so on, where a tow passes over two other tows and then returns underneath for a length equal to that of the overpass. Generally, following a tow in a twill weave, it goes over a certain number of threads and then under the same number. The over/under pattern creates a diagonal arrow-like appearance, sometimes referred to as the "twill line."

It is superior to satin weaving in terms of fabric stability, but not as good as plain weaving.

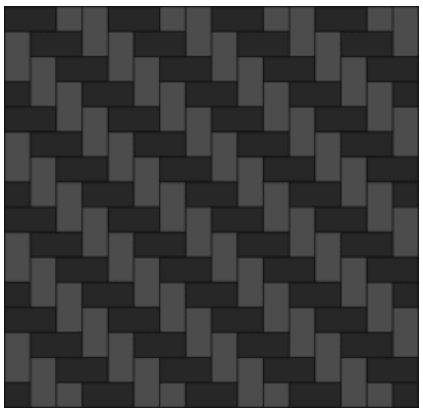

Figure1.5: Twill fabric

We also have satin weave, which features exceptional drapability and a smooth, seamless appearance. The drapability of this type of composite allows it to easily

conform to and wrap around complex contours. This fabric has low stability due to its high formability. [28]

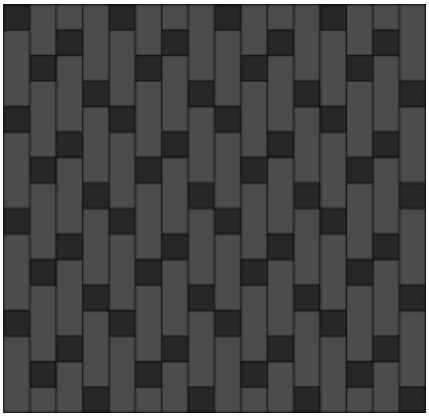

Figure1.6: Satin fabric

A series of thermal treatments are applied to the fibers to improve their processability and bonding with the resin.

Thermal treatments can be divided into surface treatments and sizing treatments. Surface treatments, through the addition of functional oxygen groups, enhance fiber adhesion to the matrix and vary depending on the type of matrix and the mechanical properties desired.

Sizing processes, on the other hand, involve applying coatings to the fibers. This process also improves fiber processability and the bonding between the two elements of the composite.

Fibers are largely used in the form of pre-impregnated materials. These materials are used to produce high-performance panels with very low weight, such as for manufacturing doors, fenders, etc.

Carbon fibers are obtained by graphitizing textile organic fibers of rayon or polyacrylonitrile (PAN) in an inert atmosphere at temperatures exceeding 2000°C. The starting fibers are known as precursors.

This process requires high energy consumption, so it's worth trying to minimize waste from the fiber production process.

Thus, efforts have been made to recover carbon fiber waste, which is then reused in short or long fiber composite materials. This approach leads to significant reductions in energy consumption, costs, and associated emissions.

Recycled carbon fibers can be obtained mainly in two ways: either by recovering waste from virgin fibers obtained from weaving, or through recovery processes of fibers from post-cured composite materials.

The possible processes used for recycling carbon fibers are:

1. **Pyrolysis**: Pyrolysis is one of the most common methods for recycling carbon fibers. It involves heating composite materials in the absence of oxygen at high temperatures (typically between 400 and 700°C). This process consists of the following stages:
    a) **Decomposition of the polymer matrix**: The matrix (usually resin) is thermally degraded, releasing volatile gases.
    b) **Recovery of fibers**: Carbon fibers remain intact because they are resistant to high temperatures and are not burned. However, the surface quality of the fibers may be compromised.
2. **Solvolysis**: In this process, composite materials are treated with solvents at high temperatures and pressures to break down the polymer matrix, leaving the carbon fibers intact. This process can be carried out at lower temperatures compared to pyrolysis but requires the use of chemical agents such as alcohols and organic acids.
3. **Oxidation**: In this process, composite materials are treated with heat in the presence of oxygen. The polymer resin burns completely, leaving all the carbon fibers intact. This process is simpler compared to pyrolysis, but the fibers obtained tend to be more damaged due to surface degradation during combustion.
4. **Microwave Pyrolysis**: This is an advanced version of pyrolysis that uses microwaves to heat the composite material. This method is considered more energy-efficient compared to classic pyrolysis as microwaves heat the material directly. The fibers tend to heat up quickly, accelerating the degradation process of the polymer matrix.
5. **Thermal Electrodes**: In this process, electrodes are used to selectively heat the carbon fibers within a composite material, decomposing the matrix without damaging the fibers. This method is still under study and experimentation.
6. **Mechanical Grinding**: In some cases, materials are ground into powder to produce fine powder or short fibers. Although this method does not allow for

the recovery of long, high-quality fibers, it can be useful for less demanding applications or as filler reinforcements in new composite materials. [24]

It is estimated that 30% of carbon fibers from industrial production processes become waste. The production of virgin carbon fibers requires high energy consumption, while recycling fibers through pyrolysis consumes about one-tenth of the energy required for virgin fibers. Additionally, recycling fibers eliminates the costs associated with the precursors of carbon fibers, which account for about 50% of the total cost of virgin carbon fibers. [29]

Recycled fibers exhibit mechanical properties comparable to those of virgin fibers. They have similar stiffness but a reduction in maximum strength of about 15%. Recycled carbon fibers lead to a reduction in production costs of approximately 45-50%.

These positive aspects have led to the development of a range of recycled fabrics such as non-woven fabrics (TNT) or Carbon Task. Their use is more appreciated in the production of non-structural components like flanges and exterior body parts.

The company *Angeloni Group S.r.l.* provided us with two long-fiber materials pre-impregnated with a bio-resin and three short-fiber materials obtained through the recycling of TR50 virgin fiber waste. Two of the short-fiber materials are pre-impregnated with the same bio-resin used for the long-fiber materials, while the other short-fiber material is impregnated with a synthetic resin, allowing us to compare the mechanical properties of the biomaterial with its synthetic counterpart.

The two long-fiber materials are:

- **C 370 MR60 24K IMP512BIO 38% Angeloni**: This is a long-fiber material with a plain weave, featuring a carbon areal weight of 370 grams per square meter, with 24.000-filament MR60 tows. The shared bio-resin is IMP512 with a percentage of 38%.
- **C 630 TR50 12K IMP512BIO 34% Angeloni**: This is a long-fiber material with a 2x2 twill weave, featuring a carbon areal weight of 630 grams per square meter, with 12.000-filament TR50 tows. The bio-resin percentage in this case is 34%.

The IMP512 is a thermosetting epoxy resin with 15% bio-origin content that can be processed both in the press and in the autoclave. This 15% of bio-origin content is made of a 10% coming from natural origin composition and a 5% coming from mass balance. It has a post-cured average density of 1.21 g/cm^3 and a maximum glass

transition temperature of 145°C. Among its other characteristics are good UV and weather resistance, making it suitable for aesthetic applications.

The discussion will then shift to the characterization of three mildly needled short-fiber composite materials, whose fibers were obtained through the recycling of TR50 virgin carbon fibers from other weaving processes. The materials studied are:

- **C100Carbon Task IMP512BIO**: This material has a carbon areal content of 100 grams per square meter, immersed in the IMP512 bio-resin used also for the long-fiber materials.
- **C200Carbon Task IMP512BIO**: This material is similar to the previous one but with a carbon areal weight of 200 grams per square meter.
- **C200Carbon Task IMP509**: This material also has 200 grams of carbon per square meter but is impregnated with a standard synthetic resin.

The IMP509 is a standard epoxy resin with characteristics similar to IMP512BIO. IMP512BIO is derived from IMP509 by replacing some synthetic precursors with their bio-origin counterparts. It has identical average density and glass transition temperature as the other studied resin and excellent weather resistance.

This choice of materials is very useful as it allows for a comparison between the behavior of the same bio-resin with different carbon areal weights, both in combination with long and short fibers.

The choice to impregnate the Carbon Task with two resins that are very similar in properties but of different origins will allow us to analyze the effect of the bio-component on the mechanical properties of two otherwise very similar materials.

Furthermore, impact tests using a drop tower will enable us to observe the differences in energy absorption capacity between the long-fiber and short-fiber materials and between the bio-resin and the synthetic resin.

It will also be interesting to observe the processability of the short-fiber materials, comparing their behavior when processed in a press versus in an autoclave.

2.→Test and Instruments

In order to investigate and deepen the understanding of the behavior of the bio-based materials described earlier, a series of mechanical, thermal, thermomechanical tests were carried out to assess their performance and the quality of the production process followed. Optical microscopy was also used to assess the quality of the produced laminates.

To begin with, a series of tensile tests were performed at 0°, 90°, and 45° relative to the main fiber direction in order to evaluate the tensile strength and the elastic modulus in different directions.

Subsequently, a series of compression tests were conducted at 0° and 90° respect to the main material direction to assess the compression performance of the materials, along with Interlaminar Shear tests to evaluate the adhesion strength between the fibers and the matrix.

Additionally, three-point bending tests were performed to evaluate the flexural behavior and drop tower impact tests were conducted to assess energy absorption in the event of an impact.

Finally, for each material sample, a Dynamic Mechanical Analysis was carried out to study the viscoelastic properties of the materials, as well as a Differential Scanning Calorimetry test to evaluate the quality of the experimental production process that was followed.

2.1→Mechanical characterization: tensile, compression, flexural and interlaminar shear tests

Tensile tests are mechanical characterization tests that involve applying a mono-axial load (F), initially zero, to a specimen of standard dimensions, as described by the relative standards. The load is then gradually increased until the maximum value is reached, determining the fracture point.

This test is essential for measuring various mechanical properties, such as tensile strength (Rm), Young's modulus (E), and maximum strain at break. [40]

Compression tests are mechanical tests used to measure a material's resistance to compression, i.e., its ability to withstand a load that tends to compress it.

This loading condition is commonly encountered in engineering applications, such as the automotive and aerospace industries.

The test allows for determining important mechanical properties, such as compressive strength, resistance to deformation, and identifying any defects that could affect performance.

During the compression test, the material specimen is placed between two parallel plates, and a unidirectional force is applied along the compression axis. The load is gradually increased until the material either breaks or undergoes permanent damage.

The applied force and material deformation are recorded throughout the test, allowing the stress-strain curve to be plotted. [41]

Three-point bending tests, on the other hand, provide values for the flexural modulus, stress, and strain of the studied material. This test is carried out on a universal testing machine (tensile tester) equipped with a three-point bending device.

The standard-length specimen is placed in the three-point bending device and subjected to an increasing load. During the test, the load and deformation are measured, allowing the flexural modulus and flexural breaking load to be measured.

The main advantage of the three-point bending test is the ease of specimen and test preparation. However, this method also has some disadvantages, such as the fact that the results are sensitive to specimen geometry, load type, and deformation speed. Therefore, it is crucial to strictly follow the relative standards.

Interlaminar shear strength is a critical property of laminated materials with a brittle matrix made from epoxy resin.

It is usually determined using a short beam shear test. Shear stress is always present in bending tests.

If the specimen length is reduced relative to its thickness, the shear stresses that occur, in comparison to the normal stresses generated by the bending moment, become very high. This allows the generation of shear stresses in brittle matrix materials, enabling the measurement of shear resistance.

In this case, the specimen is subjected to an increasing load until fracture occurs, and both the load and corresponding deformation state are measured. Depending on the fracture type, it is possible to assess the shear resistance of the matrix or the quality of the fiber-matrix bonds.[42]

For the mechanical tests such as compression, tensile, three-point bending, and interlaminar shear tests, the *MTS Insight 150 EL* electromechanical testing machine,

Model number 820,150-EL, MTS Part number 56-906-702, was used, available at the *Dallara Automobili* research laboratory.

The machine has a load cell of ±150 kN and a resolution of 0,002 kN, class 0.5 and is equipped with 250 kN hydraulic grips and a coder with a range of ±300 mm and a resolution of 0,001 mm, calibrated until 18/07/2025.

Additionally, a biaxial extensometer MTS, model no. 632.85F-14, with a gauge length of 25 mm, and an axial extensometer MTS model no. 634.31F-24 with variable length were used, both calibrated until 18/07/2025. [38]

Figure 2.1: *MTS Insight 150 EL*

The tensile tests at 0° and 90° relative to the main fiber direction of the composite materials were carried out according to the ASTM D3039 standard, while those at 45° were conducted following the ASTM D3518 standard.

For the tensile tests at 0°, 90°, and 45° on short fiber specimens, the ASTM D638 standard was applied.

The compression tests at 0° and 90° were conducted according to the Boeing modified ASTM 695 (SACMA SRM 1R-94) standard.

Using the same equipment, Interlaminar Shear tests were performed following the ASTM D 2344 standard, and three-point bending tests were carried out in accordance with ASTM D790.

2.2→Drop tower test

The drop tower test is a type of impact test used to measure the energy absorbed by a material during high-speed impacts. The testing system consists of a falling mass guided by two columns, instrumentation for measuring force, a device to hold the sample, and a data collection system. [43]

The sample is fixed to the bottom of the drop tower, and a mass is dropped onto it. The acceleration and force at the moment of impact are measured.

At this point, depending on the material's behavior, the absorbed energy is calculated either by considering the difference in the mass of the specimen before and after impact (if the sample has undergone pulverization) or by calculating the difference in height of the specimen before and after impact (if it has fractured in a petal-like manner). The energy absorption value is measured in SEA [J/g]; Joules of energy absorbed by the material per gram of mass.

Energy absorption tests on the studied materials were conducted in a drop tower designed by *Dallara* with a maximum free-fall height of 4,7 m, a maximum impact energy of 3 kJ, and a maximum measurable acceleration of 20.000 g.

For the energy absorption tests, internal standards were followed, with a free-fall length of 1,83 m, an impacting mass of 24,2 kg, a theoretical impact speed of 6 m/s, and a theoretical kinetic energy of 434,3 J.

Figure 2.2: Example of drop tower

2.3→Dynamic Mechanical Analysis

Dynamic Mechanical Analysis (DMA) is a thermal analysis technique used to study the viscoelastic properties of materials. It involves applying an oscillating force at a specific frequency to a sample at a given temperature.

DMA is used to measure the mechanical properties of a wide range of materials. Many materials, including polymers, exhibit both solid elastic behavior and fluid viscous behavior, which is why the term "viscoelastic" is used. [44]

Dynamic Mechanical Analysis differs from other mechanical tests in two significant ways. First, typical tensile tests focus only on the elastic component, but in many applications, the non-elastic or viscous component is critical. It is the viscous component that defines impact resistance. Additionally, tensile tests primarily operate outside the linear viscoelastic range, whereas DMA works within the linear viscoelastic range, making it more sensitive to the structure of the material being studied.

The most common version of DMA is the dynamic oscillation test, where a sinusoidal stress (or strain) is applied to the specimen, and the resulting sinusoidal strain (or stress) is measured. The phase difference (δ) between the excitation and the system's response is also measured. The phase lag will be 0° if the material behaves perfectly elastically and 90° if its behavior is purely viscous. Viscoelastic materials display intermediate behavior.

The complex modulus (E^*) can be calculated from the ratio of stress to strain (2.1). From the values of the elastic modulus and the phase difference (δ), it is possible to calculate the storage modulus (E') and the loss modulus (E'') (2.1).

$$\begin{aligned} E^* &= stress/strain \\ E' &= E^* cos(\delta) \\ E'' &= E^* sin(\delta) \\ tan(\delta) &= E''/E' \end{aligned} \tag{2.1}$$

The storage modulus (E') corresponds to the elastic part of the stiffness of the tested specimen, while the loss modulus (E'') represents its viscous component and is related to the specimen's ability to dissipate mechanical energy through the movement of molecules or other irreversible phenomena. The tangent of the phase difference, tan(δ),

is another common parameter that provides information on the relationship between the elastic and viscous components of the modulus.

Through dynamic mechanical analysis, it is therefore possible to determine the glass transition temperature, the composition of the polymers, and parameters such as the complex Young's modulus (E^*), storage and loss moduli, in addition to the damping factor ($tan\ \delta$) and viscous flow (creep).

The dynamic mechanical analyses were performed using the *DMAQ800*, according to the normative ASTM D7028. This device can apply a maximum force of 18 N and a minimum force of 0,0001 N with a resolution of 0,00001 N. It features a strain resolution of 1 nanometer and an elastic modulus measurement range between 103 and 3x1012 Pa, with an accuracy of ±1%. It simulates a frequency range from 0.01 to 200 Hz and a dynamic deformation of the specimen up to 10.000 μm. The temperature range operates within spans from room temperature up to 600 °C, with a heating rate between 0,1 and 20°C/min and a cooling rate between 0,1 and 10°C/min. [37]

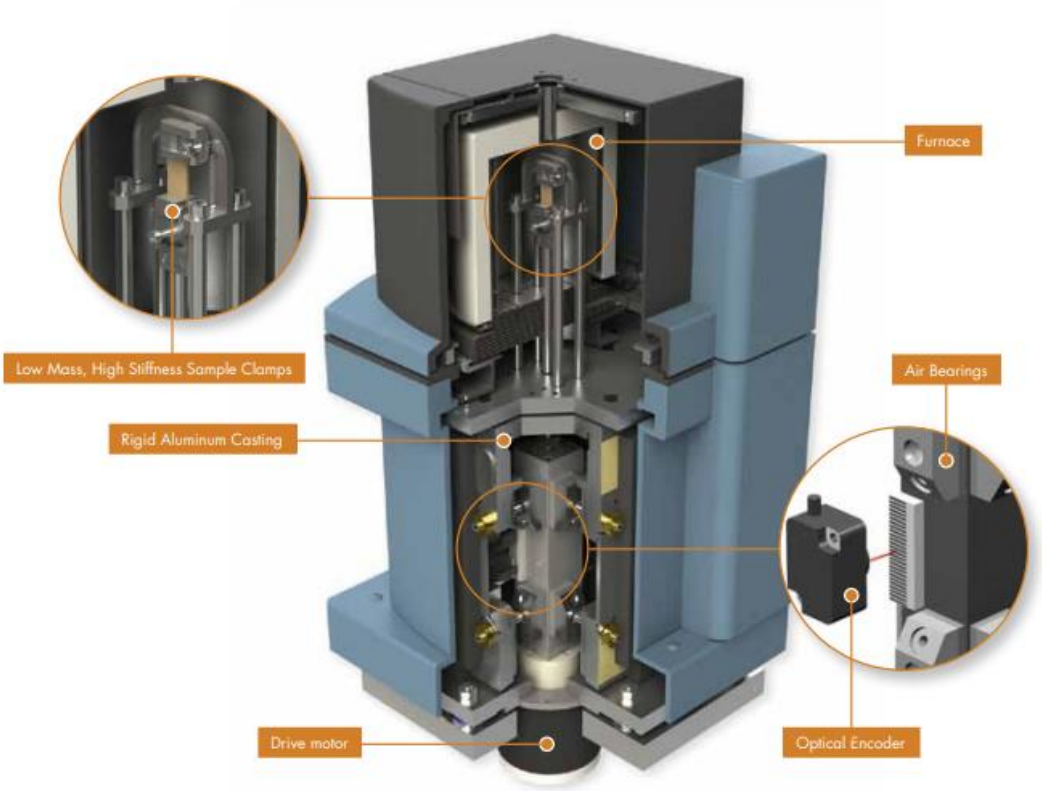

Figure 2.3: *DMAQ800*

2.4→Differential Scanning Calorimetry

Differential Scanning Calorimetry (DSC), together with Differential Thermal Analysis (DTA), is one of the primary thermal analysis techniques used to characterize various materials, including polymers, metals, and ceramics. The basic principle of this technique involves obtaining information about the material by heating or cooling it in a controlled manner. Specifically, DSC measures the difference in heat flow between the sample under examination and a reference sample, as both are subjected to a variable temperature defined by a pre-established program. The apparatus is prepared by placing two identical crucibles (called pans) on the holders, chosen to withstand the test temperatures without interacting with the sample. One of the crucibles remains empty and serves as the reference for differential measurement. The furnace is hermetically sealed using the control unit to isolate the testing environment from the outside. Once the thermal program (usually a linear temperature ramp) is started, an inert atmosphere of *Ar* or N_2 is introduced into the furnace containing the material to be analyzed, with a continuous and uniform flow. When the test begins, the heat supplied by the furnace heats both the sample and the reference pan in the same manner.

Any temperature variation between the two is due to phenomena occurring in the material under analysis: an exothermic reaction will raise the sample's temperature, while an endothermic reaction will lower it. Throughout the experiment, a system of thermocouples collects temperature data and sends it to a computer, which processes the data with specialized software to generate the output for the user.

Once the test is completed, the cooling system allows the operator to open the machine and remove the pans. [45] The differential scanning calorimetry tests presented in the present thesis were conducted, according to the standard ASTM D3418 for T_g calculation and according to ASTM E 2160 for residual enthalpy evaluation, using the *DSC1 Mettler Toledo* in the Quality control department of *Dallara Automobili*.

The temperature range of the machine spans from 30°C to 700°C, with an accuracy of ± 0,2°C and a heating rate between 0,02 and 300 K/min. [39]

Figure 2.4: *DSC1 Mettler Toledo*

2.5→Micrographs

The microscope is the instrument used to magnify objects, or their details, that we cannot see with the naked eye, so as to make them visible. It is made up of two systems of lenses inserted in a tube (lens tube). The lens on which we place our eye is called the eyepiece, while at the other end of the tube, near the object to be observed, we find another lens, the objective. Generally, microscopes have at least three objectives, with different magnification power, placed on the rotating objective turret. The eyepiece, tube and objectives form the optical system of the microscope. In practice, it is as if it were a double magnifying lenses: the objective magnifies the object and the eyepiece magnifies the image produced by the objective.

In addition to the optical system, the microscope has an illumination system and a support structure (stand). The support structure of the microscope, called a stand, includes the support base, the stage and a support to which the lens tube is connected. On the support we find the micrometric screw, which can move the lens tube closer or further away from the slide to focus the object and obtain a clear image. The resolving power indicates the ability to distinguish two very close points as separate. The optical microscope has a resolving power of approximately 0.3 microns: this means that we can enlarge the image until two points that are 0.3 microns apart are visible. This is the maximum resolution limit of the optical microscope: two points less than 0.3 microns apart cannot be distinguished, because visible light does not allow it. To distinguish even smaller details, we must use the electronic microscope, in which light is replaced by electrons.[46]

The microscope used for micrographic observations is the *Leica DM2700* optical microscope, located in the *DARC laboratory* at *Dallara Automobili*. It has a maximum magnification factor of 1000x and a motorized stage. Its objectives range from 2,5X to 50X.

Figure 2.5: *Leica DM2700*

3.→Material processing and sample manufacturing

After a brief overview of the possible ways of producing composite materials, we will move on to a description of the production process of the studied specimens. There are different ways of making composite components. The process varies depending on the type of component to be made and, therefore, depending on what mechanical and geometrical characteristics one wants to provide it with.

Once you have decided on the matrix and the fibers you want to use to make the material, the coupling process can be carried out in different ways depending on the type of component you want to go and create.

3.1→Composites materials production processes overview

Composite fabrication technologies vary according to the shape, size, and properties required for the finished part.

The most popular composite manufacturing processes are: manual impregnation without the use of pressure or vacuum, pultrusion, filament winding, resin transfer molding, resin infusion under flexible tool, autoclave molding, and press molding.

The manual impregnation process without the application of pressure or vacuum is still widely used for work on large surfaces such as swimming pools and boat hulls for which production is typically done in small batches and is the most widely used fabrication process in civil engineering. Reinforcements in fabric or mat form, are laid inside the mold and then the fibers are soaked in catalyzed resin and then manually consolidated using metal or plastic rollers for the purpose of removing excess resin. Curing generally takes place at room temperature. [48]

Another production process is the pultrusion. The meaning of the term pultrusion is extremely clear when one considers the basic technological scheme of the process.

In fact, while extrusion of aluminum or thermoplastics is accomplished by a pushing action on the material to force it through the mold, in the case of reinforced plastics, the same shape can be obtained by exerting a pulling (pull) force on the fibers forcing them to pass, after being wet with resin, into the mold. Thus, the pushing action typical of extrusion is replaced by the pulling (pull) action, hence the term "pultrusion." [48]

Filament Winding, on the other hand, is a technique that has been known for more than thirty years but advantageously used only in recent years due to the introduction of reliable materials and expedients that have made production easier and more economical.

The process basically consists of winding resin-impregnated continuous filaments onto a rotating body, called a mandrel, whose shape is identified in the geometry of the part to be produced. Curing of the resin is achieved by placing the part in an oven or autoclave. [48]

The resin transfer molding (RTM) process refers to a technology by which polymer matrix composites are fabricated by injecting catalyzed resin into a cavity having the shape of the part to be made and in which dry reinforcement has been preliminarily placed. The cavity is obtained by closing the mold and counter mold, one against the other. [48]

RIFT (Resin Infusion Under Flexible Tooling) processing, a variant of RTM, is performed using the flexible polymer bag instead of one of the faces of the rigid mold; it is more economical and by operating the vacuum inside, the resin is pushed into the dry reinforcement so as to reduce the operator's contact with the resin in its liquid state and all its volatile components emitted during placement. [48]

Autoclave forming is a technology to produce composite elements by the use of the autoclave; it makes it possible to obtain laminates with much higher mechanical properties than the more traditional and economical technologies analyzed so far. With the use of the autoclave, it is possible to intensify the compaction action by increasing the pressure during the cure cycle to about 7-10 atm and the temperature up to 200 °C. Newer autoclaves also offer the possibility of varying the pressure and temperature during the curing cycle according to the laws most appropriate for the particular type of resin used.

Higher pressure ensures the absence of voids between layers. This type of fabrication is adopted when parts with very stringent mechanical properties are to be made as required, for example, for aeronautical, racing, space and medical use. [50]

With this type of process, the molding of prepreg fabrics and infused fabrics with the Film Infusion technique typically requiring the use of high temperatures and vacuum consolidation is carried out.

To conclude it is possible to describe the forming process in hot press. First, we process the prepreg material with the hot press. The part is shaped into various shapes, and then the different layers are stacked on top of each other depending on the final thickness of the part and the desired fiber inclination. The set of stacked layers is

called a kit. Then the kit is placed inside the press, which when put into operation, will apply pressure and heat. [48][49]

3.2→Production processes of the experimental samples

The materials studied were provided to us in the form of rolls of prepreg composite material. Prepreg is a term used for pre-impregnated fiber-reinforced composite materials in which a matrix, such as epoxy resin, is already present.

The fibers, of a continuous type, are typically arranged to form a fabric, while the matrix is used to attach them to each other and possibly to other components during manufacture. The matrix is only partially cross-linked so that it can be easily handled; this is called B-stage material and requires storage at low temperatures to prevent completion of cross-linking. Stage B prepregs are always stored in cooled areas since heat accelerates polymerization.

There are several advantages and disadvantages of the B-stage prepreg process in comparison with the hot-chamber injection system. Prepreg allows fibers to be impregnated on flat workable surfaces, i.e., in industrial processes, and then give the impregnated fibers a shape that would be problematic for the hot-chamber injection system. Prepreg also allows a significant number of fibers to be impregnated and then stored in a cooled area for long periods, proceeding to cross-linking later. Unfortunately, the process can be time-consuming compared to the hot-chamber injection system, so a greater cost of preparing the prepreg is at the material supply stage. [51] The rolls of prepreg material were then stored in cold storage between -18°C and -20°C to slow down the resin cross-linking process that had already been triggered in the previous process.

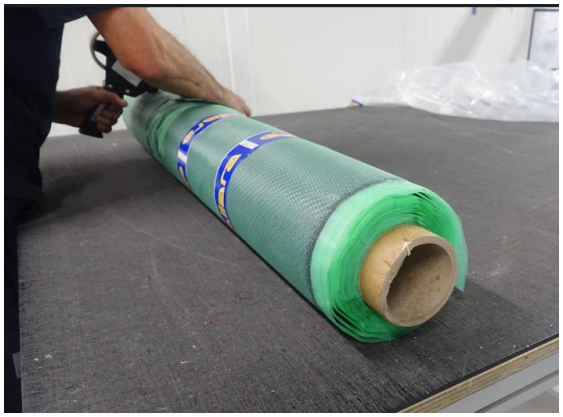

Figure 3.1: Prepreg roll

From them, templates of the specimens that wanted to be produced were then cut and a number of layers were stacked depending on the material considered and the thickness required by the testing standard.

The cutting process can be done manually, in the case of simple geometries and for low volumes, or in a fully automated manner.

Plotter cutting machines are semi-automated machines. They consist essentially of a feeding system into which the pre-impregnated composite material is fed, a table equipped with a vacuum system to constrain the sheets while cutting is being performed, a 2-axis or multi-axis handling system, and the tool required for cutting.

Figure 3.2: Plotter cutting machine

Given the high cost of prepregs and the scarcity of time, it is of utmost importance to maximize production by minimizing waste during cutting operations.

Nesting refers to the application of an algorithm in order to arrange cutting patterns (or icons or geometries or shapes) to minimize raw material waste. [52]

Once the specimen shapes have been cut, the different layers of sticky pre-impregnated material for partial resin cross-linking are glued on top of each other according to the desired thickness and fiber direction.

Then, after the lamination process is finished, the fabricated composite material kits are placed in the appropriate molds and a layer of release film and a vacuum fabric (breather/ bleeder) are placed on them, the former to allow the specimen not to stick to the mold at the end of the production process and the latter to allow proper air aspiration during vacuum creation.

This is then placed inside a bag (vacuum bag) that is closed with sealant tape, and a valve (Vac Valve) is applied to the bag, which uses a vacuum pump to suck air into the bag, which escapes assisted by the vacuum fabric.

Figure 3.3: Vacuum bag with Vac valve

This operation performed by skilled and experienced technicians makes the bag adhere perfectly to the laminate by compressing it in contact with the mold.

At the end of this stage, the molds are placed inside the autoclave and connected to its vacuum circuit.

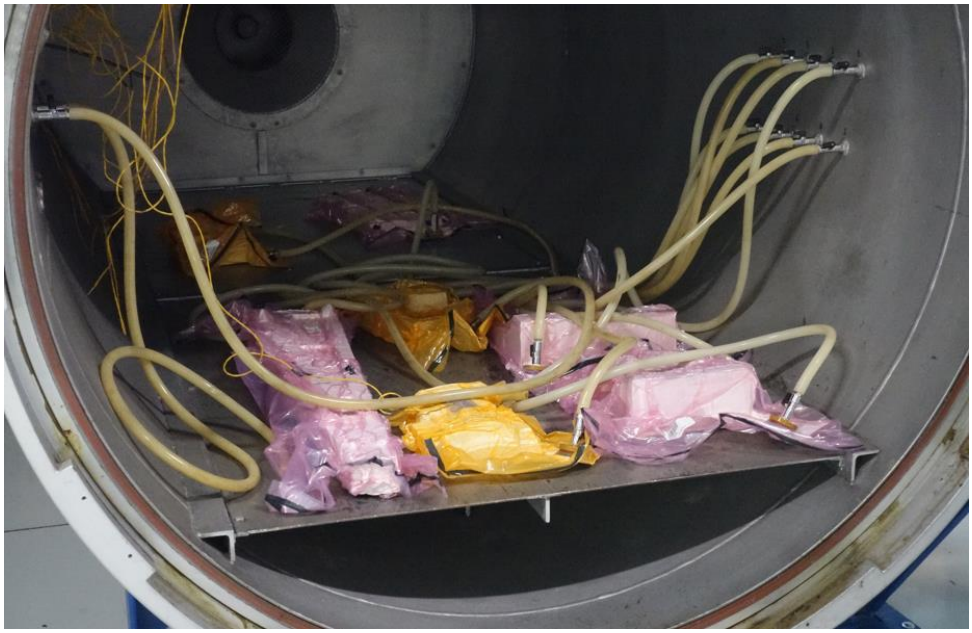

Figure 3.4: Vacuum circuit

Next, the curing cycle (Cure Cycle) is set with a specific program, and the time temperature and pressure functions are then set.

The internal pressure of the autoclave compresses the material in contact with the mold, and the vacuum inside the bag will suck out any air and residual solvents, obtaining a part with characteristics otherwise unobtainable with other technologies.

This type of process allows great freedom in making any type of geometry and the possibility of obtaining artifacts with structural and other strength capabilities that otherwise would not be obtainable. [47]

The long-fiber composites that were supplied to us by *Angeloni Group* were made with the goal of obtaining materials with high mechanical performance and were therefore autoclaved in order to obtain their maximum performance.

They were autoclave processed according to the suggested cure cycle of 90 minutes at a cure temperature of 135°C, a pressure of 6 bar, and a heating rate of 2°C/min.

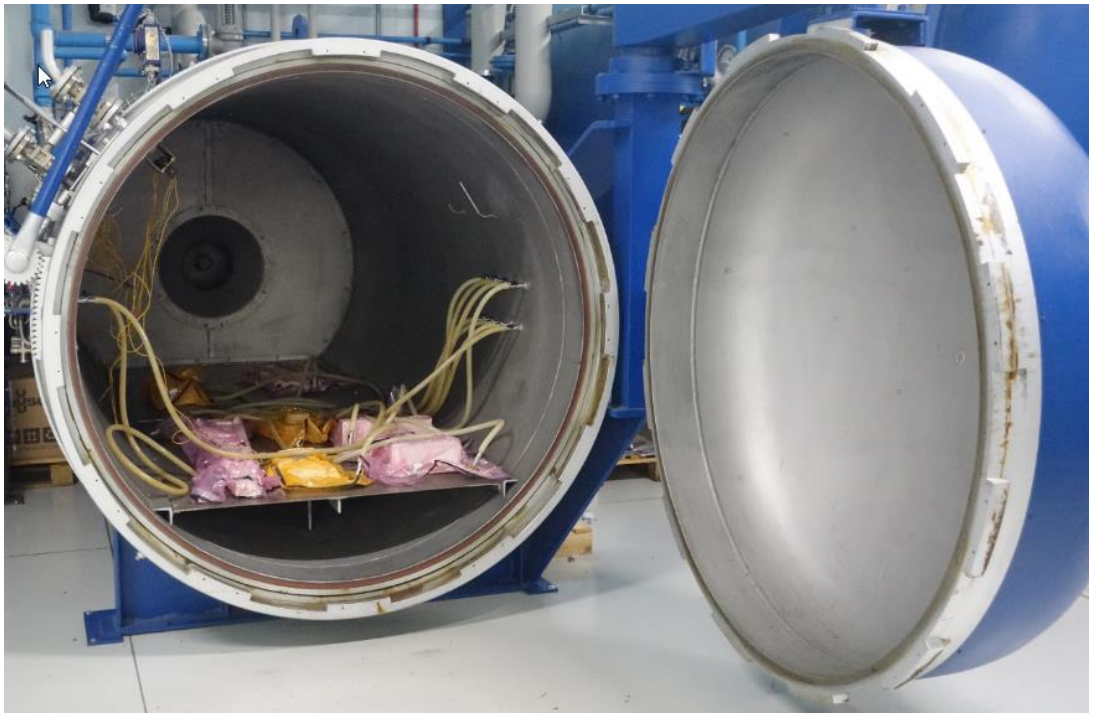

Figure 3.5: Autoclave

Short-fiber materials, on the other hand, originate from recycled fibers obtained from the weaving waste of long-fiber materials. Their purpose, therefore, is the manufacture of nonstructural components with a more sustainable production process that leads to the reduction of resource consumption and especially of energy consumption. Consistent with the above, they were processed by press.

The press process, although it does not allow the production of components with the same performance as those processed in an autoclave, provides a great reduction in production time and cost as well as ensuring the maintenance of good mechanical properties.

In the manufacturing process of short-fiber materials, one of the main problems is the evacuation of air during production.

This is because they are made from fibers that are only partially sorted, which makes it difficult for air to pass through evenly when pressure is applied during production of the component.

Moreover, in the press process, higher pressures can be used than those obtained in an autoclave and is therefore very suitable in the production of short-fiber components.

The press molding process, in addition to providing a reduction of energy consumption, also has characteristics that make it preferable to the autoclave process for the production of short-fiber materials.

Figure 3.6: Press

Press technology, sparsely used in the past, has recently found wide use due to the availability of pre-impregnated fibers and new resin matrices specifically designed for this process.

The pre-impregnated composite material is placed on an open, heated mold, usually metallic and obtained by CNC machining.

It is then closed with the counter mold and pressed. Heat and pressure are maintained with dedicated curing cycles.

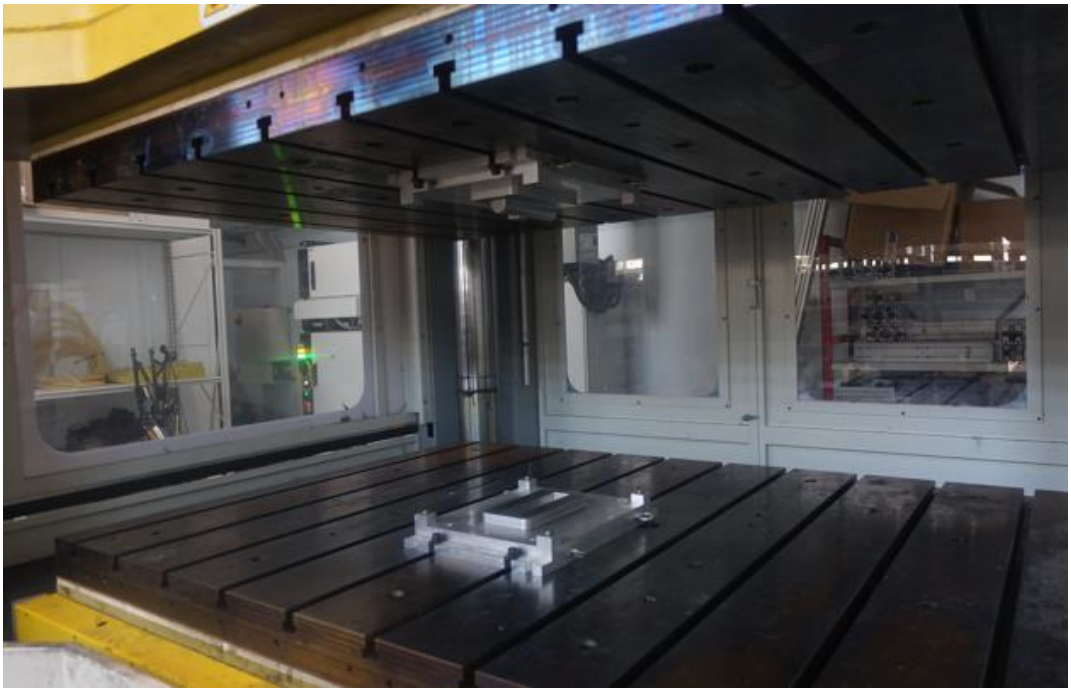

Figure 3.7: Heated mold

This technology allows the production of both small and large parts with complex conformations, such as holes and concavities, but without the need for any subsequent machining.

In particular, it allows a high speed of the curing cycle as well as the possibility of using multi-cavity molds for the production of several parts simultaneously.

For this study, specimens of the short-fiber materials, therefore, in accordance with what has just been said, were produced by the press production process.

The press cycle suggested by *Angeloni Group* using a force of 30 tons, a cure time of 15 minutes and a temperature of 135°C was followed.

Since the production process of short fiber material was still under study, a pre-heating time of 145 seconds was experimentally identified for the specimens for the energy absorption tests.

Instead, a preheating time of 100 seconds was identified for the short-fiber composite panels from which all other specimens were cut for the other tests.

Figure 3.8: Omega specimen

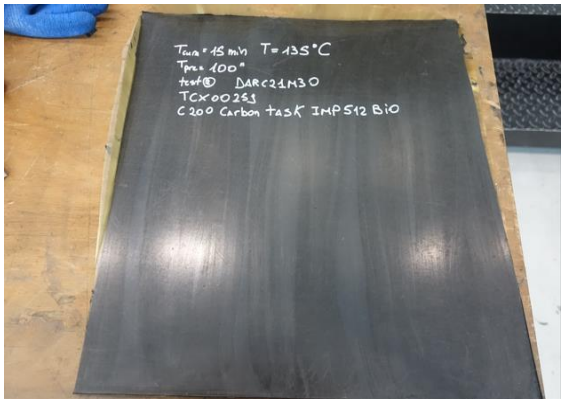

Figure 3.9: Shot fiber press processed panel

The goodness of time value obtained will then be verified through DMA and DSC tests performed on the samples of the short-fiber materials.

A panel of C200 Carbon Task IMP512 BIO short-fiber materials was also made in autoclave to evaluate possible processing of the short-fiber materials.

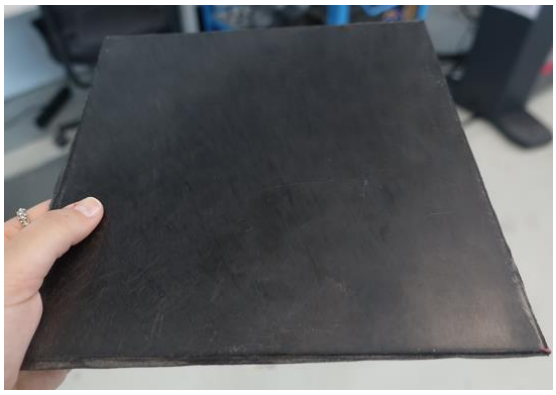

Figure 3.10: Shot fiber autoclave processed panel

The cure cycle followed was suggested by the manufacturer with a cure time of 90 minutes at a temperature of 135 °C and a pressure of 6 bar.

3.3→ Comparison between press and autoclave production processes of short-fiber composite materials

Since the materials analyzed are new materials about which there is not much information, a series of micrographs were taken in order to evaluate the quality of the manufacturing process used to make the short-fiber specimens.

The instrument used was the *Leica DM2700* optical microscope, as indicated in the section on tests and instruments used.

First, micrographs were made on the omega-shaped specimens that were used for energy absorption tests, for all short-fiber materials. These specimens were made through compression molding process.

Next, micrographs were taken from a section of the test panel of C200 Carbon Task IMP512 BIO, which was made in autoclave.

3.3.1⟶Micrographs press processed samples

A series of micrographs were made on the specimens of the short-fiber materials made in the press. Sections were then cut down and polished so that observation could be conducted under an optical microscope.

The following images show the specimens of the short-fiber materials from which the sections on which the observation was then performed were extracted.

Figure 3.11: DARC21M31-C200 Carbon Task IMP512 BIO

Figure 3.12: DARC21M35-C200 Carbon Task IMP509

Figure 3.13: DARC21M33-C100 Carbon Task IMP512 BIO

Given that the samples considered have a typical omega shape, the air inside them will encounter varying levels of resistance depending on the part of the coupon considered. Therefore, images were acquired across the entire section to assess the presence of potential porosity caused by air trapped during processing.

Let us start by analyzing the micrographs of the C200 Carbon Task IMP512 BIO.

In the following micrograph of the apical part of the sample, it is possible to observe the absence of porosity and a measured average thickness of 1850 µm.

This is the area where it is easiest to apply homogeneous pressure, and therefore where it is simpler to allow the sample to expel air before the complete crosslinking of the resin.

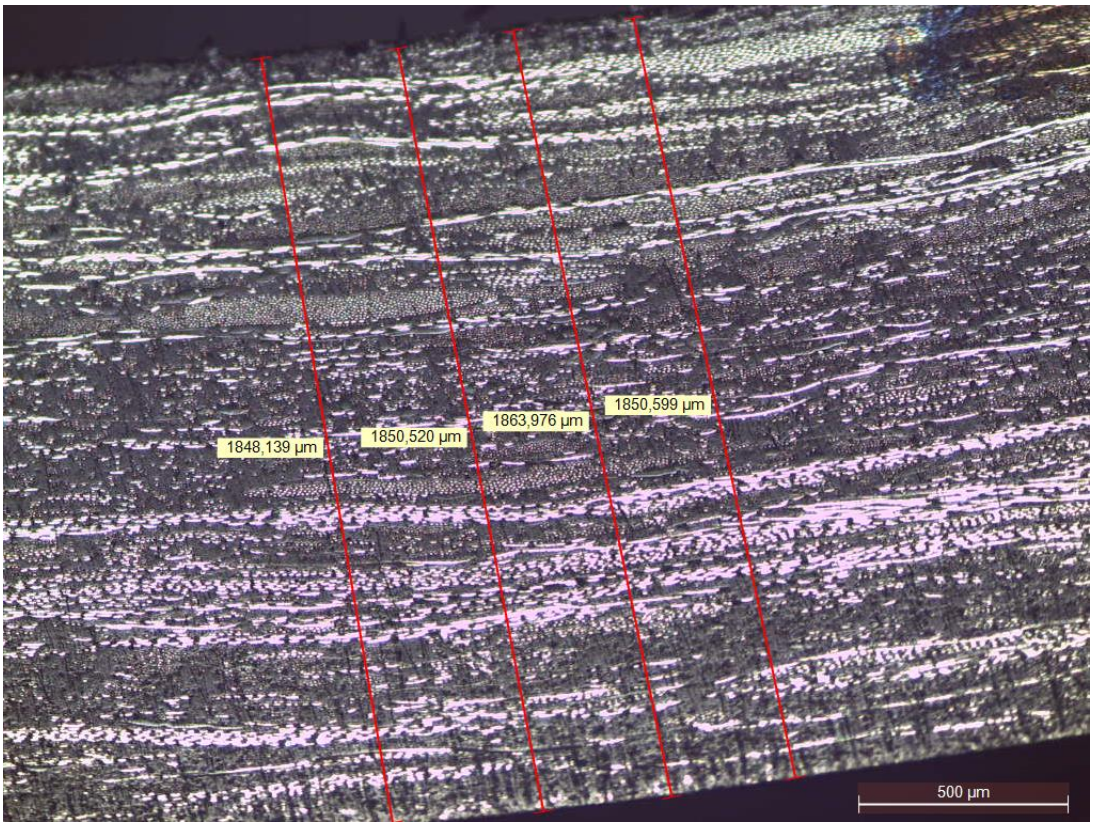

Figure 3.14: Apical part of DARC21M31 sample

Moving on to the observation of the lateral parts of the specimen, it is possible to note the presence of numerous pores.

These areas are, in fact, where the air has the most difficulty being evacuated during the molding process. However, this may not be due to an issue related to the chosen production process, but rather to the critical shape of the specimen being studied.

The size of the pores varies both in length and width.

As a result, the measured thickness of the specimen in these areas is greater than that recorded for the apical part, with a value of 2400 μm.

These pores, due to their location and small size, had only a minimal effect on the energy absorption values measured in the drop tower tests.

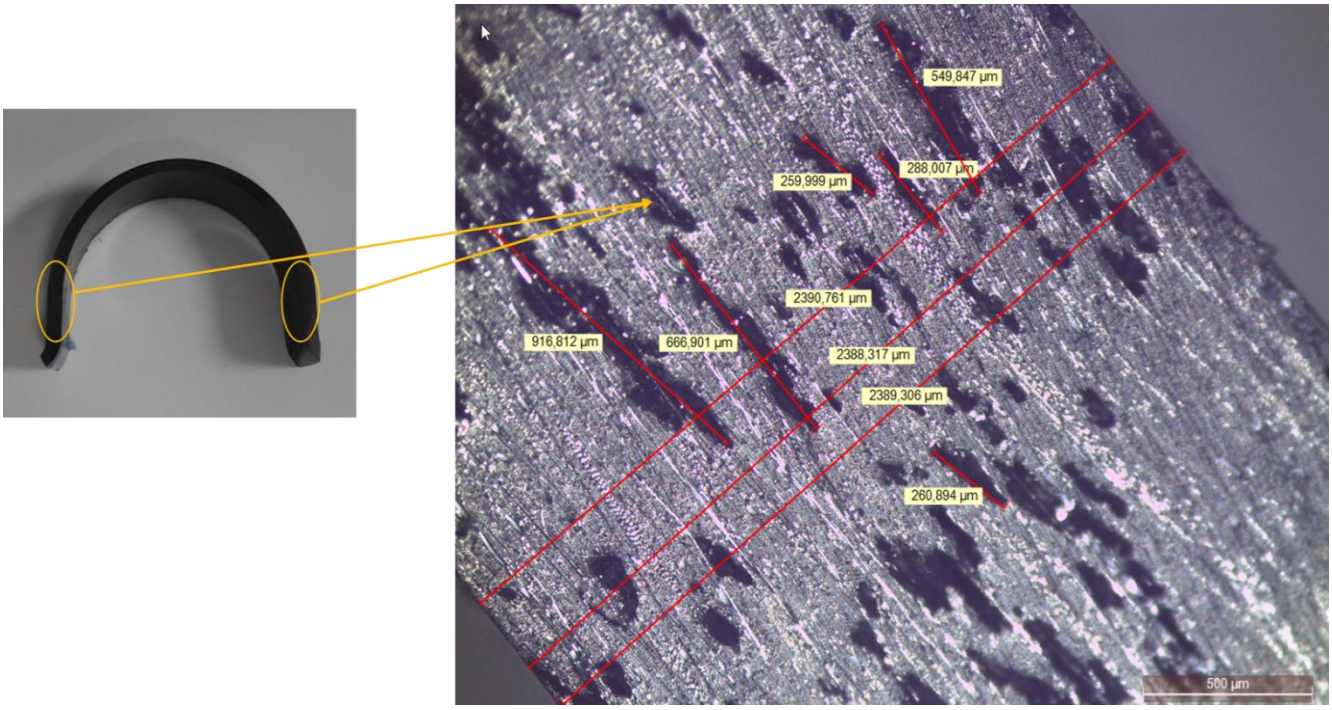

Figure 3.15: Side of DARC21M31 sample

Let us now analyze what was observed for the C200 Carbon Task IMP509 specimen, the short fiber material that was impregnated with a standard resin.

From the following images, it is possible to observe the absence of porosity not only in the apical part, where it was expected due to the ease with which a strong and uniform load can be applied, but also throughout the rest of the specimen. The measured thickness in the apical part, in this case, is approximately 2400 μm

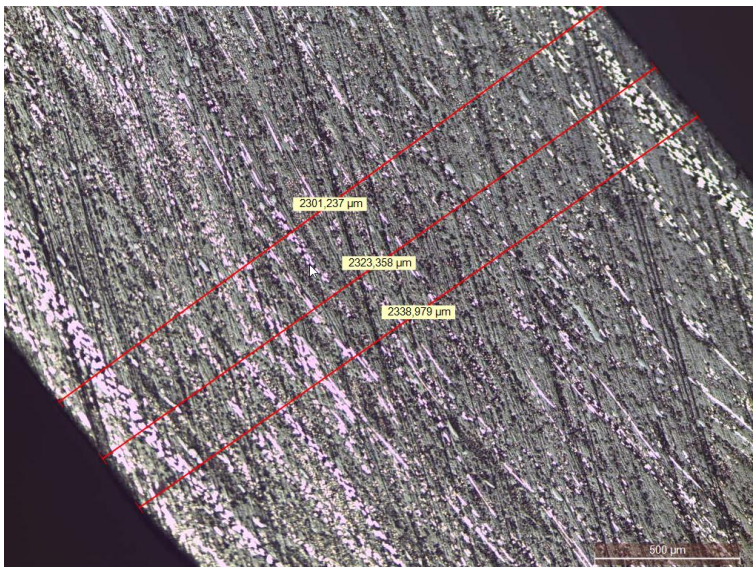

Figure 3.16: Apical part of DARC21M35 sample

In the following image, it is possible to observe how the resin has uniformly wet the fibers without trapping any air bubbles inside

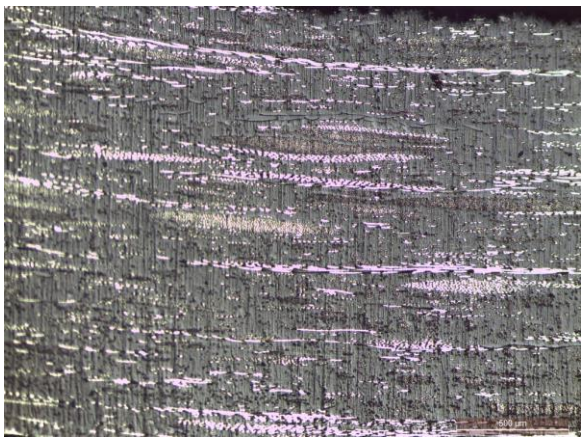

Figure 3.17: Micrograph of DARC21M31 sample

Also in this case, porosities were observed on the sides of the specimen but in much lower quantities than those found in the specimen impregnated with the bio resin.

It is possible, therefore, to say that these are due to the particular shape of the specimen.

Considering the location, the small number and the dimensions, it is possible to affirm that the porosities recorded had a negligible effect on the energy absorption values measured on these specimens.

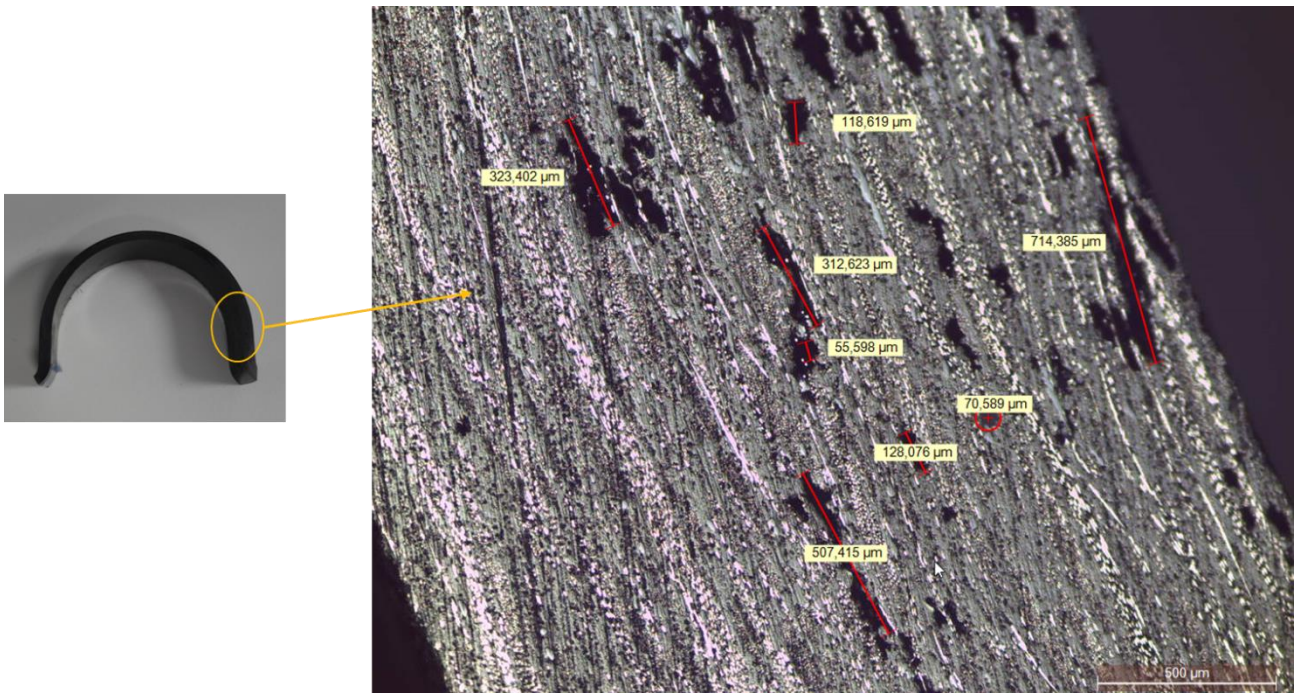

Figure 3.18: Sides of DARC21M35 sample

Let us now move on to the observation of the samples of the short-fiber material impregnated with the resin IMP512 BIO but with a lower areal weight of carbon per square meter, the C100 Carbon Task IMP512 BIO.

From the images acquired with the microscope it is possible to highlight the presence of rare porosities and well dispersed in the section of the sample.

Their size is about 30 µm, therefore, much smaller than the size of those measured in the other two materials studied. The thickness measured in the apical area of the sample, in this case, is 2170 µm.

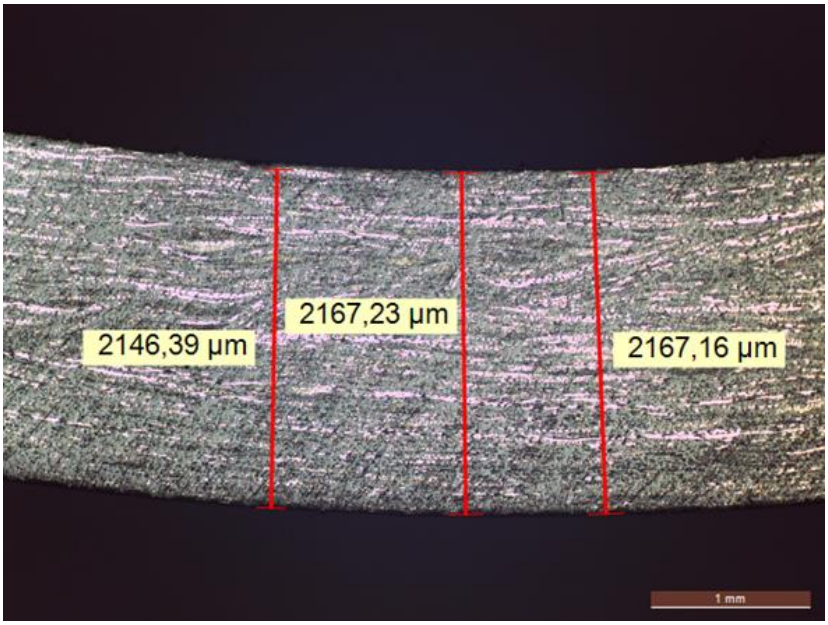

Figure 3.19: Apical part of DARC21M33 sample

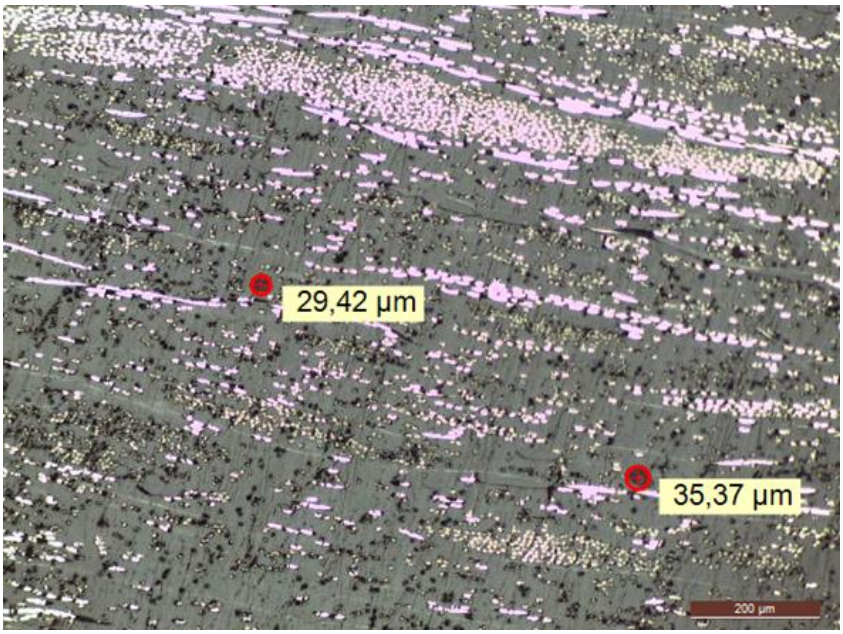

Figure 3.20: Porosities of DARC21M33 sample

As shown in the following micrographs, only a few porosities were found located on the sides of the specimen. Specifically, they were observed only at the outer edge of the specimen on the right side and near the inner surface of the left side.

The sides of the "omega" specimens are in fact, even for materials with a good impregnation capacity, the points where the evacuation of air is more difficult. Even in these areas, the porosities have a much smaller size than those recorded in other materials with a diameter ranging from 60 to 90 μm.

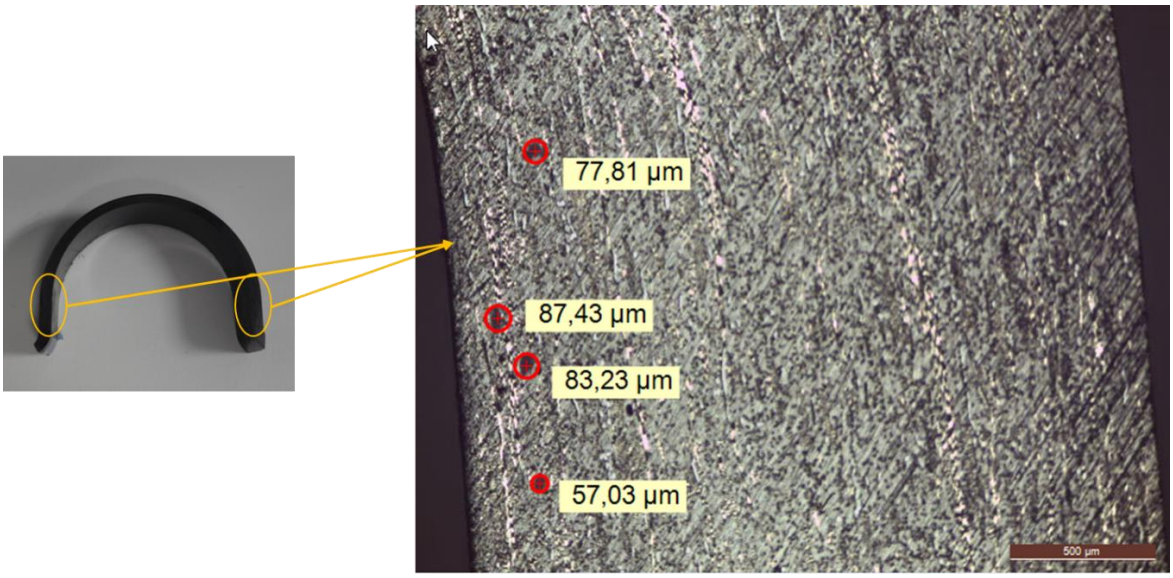

Figure 3.21: Sides of DARC21M33 sample

The rest of the sample was very homogeneous, and no significant porosity was recorded in most of it.

Figure 3.22: Micrograph of DARC21M33 sample

To sum up, we can observe that the C200 Carbon Task IMP512 BIO and the C200 Carbon Task IMP509 have very similar porosities in terms of size and location.

In the C100 Carbon Task IMP512 BIO specimens, however, it was possible to find the presence of porosities that were much lower in number, smaller in dimensions and distributed more homogeneously over the entire section compared to the other two materials studied.

It is therefore possible to say that C100 Carbon Task IMP512 has a better fiber impregnation capacity, for the production of omega-shaped specimens through press process.

It can also be deduced that the use of the BIO version of the resin (IMP512 BIO) compared to the synthetic version (IMP509) does not have a significant influence on the quality of the impregnation of the specimens.

It is, however, noteworthy that with a reduction in the carbon areal weight, the resin is able to better impregnate the carbon fibers, thus obtaining more homogeneous specimens.

3.3.2⟶Autoclave processed sample micrographs

To evaluate the possibility of processing fiber materials also with a different production process, a small test panel of C200 Carbon Task IMP512 BIO was created in autoclave.

The cycle followed was the one suggested by *Angeloni Group* with a duration of 90 minutes, a curing temperature of 135 °C and a pressure of 6 bars.

The thickness of the specimen obtained in the autoclave was then measured and an increase in thickness was found compared to what was measured for the specimens processed in the press.

Figure 3.23: Thickness measuring of autoclave processed panel

The thickness ranges from a value of approximately 1850 μm for the specimens processed by press to a value of 2300 μm for those processed in autoclave.

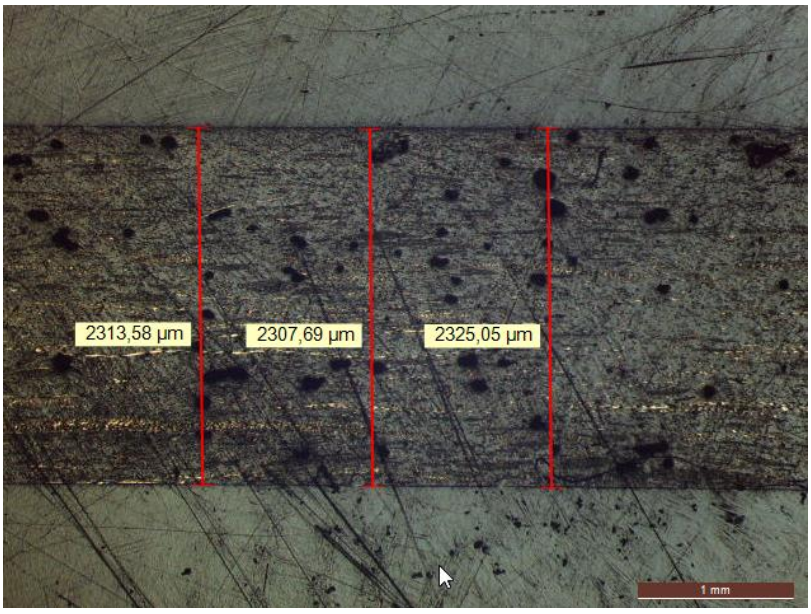

Figure 3.24: Micrograph of autoclave processed panel sample

This non-negligible variation in thickness suggested the presence of porosity in the autoclaved specimens and for this reason, the autoclaved specimen was sectioned and polished and a series of micrographs were made.

As expected from empirical observations, it was possible to observe the presence of numerous porosities both in the 0°C direction with respect to the main direction of the fibers and in the 90°C direction. The porosities are present and distributed uniformly over the entire section and have a size that varies from 40 μm to 90 μm.

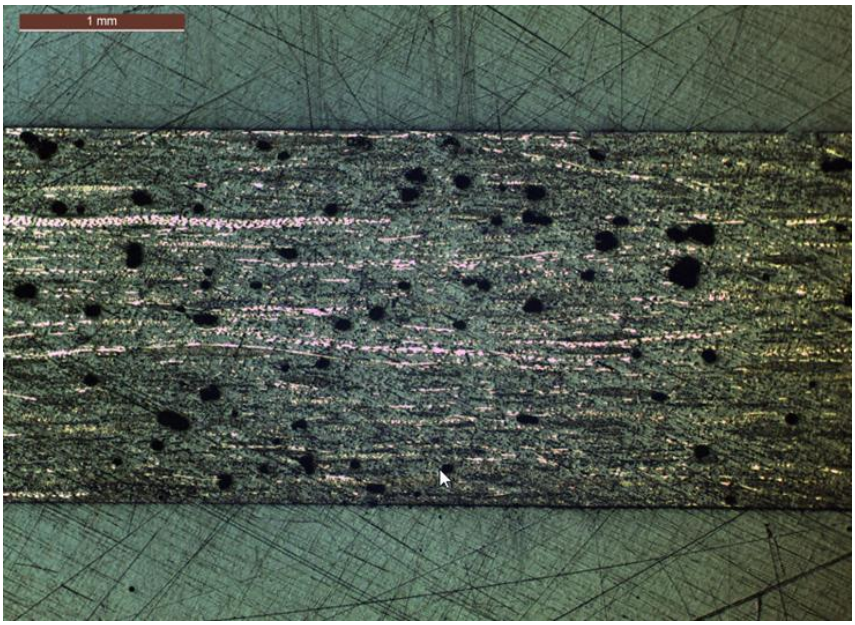

Figure 3.25: Porosities of autoclave processed panel sample

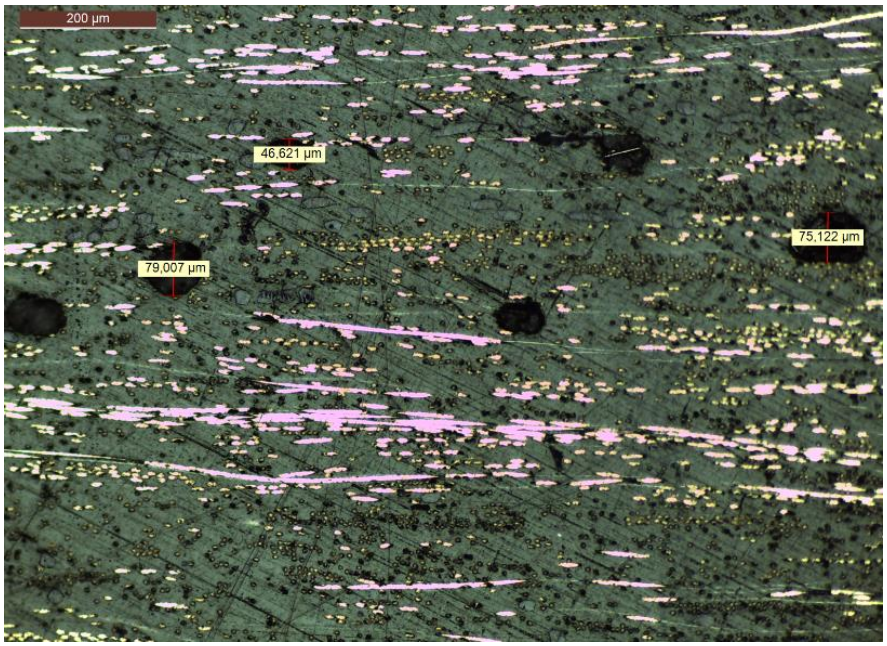

Figure 3.26: Dimension measurement of sample porosities

It is therefore evident that the pressure applied in the autoclave is not sufficient to allow the perfect evacuation of air in short-fiber components even for specimens with a very simple shape such as a flat panel. The consequent presence of porosities reduces the mechanical characteristic of the processed components. In conclusion, the most suitable production process for short-fiber specimens is the press one.

3.4→ Samples final shaping process

After analyzing the molding process of both long fiber specimens and short fiber specimens, let us now analyze the last steps to get to the final shape of our specimens.

Once the shape has been impressed on our coupons in an autoclave or through the molding process in a press, they are passed under the waterjet cutter where, with the help of CAD files, they are given the final shape and the precise measurements required by the regulations of the test for which they were made.

CNC (computer numerical control) waterjet cutting machines have become extremely popular for 2D cutting.

Some of the main advantages of waterjet cutting are the linearity of the cut and the absence of a heat-affected zone.

To understand why this technique offers such advantages, let us take a quick look at how waterjet cutting works.

Unlike a thermal cutting process, the waterjet process is a mechanical sawing process. The effect is similar to that of a band saw, which is a thin sheet of metal with sharp teeth that pulls through the material.

Similarly, the water jet cutting process uses a thin stream of water with sharp pieces of rock that are pushed through the material.

The pieces of rock, or abrasive, are usually made of crushed garnet.

Garnet is made from a relatively hard rock and is also commonly used in sandpaper. Each grain of abrasive that passes through the system will wear away some of the material.

However, pouring abrasive jets of water onto a component is not enough to cut it. What makes the process work is the speed at which the abrasive hits the sheet metal.

The momentum of an object is equal to its mass multiplied by its velocity. A grain of abrasive has little mass, so to have an effect, it must have a high velocity to accelerate the abrasive fast enough to cut through hard materials.

Water is pressurized to "ultra-high pressure" and then released through a small orifice.

Typical water jet cutting pressure is between 50.000 and 60.000 PSI (per square inch). Many newer systems are pressurized up to 90.000 PSI.

Water at this pressure is then released through a small orifice machined from diamond or sapphire, usually in the range of 5 to 15 thousandths of an inch in diameter. The resulting water flow is supersonic, meaning it is faster than the speed of sound.

The formation of the water flow from the jewelry orifice and the mixing of the abrasive into the flow occurs inside a waterjet cutting head.

To get the abrasive into the water, the flow passes through a funnel-shaped chamber, where the abrasive is picked up by the water flow and accelerated. The water flow, now carrying abrasive particles, then passes through a concentration tube, or nozzle, with which all of the abrasive is completely inserted into the water flow and moved in the same direction.

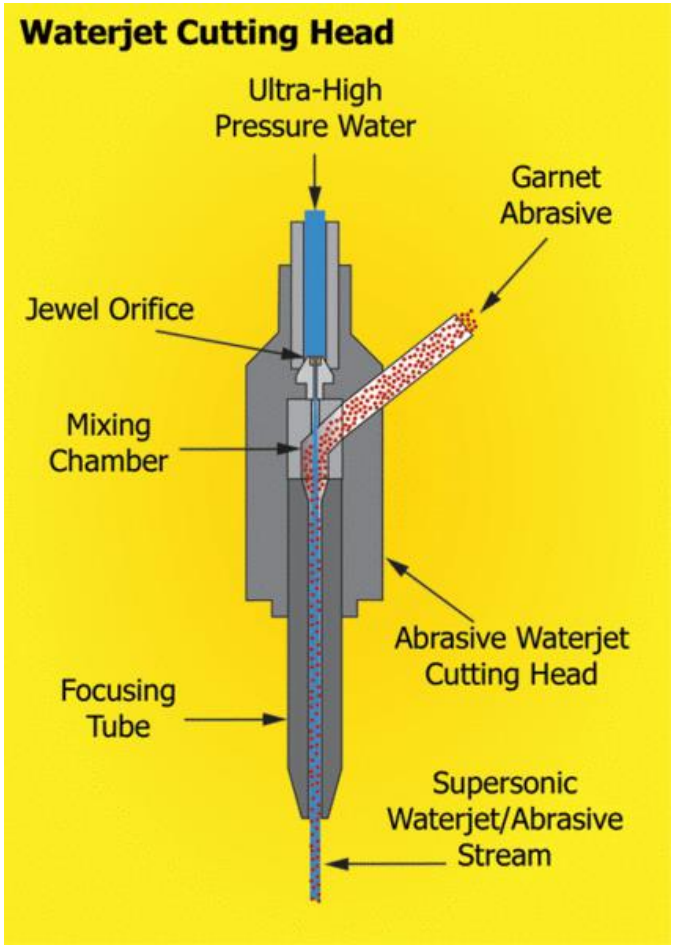

Figure 3.27: Waterjet cutting head

As it exits the concentration tube, the supersonic flow of water and abrasive will rapidly consume any material it passes through. The water flow, once it has passed through the component, is collected in a water-filled tank beneath the part.

Since each abrasive particle only removes a small amount of material by erosion, little heat is generated. Furthermore, the heat that is produced is quickly dissipated by the water flow before it has time to heat the surrounding material.

As a result, the cut does not produce a heat-affected zone. This technology can therefore be thought of as a cold cutting process.

Not only do these fast-moving abrasive particles cut without forming a heat-affected zone, but the momentum of the water flow keeps them moving in a straight line long after they have exited the concentration tube, thus producing an extremely straight and precise cutting edge on a variety of materials. [53][54]

Figure 3.28: Example of waterjet robotic arm

Waterjet cutting, therefore, is particularly suitable for cutting materials with high mechanical properties such as composite materials. This technology allows the properties of the cut components to be maintained unchanged; a very important condition for the creation of specimens on which a study of the mechanical properties will be performed.

Water cutting still has great precision and flexibility, thus allowing the creation of very complex geometries and it is a very rapid process.

Once it has been made sure that the piece to be cut is well anchored and it has been chosen an appropriate size of the garnet to avoid delamination, water-jet cutting is an excellent technology for the cutting high-performance composite materials.

3.5→Sample tabbing

At the end of the preparation process of the specimens used for the tests we have the tabbing phase. This is a very important step especially in the production of composite material specimens.

In order to correctly perform the tensile and compression tests, the specimens must be equipped with tabs at their ends. This is to allow the grips of the tensile machine to correctly grasp the specimen during the test.

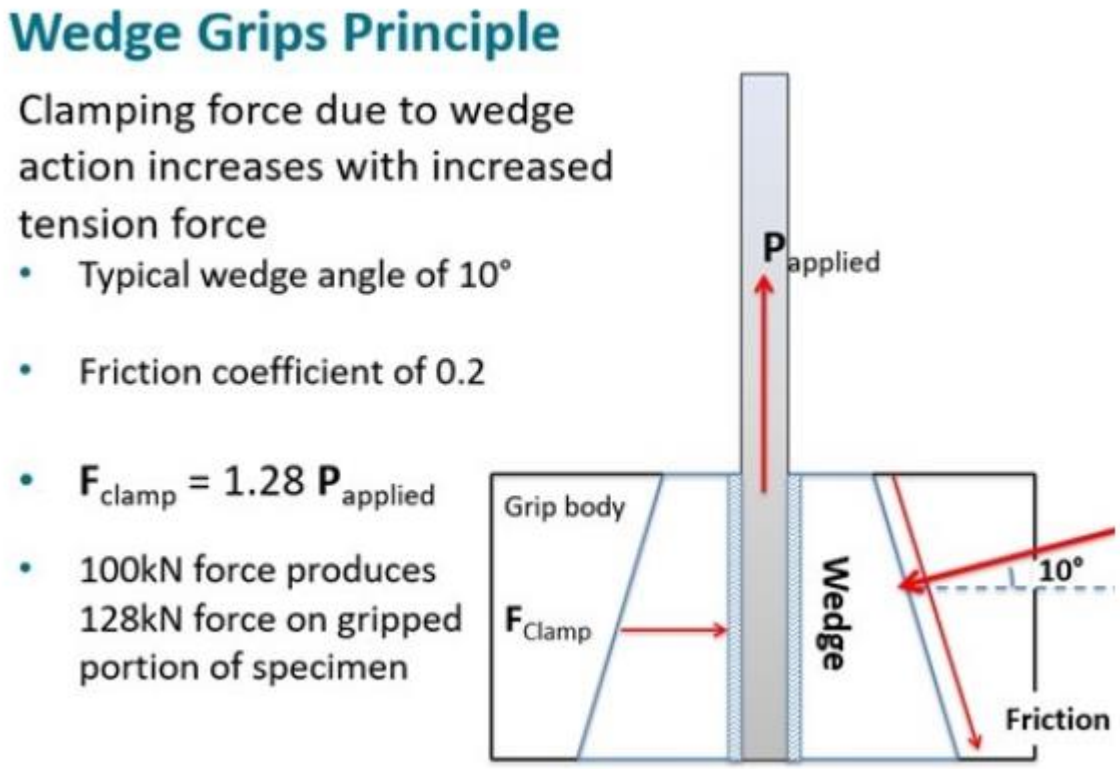

Figure 3.29: Wedge Grips principle

Assuming, in fact, to use wedge grips with a typical angle of 10° and considering a friction coefficient between specimens and wedges of 0,2, the clamping force applied to an un-tabbed specimen will be approximately 28% higher than the tensile force applied. This causes a significant concentration of stress on the edge of the grips that affects the correct performance of the tests.

To overcome this problem and promote failure in the calibrated central section of the specimen, tensile specimens are usually dog-bone shaped.

However, this is not always possible for composite materials, so an alternative way to alleviate the concentration of stresses through the use of tabs is needed.

Further consideration can be made regarding the damage that gripping serrations cause to the surface of the composite. They are usually aggressive enough to break the external resin-rich surface and damage the underlying load-bearing fibers. It is clear that the stress concentration must be limited, and the surface must be protected.[58]

The choice of material for the end tabs can affect both the measured properties and ease of use. The material chosen should be as passive as possible, without losing the strength needed to transfer the load from the grippers to the specimen section. It should also be strong enough to withstand the harsh tearing action of the grippers.

The most commonly used material for the tabs is a composite material reinforced or by carbon or by glass fibers, ideally with an orientation of +/-45° to the direction of load application. The material bonds easily to the composite panel and does not peel off during processing. The relatively low stiffness of the fibers in this orientation helps to minimize stress concentrations at the end of the tab and the tab is soft enough to allow the handles to bite into the surface of the tab.

As for the choice of adhesive to bond the tabs to the specimen, since the tensile load is introduced into the specimen through shear, it is important to choose an adhesive that has an appropriately high shear strength. The old CRAG standard specified that the adhesive used should have a shear strength greater than 30MPa. Beyond that, the choice of adhesive depends on the user and the *Tg* of the material being tested. Film adhesives are generally easier to use than paste adhesives and provide a controlled bond line thickness but require high temperature and pressure to cure. This is achieved with a heat press or vacuum bagging in a curing oven.[57][58]

A final consideration when it comes to tab material is the design of the tab itself. Generally, the tab should be the same width as the test specimen and for tensile testing should be at least 40 mm and up to 90 mm long.

Figure 3.30: Tabs geometry

The length you choose within that range depends entirely on the length of the wedges in the machine handles you are using. While ISO 527-4/5 states categorically that a 90°-tab termination angle should be used, ASTM D3039 is more nuanced in its approach to this. [55]

This is due to research showing that using supports with a tapered termination angle of between 10 and 15° can show an increase in tensile strength of up to 18%. This is because tapering the tabs reduces stress concentration at their terminal area and therefore promotes failure within the gauge section. However, angles less than 10° are not recommended, as this will cause the tabs to peel off during testing.[58]

The realized coupons were made according to ISO 527-4/5 standard.

Conversely, when performing compression tests, it is recommended that the supports termination area not be tapered. The reason is that the strain potential has a greater impact on the results than the stress concentration caused by the tab termination region. Therefore, we compromise on the compression design, in order to minimize the strain effects on the results. [56]

Finally, the thickness of both the adhesive and the tabbing material has an effect on the test results. Both materials act as a cushioning layer, with the closer to the material, the adhesive having the greater effect. As a general rule, a tab thickness of 1,5-2 mm and a bond line thickness of 0,5-1,3 mm generally provides optimal results, while avoiding the additional cost of using more material. [58]

Once the tabbing stage is complete, the specimens are ready for testing.

4.→Data Analysis

Bio composite materials are still new materials compared to more standard ones such as metals. They have attracted interest and studies only in recent years. So, it is of fundamental importance to undertake an in-depth analysis in order to evaluate possible effective applications.

In engineering applications and in automotive one, excellent mechanical performance is required to withstand the stress states of compression, traction, bending and impact, to which the structures are continuously subjected.

It is important to evaluate the mechanical characteristics of a material in order to understand its uses and make a comparison with the performances of the most well-known standard composites.

The focus of this work, therefore, will be the mechanical characterization of the materials supplied by Angeloni Group.

Whitin particular we choose two long-fiber materilas, both impregnated with the same IMP512 BIO resin, but reinforced with different fibers (C370 MR60 24K IMP512 38% BIO, and C630 TR50 12K IMP512 34% BIO).

It will therefore be possible to compare the data obtained for these two materials with the mechanical data of already characterized composite materials with the same reinforcement fibers but impregnated with a standard resin. In addition, a comparison of the behavior of the resin with the two types of fiber will also be possible.

As for the short fiber materials, three materials were analyzed, two characterized by the same reinforcement areal weight per square meter but impregnated one with the bio resin and the other with the standard resin (C200 Carbon Task IMP512 BIO and C200 Carbon Task IMP509) and a third material that was impregnated with the bio resin but with a different carbon areal weight per square meter (C100 Carbon Task IMP512 BIO).

It will therefore be possible, in addition to evaluating the performances of these innovative short fiber materials, and to study the behavior of the bio resin with two different carbon weights, also to make a comparison between the performances of the bio resin and those of the standard resin.

4.1→Long fiber materials

The two studied long-fiber materials are the C370 MR60 24K IMP512 38% BIO and the C630 TR50 12K IMP512 34% BIO.

The C370 MR60 24K IMP512 38% BIO is a long-fiber material that has an areal weight of 370 grams of dry fibers per square meter. The fibers with which it is reinforced are MR60, fibers characterized by high tensile strength and an average tensile modulus value, and they are collected in 24K carbon fiber threads. This material is impregnated with the IMP512 Bio resin (15% bio-origin) with a percentage of resin of 34% in the prepreg material.

The C630 TR50 12K IMP512 34% BIO is a long-fiber material with an areal weight of 630 grams per square meter. The fibers with which it is reinforced are TR50, fibers characterized by a tensile modulus value slightly lower than the MR60 and with a very similar tensile elastic modulus. They are grouped in filaments of 12K carbon fibers each. This material is also impregnated with the IMP512 BIO resin, with a percentage of 34% in the pre-impregnated material.

During the creation of the first set of tensile tests, it was possible to observe the presence of misalignment of the fibers of the fabric of both composite materials studied. The misalignment, as can be seen from the following photo, varies randomly across the entire extension of the fabric causing a strong difference between the data obtained at 0° and 90°. The data obtained in the two directions should be very close since the fabric is symmetrical.

Figure 4.1: Fiber misalignment of C630 TR50 12K IMP512 BIO

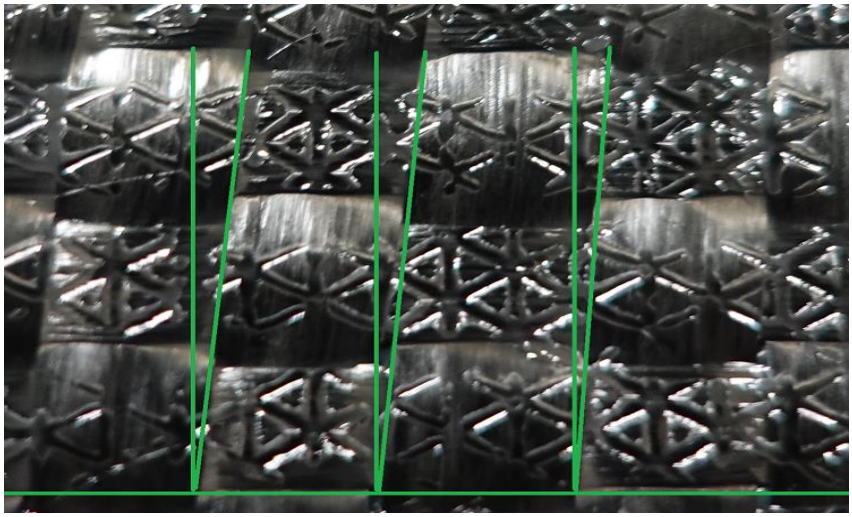

Figure 4.2: Fiber misalignment C370 MR60 24K IMP512 38% BIO

For this reason, a second set of tensile tests was created by selecting, during the plies cutting phase, the parts of the fabric where the fibers misalignment was less evident.

It was therefore possible to reduce the effect of the misalignment but not to eliminate it completely since it was present throughout the roll and distributed in an uneven manner.

4.1.1⟶Mechanical characterization of C370 MR60 24K IMP512 38% BIO

For the mechanical characterization of the C370 MR60 24K IMP512 38% BIO, a series of tensile tests were performed at 0°, 90° and 45° with respect to the main direction of the material fibers.

A series of compression tests were then carried out at 0° and 90° as well as a series of three-point bending tests.

To evaluate the performance of the fiber coupling to the matrix, a series of interlaminar shear tests were realized.

To conclude the mechanical characterization, a series of energy absorption tests were performed in order to evaluate the material performance in case of impact.

4.1.1.1⟶ Tensile tests of C370 MR60 24K IMP512 38% BIO

The tensile tests at 0° and 90° were carried out according to the international standard ASTM D3039, while the tensile tests at 45° were carried out according to the international standard ASTM D3518.

The tensile specimens have a rectangular shape, a standard width of 25 mm, and a free length of 148 mm. They were made by laminating 5 layers of pre-impregnated composite material with an expected total thickness of 1,96 mm. The actual average thickness obtained is 1,95 mm, thus obtaining specimens with an equivalent resin percentage of 37,7%, very close to the 38% declared by the supplier company. The material, therefore, does not suffer a large loss of resin during processing.

Figure 4.3: C370 MR60 24K IMP512 38% BIO tensile samples

Six specimens were tested for each direction and by measuring the load values and the corresponding elongation the stress-strain curve was obtained. The maximum force value for which the specimen reaches failure (tensile strength), and the corresponding deformation value were thus obtained.

Below it is possible to see the curves and values obtained with the relative standard deviations in different directions.

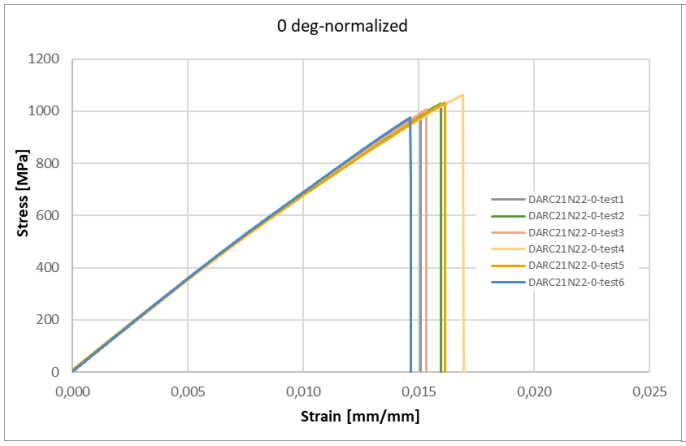

Figure 4.4: C370 MR60 IMP512 0° tensile test stress-strain curves

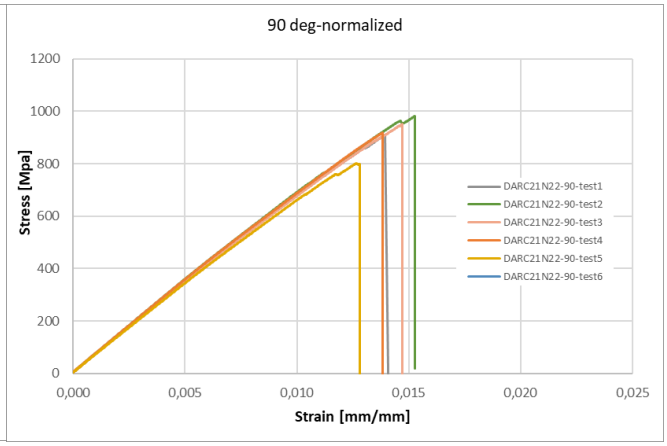

Figure 4.5: C370 MR60 IMP512 90° tensile test stress-strain curves

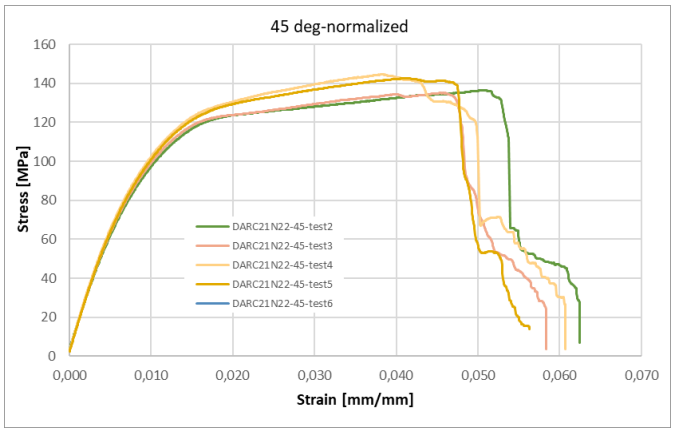

Figure 4.6: C370 MR60 IMP512 45° tensile test stress-strain curves

Direction	Normalized Tensile strength [MPa]		Normalized Elastic Modulus [GPa]	
	Value	Std. deviation	Value	Std. deviation
0°	1015,3	32,5	70,6	0,5
90°	912,6	69,0	70,1	1,2
45°	140,9	4,9	12,7	0,5

Table 4.1: C370 MR60 IMP512 tensile test results

The material has tensile strength values coherent with those of composite materials reinforced with the same fiber but impregnated by a standard matrix. It is, therefore, possible to assert that the use of bio resin does not have a significant effect on the tensile performance of the material studied.

4.1.1.2⟶Compression tests of C370 MR60 24K IMP512 38% BIO

The tensile tests were carried out according to the Boeing modified ASTM695 (SACMA SRM1R-94) standard. Fourteen specimens were tested for each direction (0° and 90° with respect to the main direction of the fibers of the composite material studied). This is the internal standard in order to have a good statistic for this type of test that could be strongly affected by coupons geometry.

The specimens have a standard size of 13 mm in width. For their realization, 6 plies were laminated with an expected thickness of 2,35 mm. The average thickness value measured is, however, 2,43 mm. The equivalent percentage of resin recorded in the specimens will be 39,6% and it is therefore slightly higher than the theoretical one.

Also in this case, the specimens were subjected to an increasing load until they reached breaking point, in the meanwhile the stress-strain curve was calculated.

The values, the corresponding standard deviations and the curves obtained in the different directions can be observed in the following images.

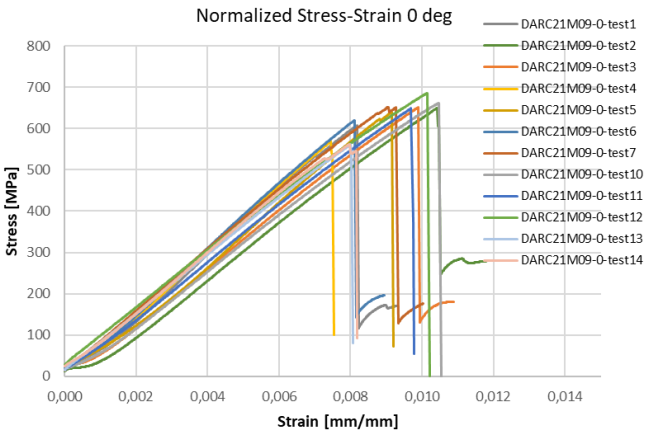

Figure 4.7: C370 MR60 IMP512 0° compression test stress-strain curves

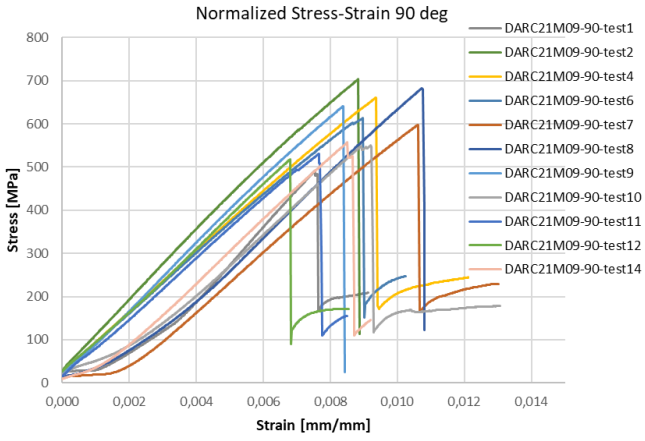

Figure 4.8: C370 MR60 IMP512 90° compression test stress-strain curves

Direction	Normalized Compression strength [MPa]	
	Value	Std. deviation
0°	625,9	42,1
90°	595,0	71,1

Table 4.2: C370 MR60 IMP512 compression test results

Even for the compression performances, the values obtained follow the trends of composite materials of the same category but impregnated with a standard resin and it is therefore possible to affirm that, also in this case, the effect of the use of the bio resin on the mechanical performances of the studied material does not have a significant effect.

4.1.1.3⟶Three point bending tests of C370 MR60 24K IMP512 38% BIO

The three-point bending tests were carried out according to the ASTM D 790 standard with a span length of 96 mm. The standard width of the specimens is 15 mm and for their production 6 layers were laminated with an expected thickness of 1,96 mm. The measured thickness value is 1,99 mm with an equivalent resin percentage of 39%. In this case the specimen was positioned in the machine where it was inserted between two anvils or parallel supports and with a central beam an increasing load was applied to it, thus managing to induce in the specimen some areas with a state of compressive stress and others with a state of tensile stress. The load was increased until the specimen broke, thus tracing the stress-strain curve and measuring the maximum bending load that our specimen can resist before breaking.

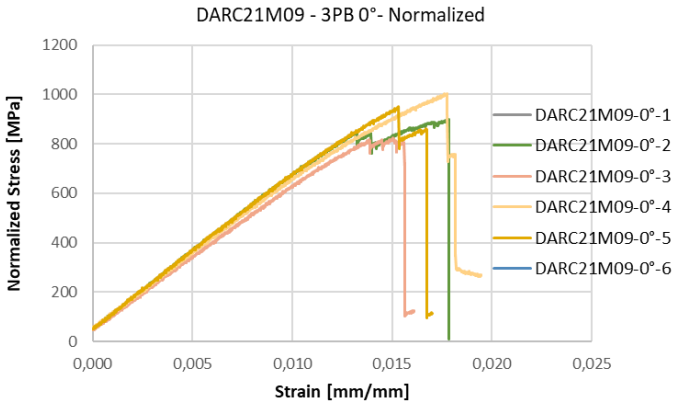

Figure 4.9: C370 MR60 IMP512 0° flexural test stress-strain curves

Material	Normalized Flexural strength [MPa]		Normalized Elastic Modulus [GPa]	
	Value	Std. deviation	Value	Std. deviation
C370 MR60 IMP512 38%	918,7	66,1	61,6	2,6

Table 4.3: C370 MR60 IMP512 0° flexural test results

The specimens all failed due to compressive stress; the material is therefore more sensitive to the state of compressive stress than to tensile stress.

As for the values obtained in this case, they are also in line with what was expected and also in this case the use of the bio resin does not have a significant effect on the mechanical properties of the material.

4.1.1.4⟶Interlaminar shear tests of C370 MR60 24K IMP512 38% BIO

A very important evaluation regarding bio-based composite materials is that of interlaminar shear stress. This test, in fact, provides information on the material's interlaminar properties and therefore also gives us indications on the quality of the coupling between fibers and matrix. The test was repeated 6 times, and the ASTM D 2344 standard was followed for its implementation. Below we can see the measured stress-strain curve and the average value of maximum interlaminar shear stress obtained with the corresponding standard deviation.

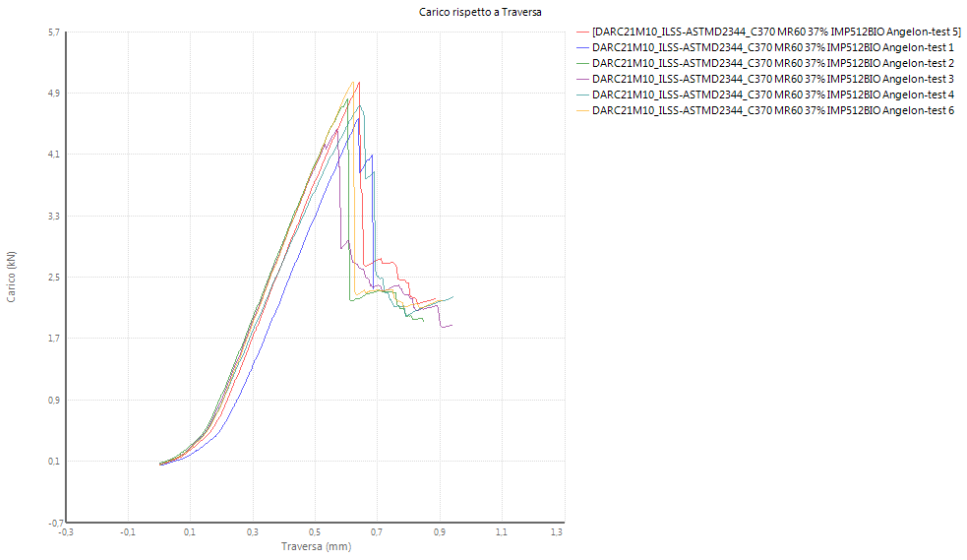

Figure 4.10: C370 MR60 IMP512 ILSS-test stress-crosshead displacement curves

Material	Normalized breaking stress [MPa]	
	Value	Std. deviation
C370 MR60 IMP512 38%	54,8	2,4

Table 4.4: C370 MR60 IMP512 ILSS-test results

4.1.1.5⟶Energy absorption tests of C370 MR60 24K IMP512 38% BIO

Let us now move on to the analysis of the energy absorption tests, these were carried out using a different machine than the one used for the tests described above.

The energy absorption tests were carried out in a drop tower. An impacting mass was dropped onto the specimens of a typical "omega" shape and the acceleration and force of the impact were measured.

Using this data, the energy absorbed by the specimen during the impact was measured in two different ways depending on the type of breakage encountered (pulverization or petal).

The specimens were made in a press with the lamination of 5 plies, obtaining an average real thickness of 2,07 mm and with an equivalent resin percentage of 40,4%.

As can be seen from the images of the tested specimens, the material showed a petal-type failure.

Figure 4.11: Petal failure of C370 MR60 IMP512's omega samples

The energy absorption was then obtained by considering the difference between the initial height of the specimen and the final height after the impact.

In the following graph we can observe the acceleration measured as a function of the test execution time.

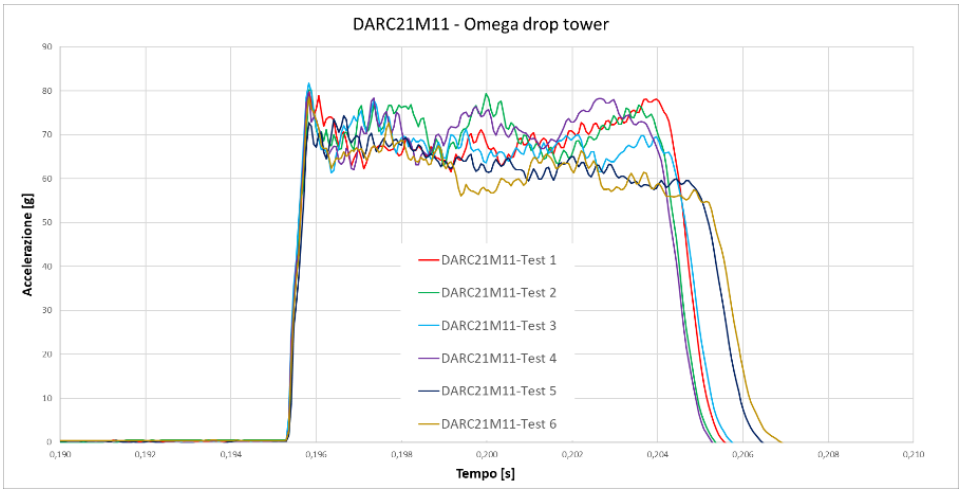

Figure 4.12: Acceleration curves of C370 MR60 IMP512's drop tower test

Material	SEA [J/g]	
	Value	Std. Deviation
C370 MR60 IMP512 38%	65,6	2,3

Table 4.5: SEA values of C370 MR60 IMP512

The energy absorption values are very good, compared to the average values of similar materials.

4.1.1.6⟶C370 MR60 IMP512 38% BIO test overview

It is concluded the analysis of the behavior of the C370 MR60 IMP512 38% BIO with a summary table of the tests performed and the values obtained.

Property	Standard	Set 1	Set 1 NORM	Set 2	Set 2 NORM
1) Tensile properties					
Tensile strength σ 0° [MPa]	ASTM D 3039	**1065,6**	**1040,0**	**980,6**	**1015,3**
Tensile modulus E 0° [GPa]		**71,6**	**69,9**	**68,2**	**70,6**
Tensile strength σ 90° [MPa]		**816,8**	**820,9**	**883,9**	**912,6**
Tensile modulus E 90° [GPa]		**69,7**	**70,1**	**67,9**	**70,1**
Tensile strength τ 45° [MPa]	ASTM D 3518	**69,8**	**69,8**	**68**	**70**
Tensile modulus G 45° [GPa]		**3,4**	**3,4**	**3,5**	**3,3**
2) Flexural properties					
3PB strength σ 0° [MPa]	ASTM D 790	**887,5**	**918,7**	-	-
3PB modulus E 0° [GPa]		**59,58**	**61,63**	-	-
3) Compressive properties					
Compressive strength σ 0° [MPa]	Boeing modified ASTM695 (SACMA SRM 1R-94)	**605,9**	**625,9**	-	-
Compressive strength σ 90° [MPa]		**576,4**	**595,0**	-	-
4) ILSS					
ILSS [MPa]	-	**54,78**	-	-	-
5) Specific energy absorption					
SEA measured [J/g]	-	-	-	-	-
SEA calculated [J/g]		**65,6**	-	-	-

Table 4.6: C370MR60IMP512 mechanical characterization overview

In the table it is possible to find the tensile data relating to the first set of tensile tests in which the problem of fibers misalignment has not yet been corrected and the data of the second set carried out on the specimens for which an attempt was made to reduce its effect as much as possible.

4.1.2⟶Mechanical characterization of C630 TR50 12K IMP512 34% BIO

The same tests presented in the previews paragraphs were also realized for the mechanical characterization of the C630 TR50 12 K IMP512 34% BIO.

The tensile tests at 0°, 90° and 45°, the compression tests at 0° and 90°, the three-point bending tests, the interlaminar shear tests and the energy absorption tests in a drop tower were therefore performed.

4.1.2.1⟶Tensile tests of C630 TR50 12K IMP512 34% BIO

A series of tensile tests were performed at 0°, 90° and 45° with respect to the main direction of the fibers, following the same regulations indicated for the other long fiber composite material. The tensile specimens also in this case have a standard length of 25 mm and a free length of 150 mm. With the aim of reaching a thickness of 2,46 mm, 4 layers were laminated.

However, specimens were obtained with an average thickness of 2,36 mm and with an equivalent percentage of resin of 31,7%, much lower than the declared value of 34%. This can be caused by the loss of a large amount of resin during the production process.

The test was repeated 6 times for each fiber direction considered and the values obtained with their standard deviations and the related stress-strain graphs can be observed in the following images.

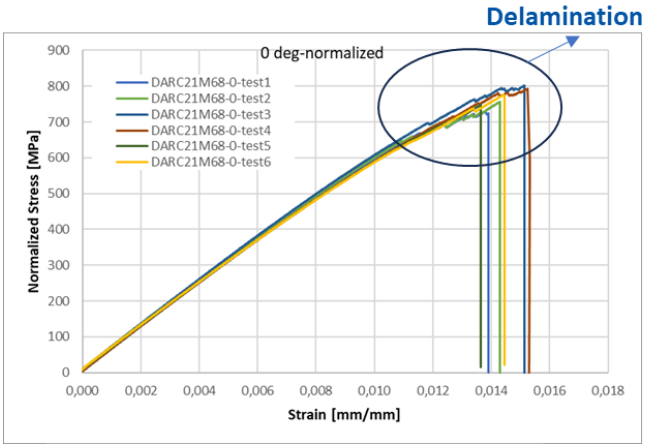

Figure 4.13: C630 TR50 IMP512 0° tensile test stress-strain curves

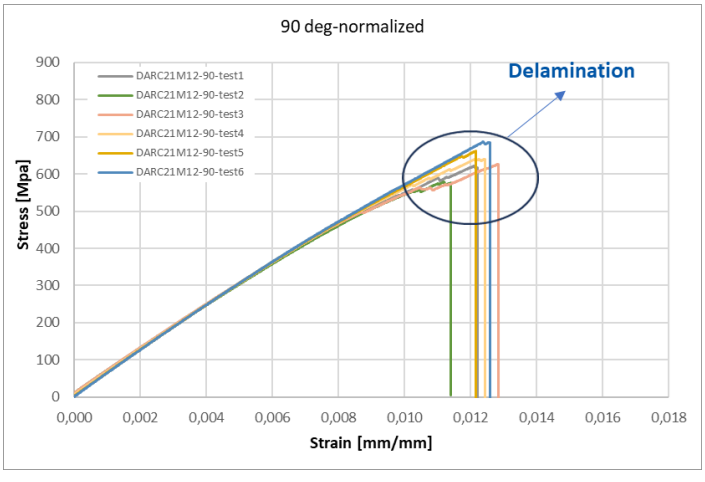

Figure 4.14: C630 TR50 IMP512 90° tensile test stress-strain curves

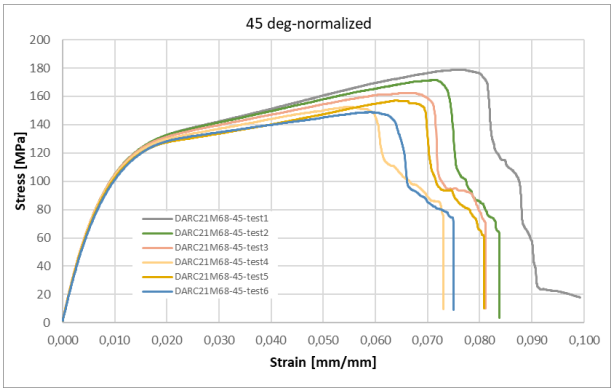

Figure 4.15: C630 TR50 IMP512 45° tensile test stress-strain curves

Direction	Normalized Tensile strength [MPa]		Normalized Elastic Modulus [GPa]	
	Value	Std. deviation	Value	Std. deviation
0°	767,3	27,5	61,8	0,9
90°	680,8	22,0	63,8	0,9
45°	161,8	11,5	14,1	0,3

Table 4.7: C630 TR50 IMP512 tensile tests results

From the apical part of the stress-strain curves of the 0° and 90° tractions it was possible to observe the effect of the delamination of the specimen before reaching the maximum stress that the material could sustain.

Figure 4.16: C630 TR50 IMP512 delaminated tensile sample

The presence of delamination seen through the curves and from the first empirical observation was then checked at the optical microscope.

To verify the type of delamination present in the specimen, some micrographs of one of the tested specimens were thus made.

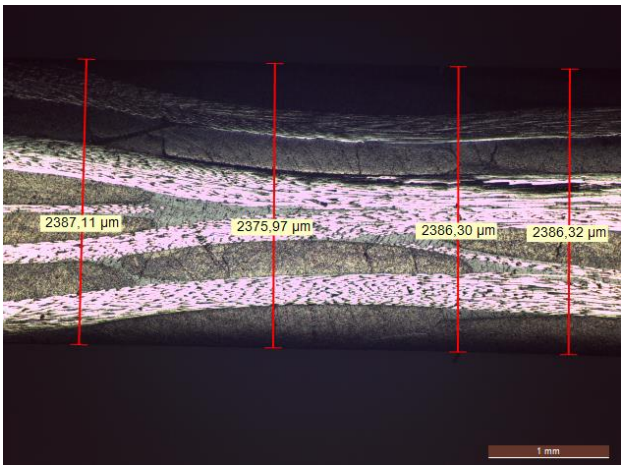

Figure 4.17: C630 TR50 IMP512 micrograph

The thickness of the sample is uniform, and the material has resin channels between the plies. Overall, the material is well impregnated, and no dry fibers were observed.

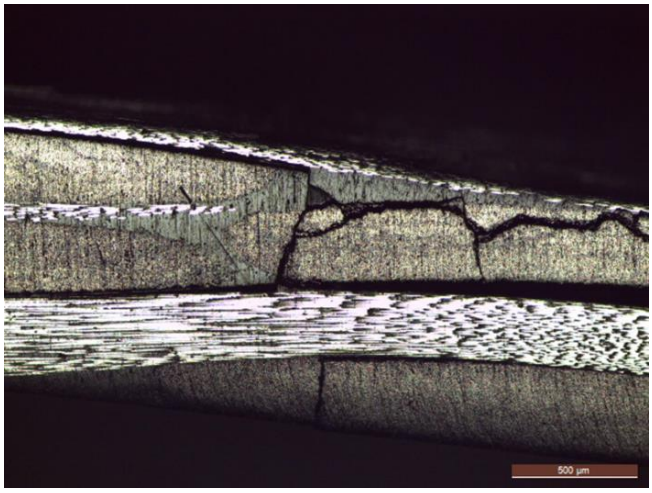

Figure 4.18: C630 TR50 IMP512's interlayer cracks

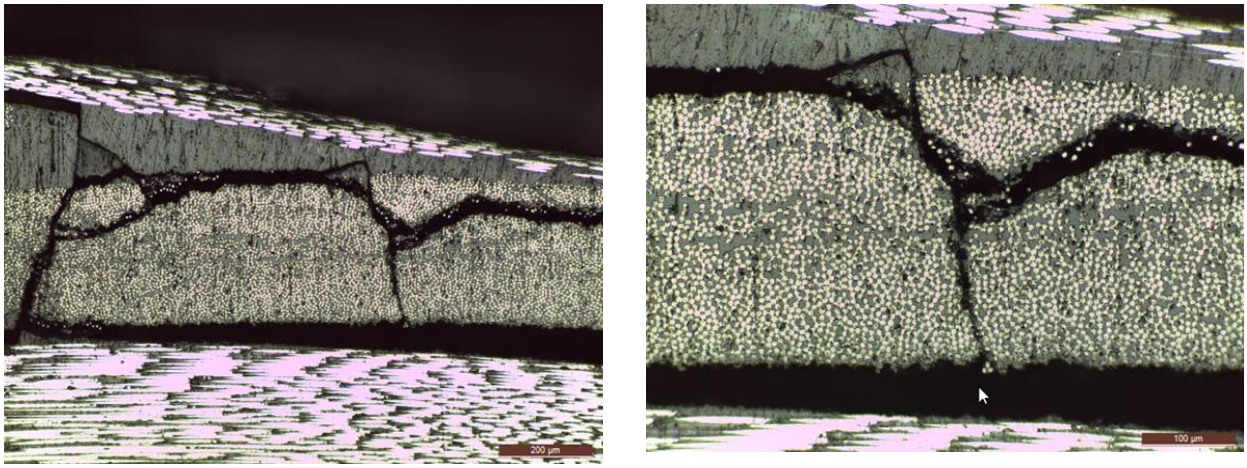

Figure 4.19: C630 TR50 IMP512's intralayer cracks

It was possible to observe with different degrees of magnification both cracks between the plies and cracks that propagated through the individual layers.

This phenomenon could be caused either by the misalignment of the fibers that were noticed during the skin cutting phase or more probably it could be caused by the low percentage of resin present in the composition of the material (31,4% in the actual composition of the processed sample) compared to the nominal value indicated by the supplier of 34%.

The 34% could be the minimum value of resin in the studied material, beyond which the material cannot perform at its maximum potential due to not complete impregnation and load distribution between the fibers.

This value, in fact, is low compared to the resin percentage values that are usually found in long-fiber composite materials.

The low percentage of resin could not allow the perfect coupling between matrix and fibers causing damage before reaching the maximum stress.

4.1.2.2⟶Compression tests of C630 TR50 12K IMP512 34% BIO

Let us now describe the behavior of the material under compression. Also in this case, a series of 14 tests were carried out both at 0° and at 90° with respect to the main direction of the fibers. The same standard that was used for the C370 MR60 24K IMP512 38% BIO was followed.

The samples have a standard length of 13 mm and for their realization 5 layers were laminated to reach a nominal thickness of 3,08 mm.

The value of the real thickness measured is however lower than the nominal one and it is 2,91 mm, with an equivalent percentage of resin of 31,1%.

For these samples it is therefore possible to record a significant reduction in resin during the processing phase of the material.

Below we find the curves and values obtained during the compression tests.

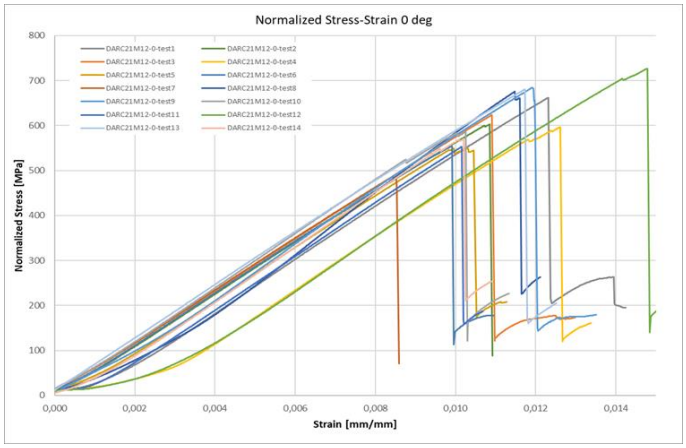

Figure 4.20: C630 TR50 IMP512 0° compression test stress-strain curves

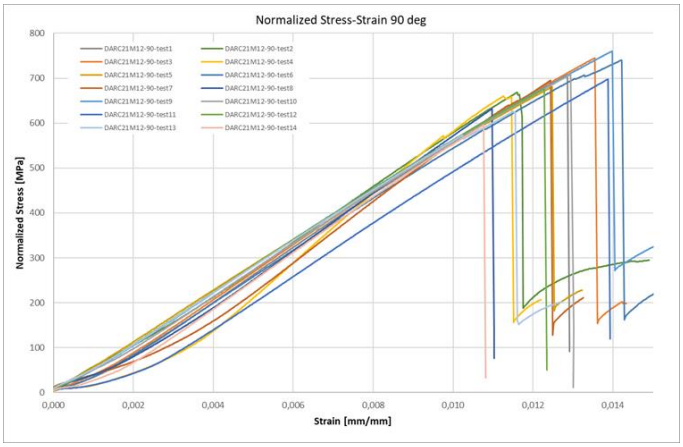

Figure 4.21: C630 TR50 IMP512 90° compression test stress-strain curves

Direction	Normalized Compression strength [MPa]	
	Value	Std. deviation
0°	631,1	63,0
90°	695,2	33,5

Table 4.8: C630 TR50 IMP512 compression tests results

The compression strength values obtained are very high compared to what would be expected from a material with similar characteristics.

This could be due to the low effective percentage of resin in the specimen (31,1%) which causes these anomalous values of maximum resistible stresses in compression.

4.1.2.3⟶Three point bending tests of C630 TR50 12K IMP512 34% BIO

A series of three-point bending tests were then performed according to the regulations indicated for the other long-fiber material (ASTM D790).

In this case, they have a standard width of 15 mm and a free length of 150 mm.

For their construction, 4 plies were laminated with an expected thickness of 2,46 mm. The average real thickness of the specimens measured is 2,35 mm with a real percentage of resin of 31,5 %. It can be recorded a significant loss of resin during the processing phase. The breakage of the specimens subjected to bending occurred for all 6 tests carried out for the state of compressive stress.

Below we have what was obtained through the series of tests carried out.

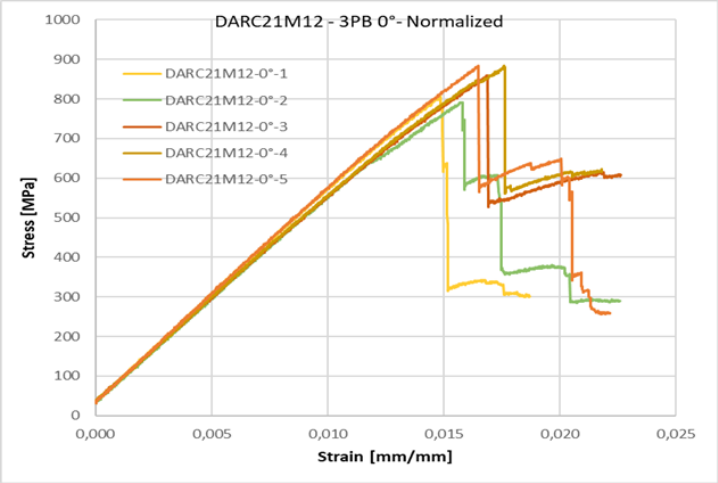

Figure 4.22: C630 TR50 IMP512 0° flexural test stress-strain curves

Material	Normalized Flexural strength [MPa]		Normalized Elastic Modulus [GPa]	
	Value	Std. deviation	Value	Std. deviation
C630 TR50 IMP512 34%	845,4	44,0	53,0	1,0

Table 4.9: C630 TR50 IMP512 flexural tests results

4.1.2.4⟶Interlaminar shear tests of C630 TR50 12K IMP512 34% BIO

At this point, a series of interlaminar shear tests were performed for 6 repetitions and the maximum shear stress that the material can resist was measured. Below we find

the curves and the maximum shear strength values of the material that were recorded during the test.

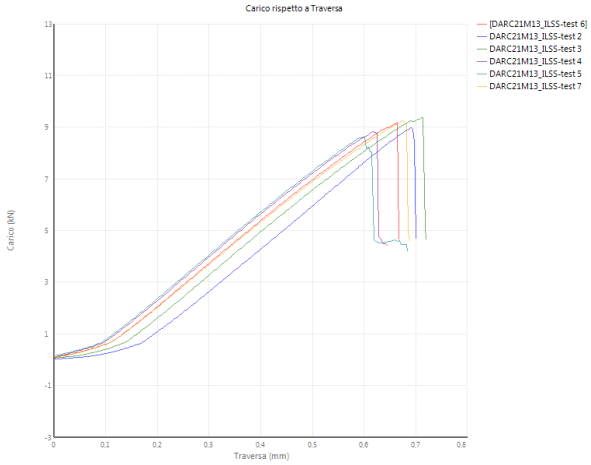

Figure 4.23: C630 TR50 IMP512 0° ILSS-tests stress-crosshead displacement curves

Material	Normalized breaking stress [MPa]	
	Value	Std. deviation
C630 TR50 IMP512 34%	62,4	1,3

Table 4.10: C630 TR50 IMP512 ILSS-tests results

4.1.2.5⟶Energy absorption tests of C630 TR50 12K IMP512 34% BIO

To complete the mechanical characterization of the C630 TR50 12K IMP512 34% BIO, energy absorption tests were performed in a drop tower. Six tests were performed by laminating 3 layers, obtaining an average thickness of 1,79 mm. The percentage of real resin present in the samples is 32,5%. As can be seen from the following images, the material presents a hybrid type of breaking mode between the pulverization and petal ones. This phenomenon could also be caused by the low value of the real percentage of resin.

Figure 4.24: Hybrid failure of C630 TR50 IMP512's omega samples

In the following graph it is possible to observe the acceleration values measured during the test, which attest to the quality of the implementation.

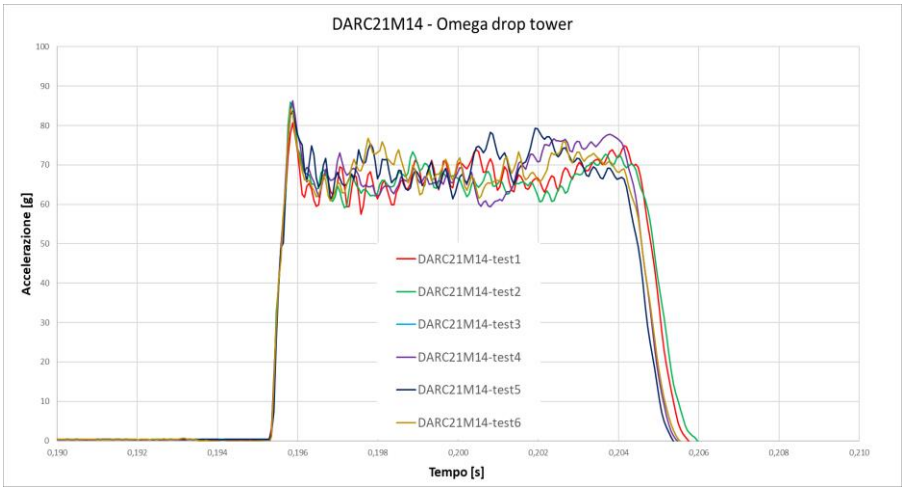

Figure 4.25: Acceleration curves of C630 TR50 IMP512's drop tower test

Material	SEA [J/g]	
	Value	Std. Deviation
C630 TR50 IMP512 34%	70,7	2,5

Table 4.11: C630 TR50 IMP512 SEA values

The C630 TR50 IMP512 34% BIO has a very good energy absorption capacity.

4.1.2.6⟶C630 TR50 IMP512 34% BIO test overview

To conclude, it is provided a summary table of all the values measured during the mechanical characterization of the C630 TR50 IMP512 34% BIO.

Property	Standard	Set 1	Set 1 NORM	Set 2	Set 2 NORM
1) Tensile properties					
Tensile strength σ 0° [MPa]	ASTM D 3039	**NT**	**NT**	**802,7**	**767,3**
Tensile modulus E 0° [GPa]		**NT**	**NT**	**64,7**	**61,8**
Tensile strength σ 90° [MPa]		**687,9**	**637,9**	**708,6**	**680,8**
Tensile modulus E 90° [GPa]		**65,1**	**60,4**	**65,9**	**63,3**
Tensile strength τ 45° [MPa]	ASTM D 3518	**86**	**81**	-	-
Tensile modulus G 45° [GPa]		**4,2**	**3,9**	-	-
2) Flexural properties					
3PB strength σ 0° [MPa]	ASTM D 790	**928,2**	**845,4**	-	-
3PB modulus E 0° [GPa]		**58,13**	**53,04**	-	-
3) Compressive properties					
Compressive strength σ 0° [MPa]	Boeing modified ASTM695 (SACMA SRM 1R-94)	**668,7**	**631,1**	-	-
Compressive strength σ 90° [MPa]		**735,8**	**695,2**	-	-
4) ILSS					
ILSS [MPa]	-	**69,9**	-	**62,4**	-
5) Specific energy absorption					
SEA measured [J/g]	-	-	-	-	-
SEA calculated [J/g]		**70,7**	-	-	-

Table 4.12: C630 TR50 IMP512 mechanical characterization overview

In the table it is possible to note the presence of two sets of specimens regarding the tractions. The first set was made before the resolution of the fiber misalignment problem, while the second was made trying to reduce the misalignment to the maximum.

Also, for the ILSS tests there are two sets, due to a problem of non-conformity of the thickness of the specimens, in fact, the test was repeated twice.

The measured value to be taken into consideration is the one relating to the second set of tests.

4.1.3⟶Comparison of long-fiber material mechanical performances

The two long-fiber materials were impregnated with the same BIO resin (IMP512) but reinforced with two types of fibers with different characteristics. Specifically, the MR60 fibers of the first material analyzed have slightly better mechanical properties in tensil and compression than those of the TR50, so the related composite materials, impregnated with the same resin, have performances in accordance with what has just been said.

It is interesting, however, to make a comparison between the values obtained for the two materials in the three-point bending, interlaminar stress and energy absorption tests.

Starting, therefore, with a first comparison between the values obtained for the three-point bending test.

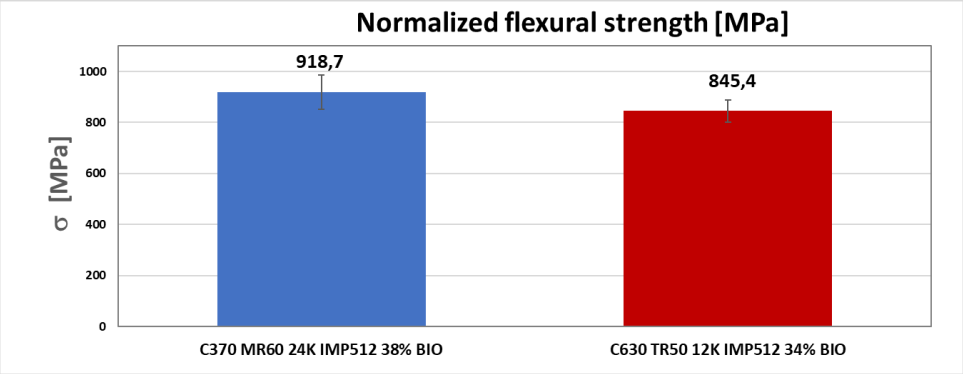

Figure 4.26: Long fiber composites flexural strength comparison

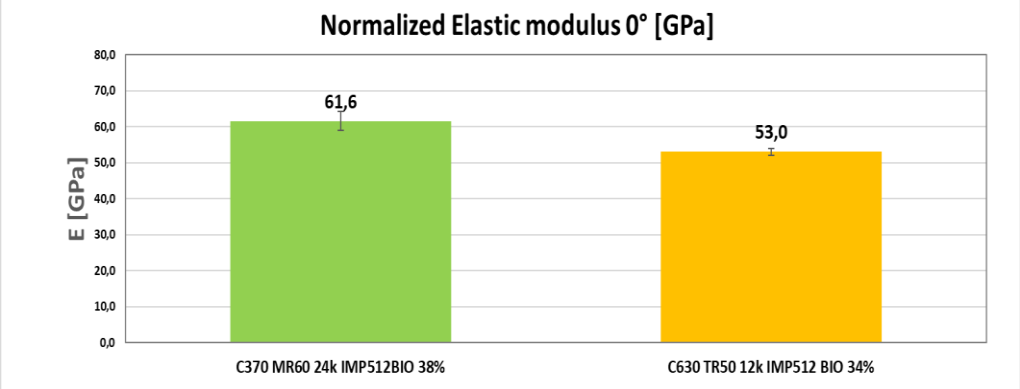

Figure 4.27: Long fiber composites flexural modulus comparison

Material	Normalized Flexural strength [MPa]		Normalized Elastic Modulus [GPa]	
	Value	Std. deviation	Value	Std. deviation
C370 MR60 IMP512 38%	918,7	66,1	61,6	2,6
C630 TR50 IMP512 34%	845,4	44,0	53,0	1,0

Table 4.13: Long fiber composites flexural performance comparison

The bending performances depend on the tensile and compressive ones of the material under examination, and it is therefore consistent with what has just been said that the material reinforced with MR60 fibers shows better values than those of the material reinforced with TR50. What has been observed for the values obtained in bending, compression and tensile confirm what was declared by the manufacturer of the fibers.

Let us now move on to a comparison of the interlaminar shear performances that allow us to have information on the coupling capabilities of the different fibers with the resin studied.

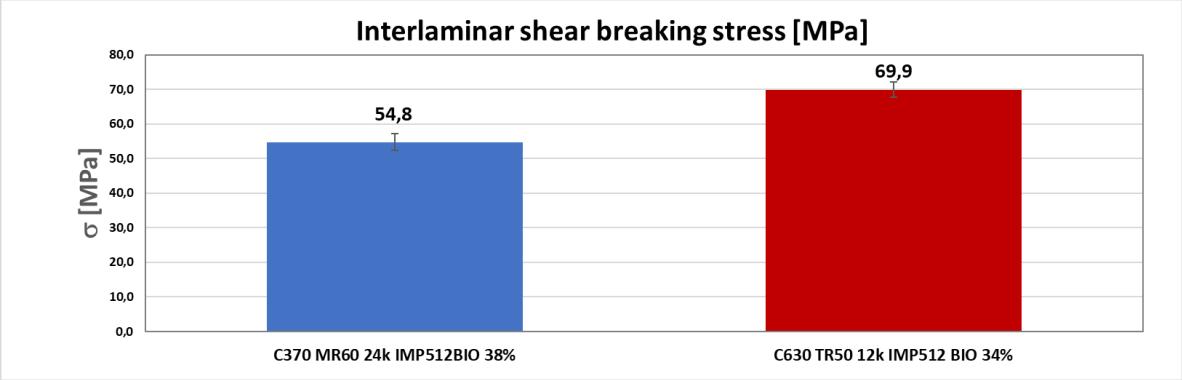

Figure 4.28: Long fiber composites ILSS strength comparison

Material	Normalized breaking stress [MPa]	
	Value	Std. deviation
C370 MR60 IMP512 38%	54,8	2,4
C630 TR50 IMP512 34%	62,4	1,3

Table 4.14: Long fiber composites ILSS performance comparison

The value of the interlaminar shear strength is greatly influenced by the number of carbon fibers present within each filament of the material. Since the C370 MR60 24K IMP512 38% BIO was made with filaments composed of 24.000 fibers, therefore larger

than those of the C630 TR50 12K IMP512 34% BIO with 12.000 fibers, it has a much tauter fabric than that of the other material. Consequently, its behavior will be more similar to that of a unidirectional material than the C630 and cracks will be able to propagate more easily. The interlaminar strength values obtained confirm what has just been said, highlighting better performance for the C630 TR50 12K IMP512 34% BIO.

It is now concluded with a comparison of the behavior of the two materials with regards to energy absorption during impact.

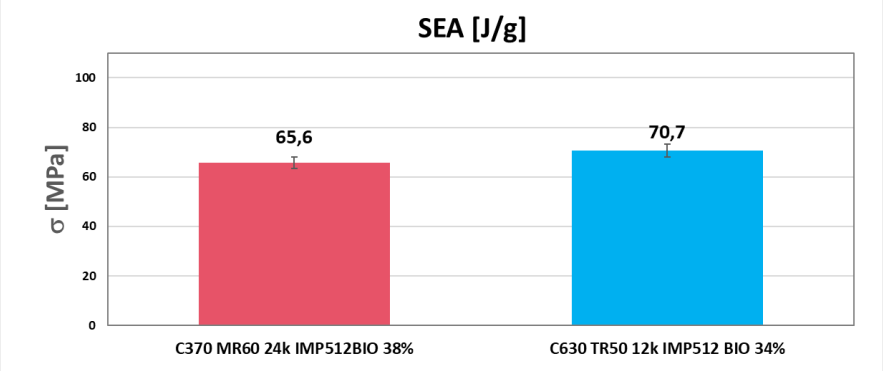

Figure 4.29: Long fiber composites SEA values comparison

Material	SEA [J/g]	
	Value	Std. Deviation
C370 MR60 IMP512 38%	65,6	2,3
C630 TR50 IMP512 34%	70,7	2,5

Table 4.15: Long fiber composites energy absorption performance comparison

Macroscopically, it is possible to highlight the different failure mode of the two materials, since the C370 MR60 24k IMP512 BIO 38% presents a "petal" type failure, while the C630 TR50 12K IMP512 BIO 34% presents a hybrid failure mode between the petal and the pulverization one, perhaps due to the low actual percentage of resin. It is also possible to observe that despite having measured very close SEA values, the C630 TR50 12 K IMP512 34% BIO has slightly better energy absorption properties than the other.

4.2→ Short fiber materials

We focused also on short-fiber materials obtained by recycling weaving waste from long-fiber materials. The materials supplied to us are the C200 Carbon Task IMP512 BIO, the C200 Carbon Task IMP509 and the C100 Carbon Task IMP512 BIO. The difference between the first two is the type of resin, in fact, the IMP512 BIO is a resin partly of bio-origin, while the IMP509 is a standard resin. The third material, on the other hand, differs from the others for a different weight of carbon per square meter.

The materials were supplied to us in the form of prepreg and were subsequently processed through compression molding.

When cutting the layers, it was possible to observe that the fibers that were evenly distributed when removed from the cold storage tended to swim inside the play and come out from the sides when, over time, the material reached room temperature.

This has been found in all short-fiber materials that have been produced and can be caused by the fact that, as stated by the supplier, the Carbon Task fabric is only lightly stitched.

Figure 4.30: Carbon Task prepreg ply

For the two materials with an areal weight of 200 grams of reinforcement per square meter it was possible to perform the complete mechanical characterization, while for the C100, we focused only on the energy absorption analysis, assuming similar mechanical properties with respect to200 g.sm. material.

All the samples, except those for the drop tower test, were made on flat panels obtained by compression molding process. For each material, the samples were made on two panels (panel A and panel B). To verify the effect due to the inhomogeneous distribution of the fibers, observed empirically during the cutting of the skins, the tensile tests at 0° and 90° were performed on both panels in order to check whether the data obtained on two different panels were consistent or not.

A first set of tensile specimens at 0°, 90°, tensile specimens at 45° to the main direction of the composite material, and compression specimens at 0° and 90° were made from panel A. A second set of tensile specimens at 0° and 90° and the flexural specimens at 0° and 90° were obtained from panel B.

4.2.1→Mechanical characterization of C200 Carbon Task IMP512 BIO

The C200 Carbon Task IMP512 BIO is a short-fiber composite material impregnated with the IMP512BIO resin of partial bio-derivation (15%). The fibers with which it was made are obtained through the recycling of virgin TR50 fiber weaving waste.

For this material, it was possible to carry out the complete mechanical characterization, performing a series of traction tests at 0°, 90° and 45° with respect to the considered main direction of the material, a series of compression tests at 0° and 90°, a series of bending tests at 0° and 90° and energy absorption tests in a drop tower.

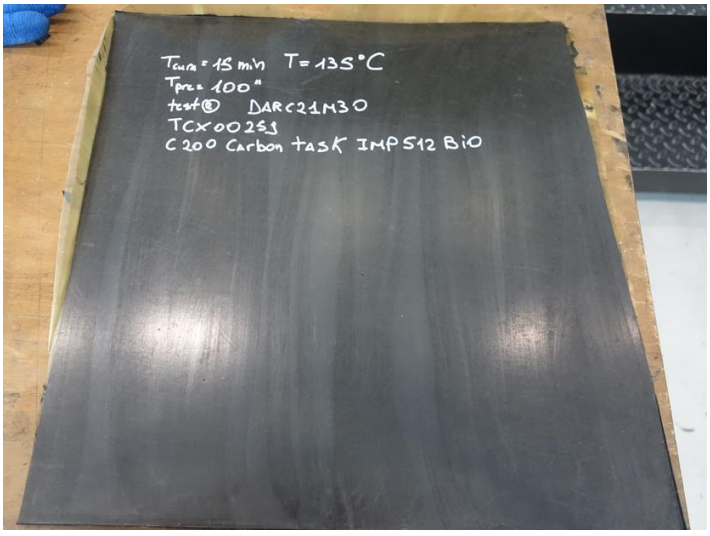

Figure 4.31: C200 Caron Task IMP512 BIO press processed panel

4.2.1.1⟶Tensile tests of C200 Carbon Task IMP512 BIO

As already mentioned, the tensile tests were carried out according to the ASTM D 638 standard. For short-fiber composite materials, in fact, it is possible to create dog bone-shaped specimens, without the aid of tabs and for this reason the testing methods are slightly different from those of long-fiber composite materials.

To evaluate a possible effect of the non-homogeneous movement of the fibers inside each skin and of the loss of resin during processing, the tensile specimens were made at 0° and 90° twice, on two different panels. In this way, it was possible to evaluate the coherence of the data obtained and the average of the values obtained on the two panels were chosen as the strength and elastic modulus values of the material.

For each set made, 6 repetitions were performed. The specimens have a standard width of 13 mm and a free length of 57 mm and for their creation, 5 layers were laminated. The expected thickness was 2,49 mm, while the average measured thickness for panel A is 1,91 mm with a resin percentage that goes from the theoretical 70% to a real 62,1%. It is therefore important to highlight a large loss of resin in the processing phase. As for panel B, the average measured thickness value is 2,11 mm with a real resin percentage of 65,2%. Also in this case, a significant loss of resin can be found in the processing phase, but to a different extent.

Let us now move on to the analysis of the data obtained in the directions studied.

Below we can obtain the stress-strain curves and the tensile strength values obtained at 0° and 90° in the two panels and those at 45° which, however, were performed only on panel A.

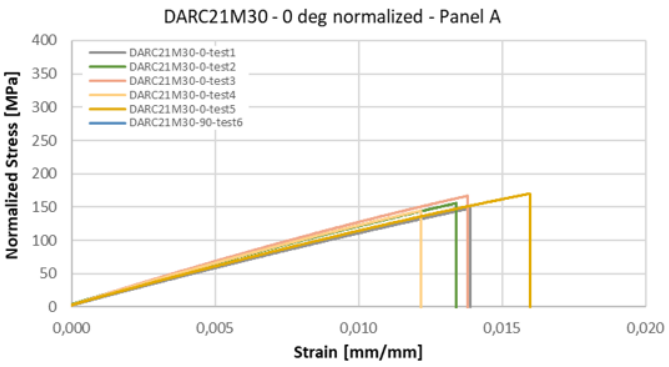

Figure 4.32: C200 Carbon Task IMP512 0°tensile stress-strain curves panel A

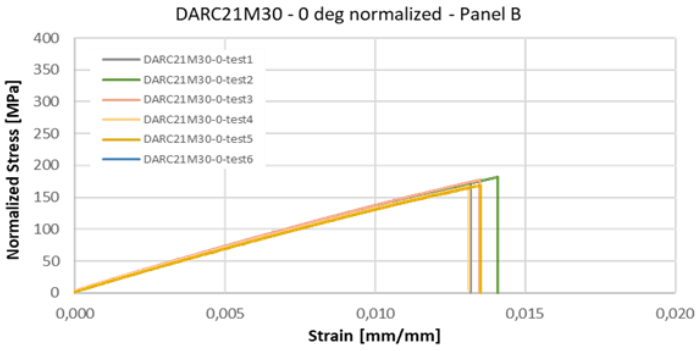

Figure 4.33: C200 Carbon Task IMP512 0°tensile stress-strain curves panel B

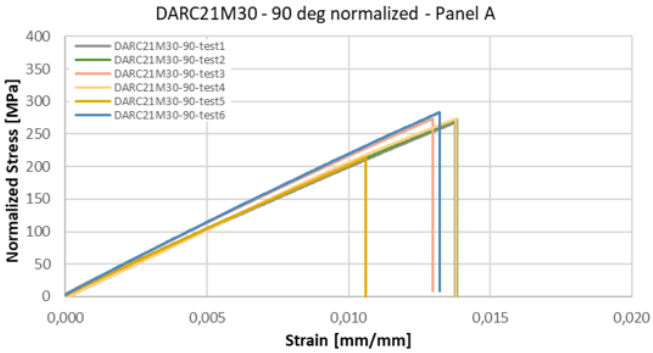

Figure 4.34: C200 Carbon Task IMP512 90°tensile stress-strain curves panel A

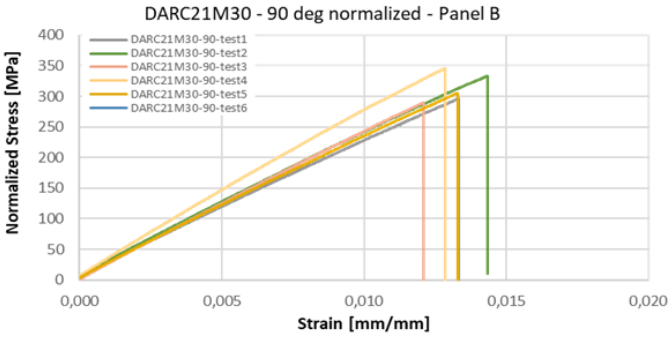

Figure 4.35: C200 Carbon Task IMP512 90°tensile stress-strain curves panel B

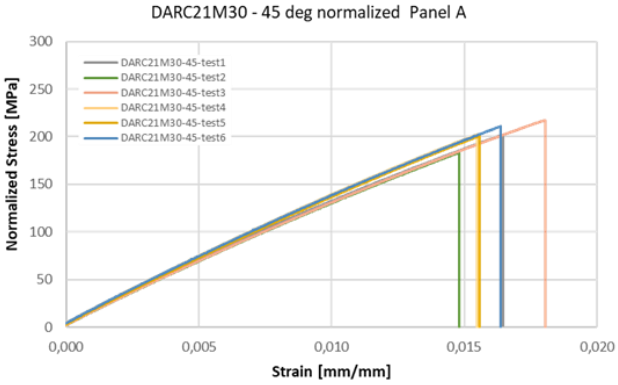

Figure 4.36: C200 Carbon Task IMP512 45°tensile test stress-strain curves

Direction	Norm. Tensile strength Panel A [MPa]		Norm. Tensile strength Panel B [MPa]		Norm. Elastic Modulus Panel A [GPa]		Norm. Elastic Modulus Panel B [GPa]	
	Value	Std. deviation	Value	Std. deviation	Value	Std. deviation	Value	Std. deviation
0°	157,1	11,3	173,4	6,0	12,3	0,8	14,0	0,3
90°	264,0	25,2	314,1	24,2	21,0	0,9	24,8	2,0
45°	202,8	11,6	-	-	13,8	0,3	-	-

Table 4.16: Tensile performances of C200 Carbon Task IMP512 BIO

As stated by *Angeloni Group*, the direction in which the Carbon Task presents the best tensile mechanical properties is 90° with respect to the main direction of the material.

Making a comparison between the values obtained at 0° and 90° in the two panels, it is possible to note a non-negligible difference between the data obtained.

Below we can observe the histograms representing the data obtained in the two panels at 0°.

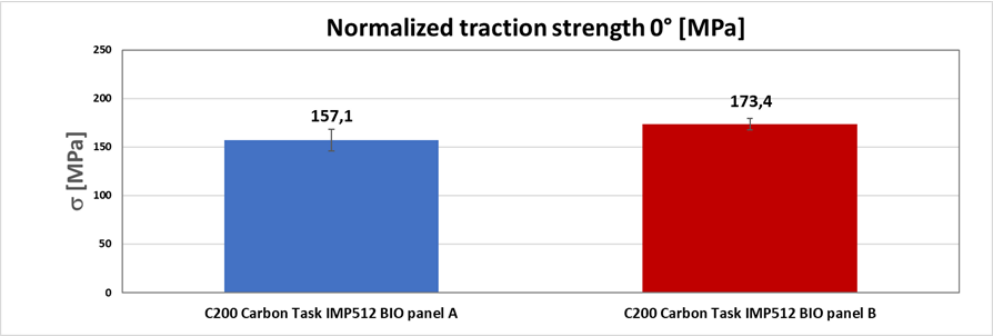

Figure 4.37: C200 Carbon Task IMP512 0°tensile strength comparison

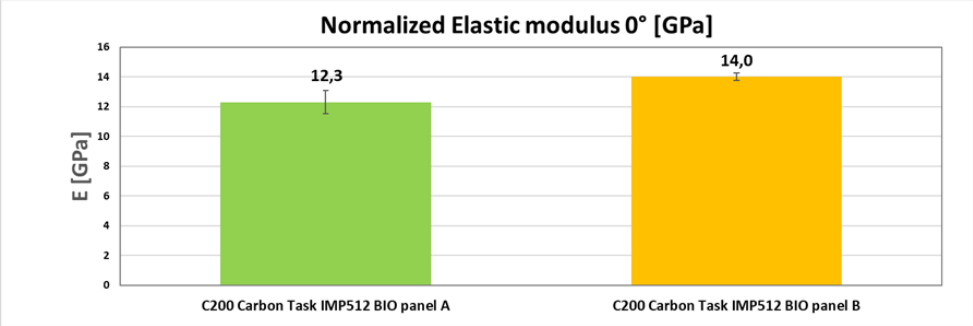

Figure 4.38: C200 Carbon Task IMP512 0°tensile modulus comparison

Let us now look at the histograms representing the values obtained at 90° in the two panels.

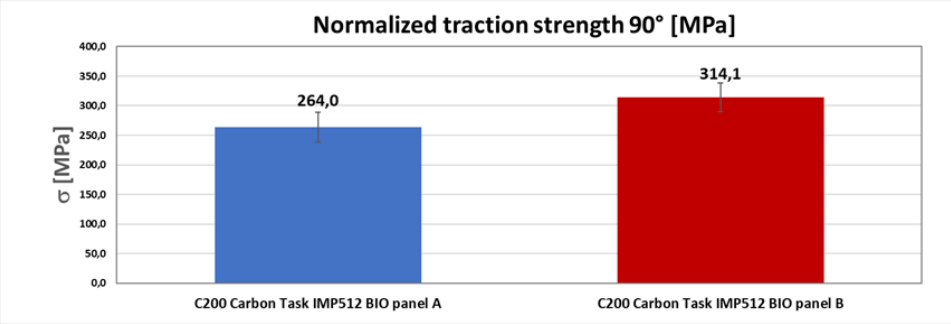

Figure 4.39: C200 Carbon Task IMP512 90°tensile strength comparison

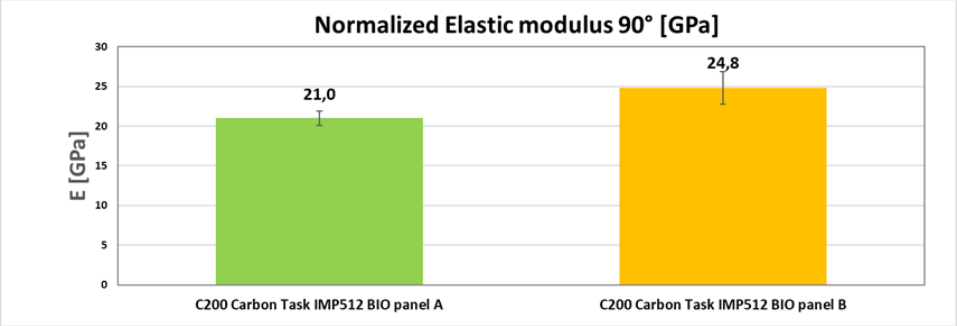

Figure 4.40: C200 Carbon Task IMP512 90°tensile modulus comparison

The difference in the data obtained in the two panels can be caused by the different loss of resin during processing in the two panels. In panel A, in fact, we have a real percentage of resin of 62,1% while in panel B we have a percentage of resin of 65,2%.

However, the most likely explanation could be an anisotropy in the non-woven recycled material due to the non-completely randomic process. This has already been observed for other non-woven materials.

Another factor that has a lot of importance on the characteristics of the material studied is the fact that Carbon Task is a material in which they are only partially sewn and for this reason they have greater mobility within the fabric. In this way it is possible to find areas in which there are accumulations of fiber and others in which they are sparser. This causes a large dispersion of the data obtained, both for the tensile strength and for the elastic modulus.

4.2.1.2⟶Compression tests of C200 Carbon Task IMP512 BIO

Let us now move on to the analysis relating to the compression tests.

The samples for the compression tests were all made from the same panel (panel A).

To make the samples, 5 layers were laminated with an expected thickness of 2,49 mm. The average measured thickness was 1,98 mm with a real percentage of resin of 63,3%. As for the tensile samples, also for the compression ones, a large loss of resin was recorded during the processing phase. The compression tests at 0° and 90° were carried out according to the ASTM 695 standard (SACMA SRM1R-94). 14 repetitions were performed for each direction.

Let us now analyze the results obtained in detail.

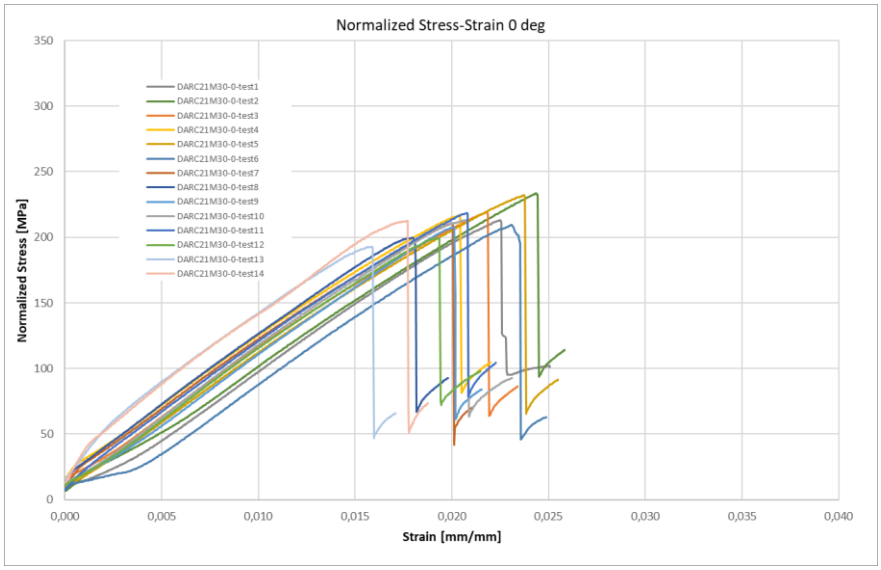

Figure 4.41: C200 Carbon Task IMP512 0° compression test stress-strain curves

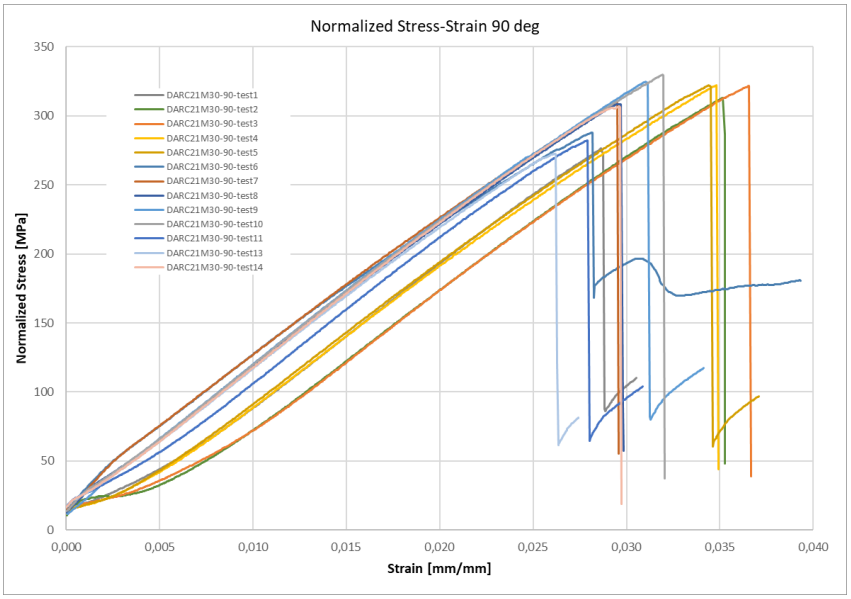

Figure 4.42: C200 Carbon Task IMP512 90° compression test stress-strain curves

Direction	Normalized Compression strength [MPa]	
	Value	Std. deviation
0°	211,0	10,0
90°	307,5	19,7

Table 4.17: Compression performances of C200 Carbon Task IMP512 BIO

Also, for the compression tests it was possible to observe a large loss of resin during the processing of the material that could have influenced the obtained data.

The best performance of the material in compression was obtained at 90° with respect to the main direction of the material, in accordance with what was declared by the supplier company. Compressive tests confirmed the anisotropy in the non-woven recycled material due to the manufacturing process. The compression tests are carried out in two series of 7 for each direction and the two smaller panels containing the single series are obtained from two different parts of the larger panel.

During the compression tests of the C200 Carbon Task IMP509, significant discrepancies were found between the values obtained from the two series of 7. For this reason, a series of micrographs were carried out for both the C200 Carbon Task IMP512 BIO and the C200 Carbon Task IMP509 to verify the possible presence of porosity in the samples coming from the two smaller panels.

We have therefore chosen two specimens from two different series to perform verification micrographs for each direction. Specifically, the DARC21M30-0°-test3 (from the first set of specimens) and the DARC21M30-0°-test8 (from the second set of specimens) were chosen to study the 0° compression specimens.

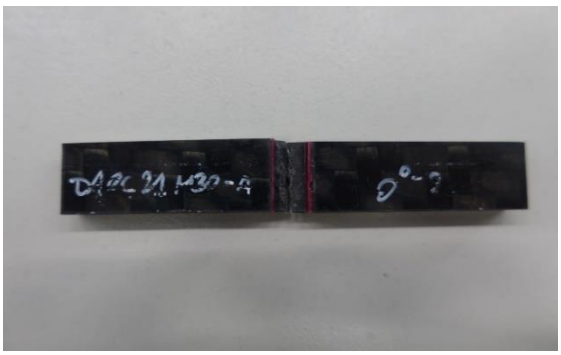

Figure 4.43: DARC21M30-0°-test3

Figure 4.44: DARC21M30-0°-test8

From the micrographs it was possible to observe that the specimens for the C200 Carbon Task IMP512 BIO at 0° are very homogeneous and free of porosity, confirming what had been suggested by the coherence of the data obtained in the two sets of compression tests. In both specimens, porosity was observed in the bonding between the specimen and the tabs even if this did not have a significant effect on the values measured during the test.

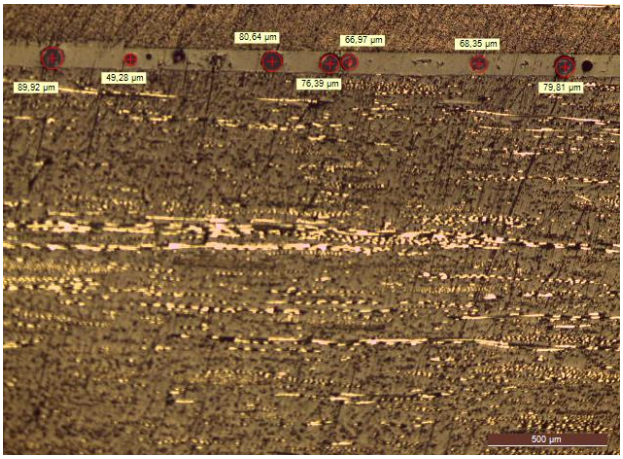

Figure 4.45: DARC21M30-0°-test3 micrograph

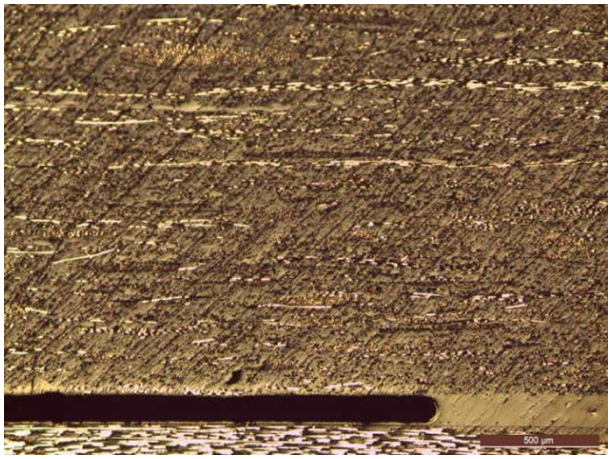

Figure 4.46: DARC21M30-0°-test8 micrograph

Let us now analyze the micrographs made on the 90° compression specimens.

Also in this case, two specimens were selected from two different sets of specimens, specifically the DARC21M30-90°-test1 (from the first set) and the DARC21M30-90°-test12 (from the second set).

Figure 4.47: DARC21M30-90°-test1

Figure 4.48: DARC21M30-90°-test12

Also, in this case both samples are very homogeneous and free of porosity confirming the coherence of the data obtained for the pressure tests.

The only observable porosities are those present in the bonding between the supports and the sample which however do not have a significant effect on the values measured during the test.

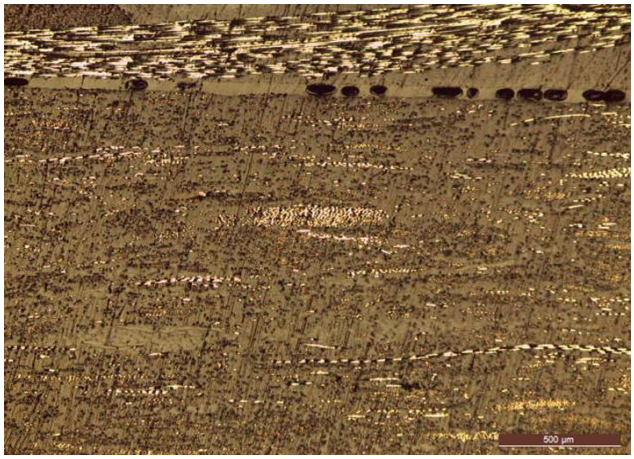

Figure 4.49: DARC21M30-90°-test1 micrograph

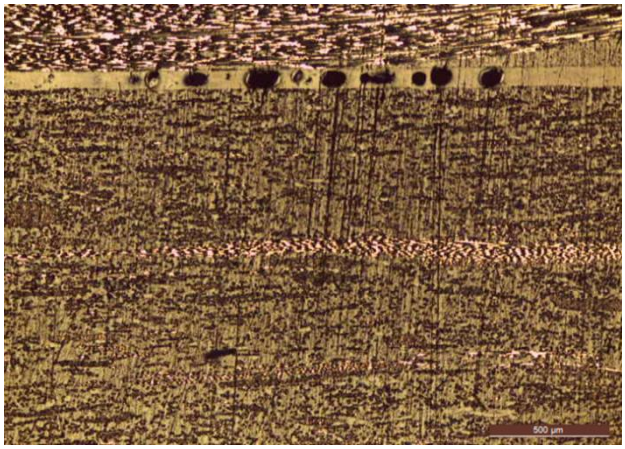

Figure 4.50: DARC21M30-90°-test12 micrograph

4.2.1.3⟶Three points bending tests of C200 Carbon Task IMP512 BIO

Let us now continue the mechanical characterization of the C200 Carbon Task IMP512 BIO with the analysis of the three-point bending tests.

The three-point bending tests were performed according to the ASTM D 790 standard with a span between the two support points of 48 mm. A series of 6 specimens at 0° with respect to the main direction of the material and 6 specimens inclined at 90° with respect to the same were obtained, all from panel B. The specimens have an average width of 15,6 mm and a free length of 150 mm. For their realization, 5 plies were laminated with a nominal thickness of 2,49 mm. The average measured thickness obtained was 2,19 mm with a resin percentage of 66,4%. As for all specimens of the C200 Carbon Task IMP512 BIO, a large loss of resin was found during the processing phase in the press.

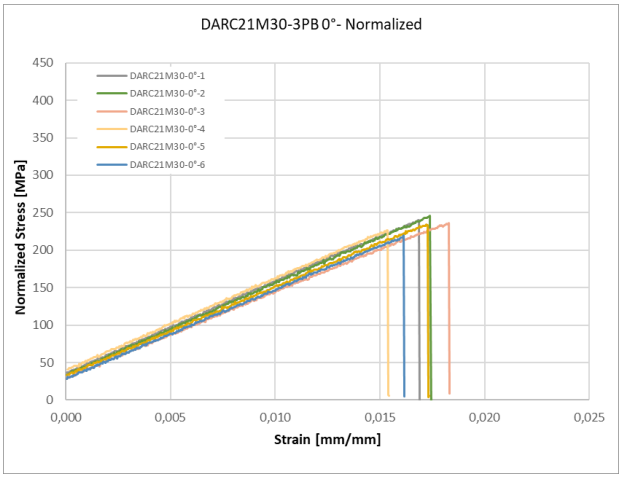

Figure 4.51: C200 Carbon Task IMP512 0° flexural stress-strain curves

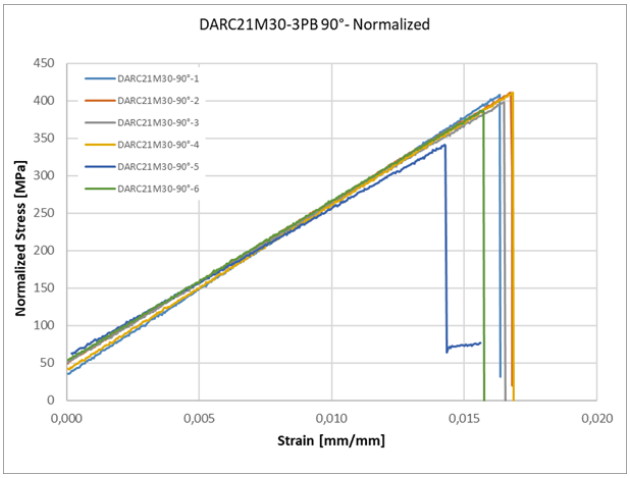

Figure 4.52: C200 Carbon Task IMP512 90° flexural stress-strain curves

Direction	Normalized Flexural strength [MPa]		Normalized Elastic Modulus [GPa]	
	Value	Std. deviation	Value	Std. deviation
0°	233,7	9,3	12,0	0,3
90°	392,7	27,0	20,2	4,1

Table 4.18: Flexural performances of C200 Carbon Task IMP512 BIO

The values obtained confirm what was declared by the supplier company, according to which the material has better performance in the direction inclined by 90° compared to the main direction of the material.

In the bending tests, a state of compressive stress is induced inside the specimen in the upper part of the specimen and a state of tensile stress in the lower part and, in this case, all the specimens tested both at 0° and at 90° reached the breakage first by traction.

4.2.1.4⟶Energy absorption tests of C200 Carbon Task IMP512 BIO

To conclude the mechanical analysis of the studied material, we now move on to the analysis of the energy absorption tests, carried out in a drop tower.

Six specimens were made and for their realization 5 layers were laminated obtaining an average thickness of 1,99 mm. The real percentage of resin obtained is 63,5%. Also,

in this case it is possible to highlight a large reduction in the percentage of resin compared to the theoretical value of 70%.

During the impact, the specimen breaks with a pulverization.

Figure 4.53: Pulverized C200 Carbon Task IMP512's omega samples

Below we can see the graph of the acceleration measured during the test execution.

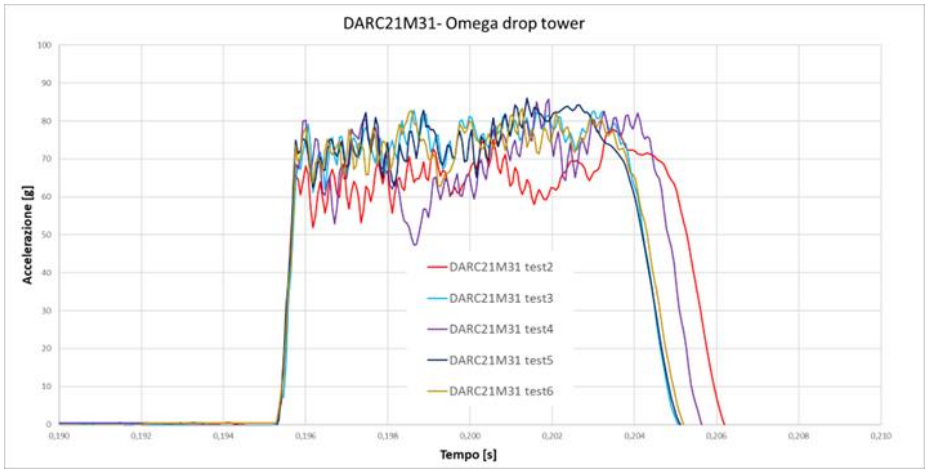

Figure 4.54: Acceleration curves of C200 Carbon Task IMP512's drop tower test

The impact energy absorbed (SEA) value can be obtained in two ways, one indicated as measured SEA and the other as calculated SEA.

The calculated SEA can be obtained by considering the difference between the height of the specimen before and after the test. The measured SEA, instead, can be obtained through the difference between the mass of the whole specimen and the tested one.

Property	C200 Carbon Task IMP512 BIO [DARC21M31]	
1) Specific energy absorption		
	Value	Std. deviation
SEA measured [J/g]	**67,7**	**4,1**
SEA calculated [J/g]	**67,0**	**4,2**

Table 4.19: SEA values of C200 Carbon Task IMP512 BIO

The two values of energy absorbed per gram of material obtained are very close and this gives us an indication of the quality of the measurement that was carried out.

The studied material behaves very well with regard to energy absorption during the impact phase.

4.2.1.5⟶C200 Carbon Task IMP512 BIO test overview

To summarize, we now include a summary table of what was obtained in all the tests carried out.

Property	Standard	Panel A	Panel A NORM	Panel B	Panel B NORM
1) Tensile properties					
Tensile strength σ 0° [MPa]	ASTM D 638	**334,8**	**264,0**	**201,4**	**173,4**
Tensile modulus E 0° [GPa]		**26,6**	**21,0**	**16,2**	**14,0**
Tensile strength σ 90° [MPa]		**199,2**	**157,1**	**364,7**	**314,1**
Tensile modulus E 90° [GPa]		**15,5**	**12,3**	**28,8**	**24,8**
Tensile strength σ 45° [MPa]	ASTM D 638	**257,1**	**202,8**	-	-
Tensile modulus E 45° [GPa]		**17,5**	**13,8**	-	-
2) Flexural properties					
3PB strength σ 0° [MPa]	ASTM D 790	-	-	**309,7**	**233,7**
3PB modulus E 0° [GPa]		-	-	**15,9**	**12,0**
3PB strength σ 90° [MPa]		-	-	**496,3**	**392,7**
3PB modulus E 90° [GPa]		-	-	**25,7**	**20,2**
3) Compressive properties					
Compressive strength σ 0° [MPa]	Boeing modified ASTM695 (SACMA SRM 1R-94)	**382,2**	**307,5**	-	-
Compressive strength σ 90° [MPa]		**267,7**	**211,0**	-	-
5) Specific energy absorption					
SEA measured [J/g]	-	**67,67**	-	-	-
SEA calculated [J/g]		**67,03**	-	-	-

Table 4.20: C200 Carbon Task IMP512 mechanical characterization overview

4.2.2⟶Mechanical characterization of C200 Carbon Task IMP509

C200 Carbon Task is a short-fiber material obtained from recycled weaving waste, with an areal weight of 200 grams of reinforcement per square meter. It is impregnated with a standard epoxy resin, specifically, IMP509.

For its mechanical characterization, a series of tensile tests were carried out at 0°, 90° and 45° with respect to the direction indicated as the main direction of the material, a series of compression tests at 0° and 90°, a series of three-point bending tests at 0° and 90° and energy absorption tests in a drop tower.

Also in this case, the samples were made on two panels (panel A and panel B).

On panel A, the first set of tensile tests were carried out at 0°, 90° and 45° and the samples for the compression tests at 0° and 90° with respect to the main direction of the material. From panel B, a second set of tensile specimens at 0° and 90° and the flexural specimens at 0° and 90° were made. The tensile strength values at 0° and 90° were calculated by averaging the values obtained for the specimens from panel A and those obtained for the specimens from panel B. The "omega" specimens for the energy absorption tests were made separately in a press with specific molds.

4.2.2.1⟶Tensile tests of C200 Carbon Task IMP509

The tensile tests were carried out according to the ASTM D 638 standard. The tensile test specimens were made on two different panels to verify the homogeneity of the tensile behavior of the material, the effect of the possible movement of the short fibers that were not very sewn inside the skins and the possible effect of the loss of resin during processing.

For each direction, 6 repetitions of the test were carried out. The specimens are characterized by a standard free length of 57 mm and for their realization, 5 layers were laminated with an expected nominal thickness of 2,48 mm.

For panel A, the average thickness measured is 2,08 mm with a real percentage of resin of 64,9%. As for the material impregnated with bio resin, it is possible to highlight a large loss of resin during processing.

For panel B, however, the average thickness measured is 2,03 mm with a real percentage of resin of 64,1%.

Below we find the stress strain curves obtained for the tensile tests at 0° and 90° obtained in the two panels and that of the 45° tests obtained from panel A.

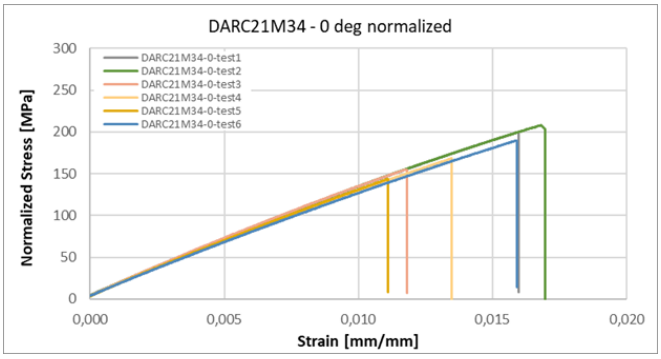

Figure 4.55: C200 Carbon Task IMP509 0°tensile stress-strain curves panel A

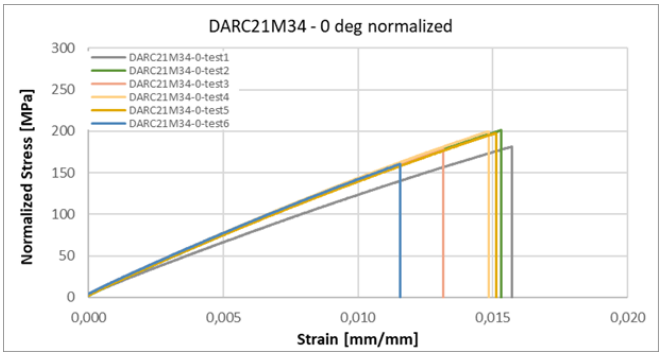

Figure 4.56: C200 Carbon Task IMP509 0°tensile stress-strain curves panel B

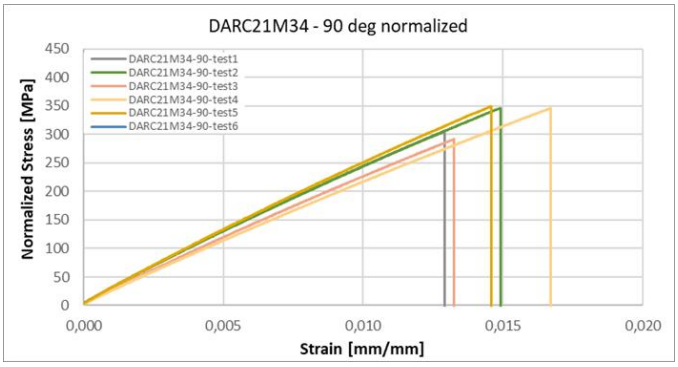

Figure 4.57: C200 Carbon Task IMP509 90°tensile stress-strain curves panel A

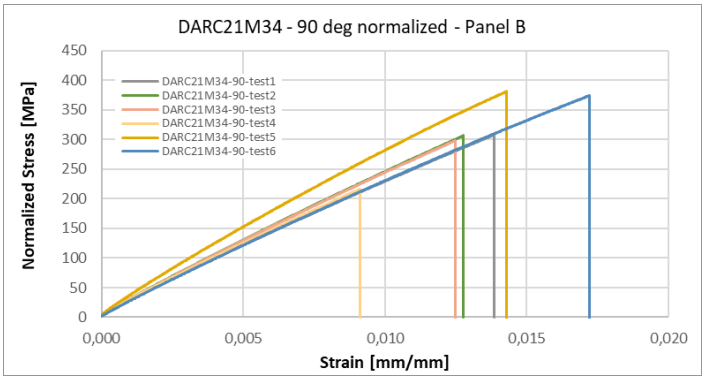

Figure 4.58: C200 Carbon Task IMP509 90°tensile stress-strain curves panel B

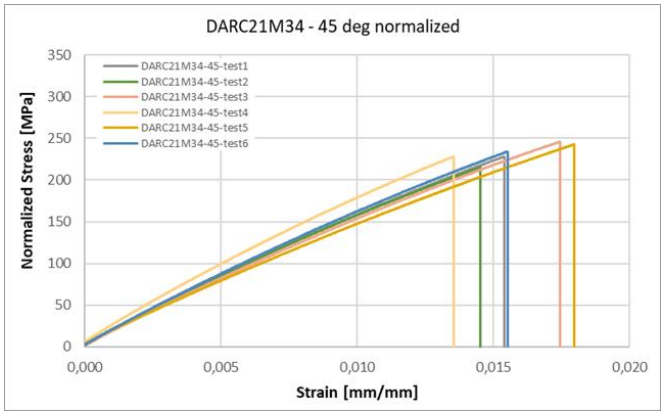

Figure 4.59: C200 Carbon Task IMP509 45°tensile test stress-strain curves

Direction	Norm. Tensile strength Panel A[MPa]		Norm.Tensile strength Panel B[MPa]		Norm. Elastic Modulus Panel A [GPa]		Norm. Elastic Modulus Panel B [GPa]	
	Value	Std. deviation	Value	Std. deviation	Value	Std. deviation	Value	Std. deviation
0°	191,6	17,1	186,6	16,0	13,4	0,4	14,3	0,8
90°	327,7	27,1	341,1	60,0	24,7	1,6	25,4	2,2
45°	232,4	11,0	-	-	16,8	1,2	-	-

Table 4.21: C200 Carbon Task IMP509 tensile performances

The data obtained confirms what was declared by the manufacturing company. The material has better tensile performance in the direction inclined by 90° compared to the direction considered the main direction of the material, confirming that the reinforcement manufacturing method induces a small anisotropy in the material.

We can now make a comparison between the values of tensile strength and elastic modules at 0° and 90° obtained in the specimens made from the two different specimens.

The following histograms show the values obtained from the tensile tests at 0° performed on the specimens obtained from the two panels.

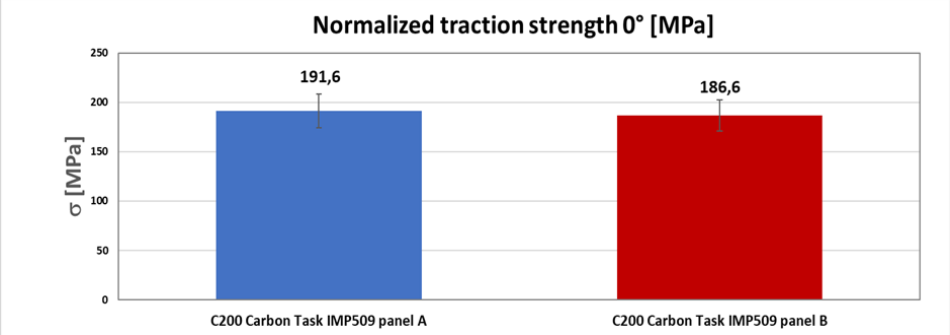

Figure 4.60: C200 Carbon Task IMP509 0° tensile strength comparison

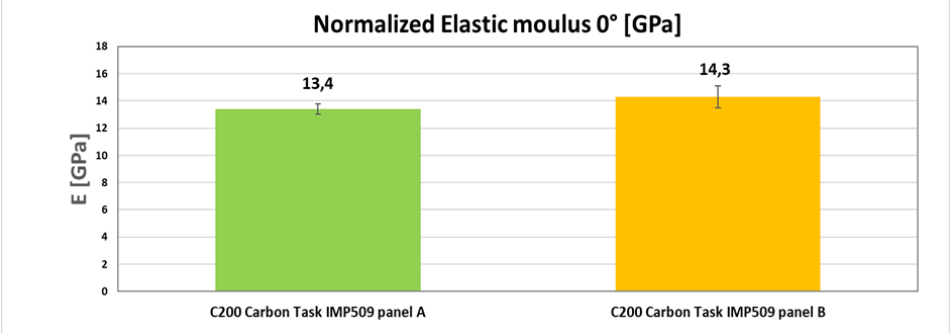

Figure 4.61: C200 Carbon Task IMP509 0° tensile modulus comparison

Below we find the values obtained in the 90° tensile tests on the two panels.

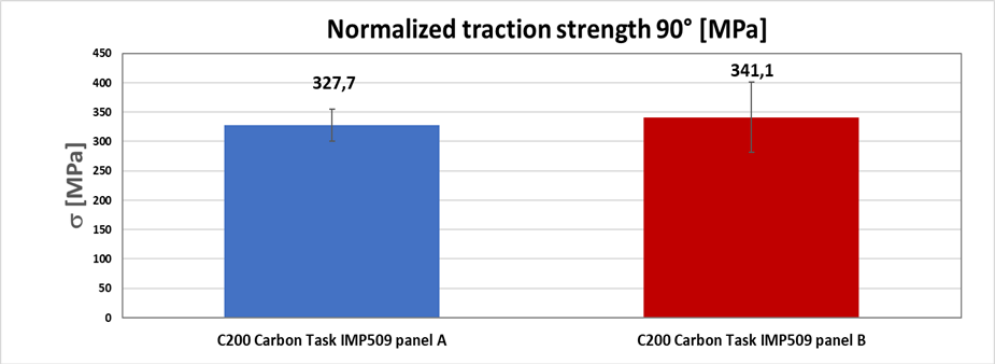

Figure 4.62: C200 Carbon Task IMP509 90° tensile strength comparison

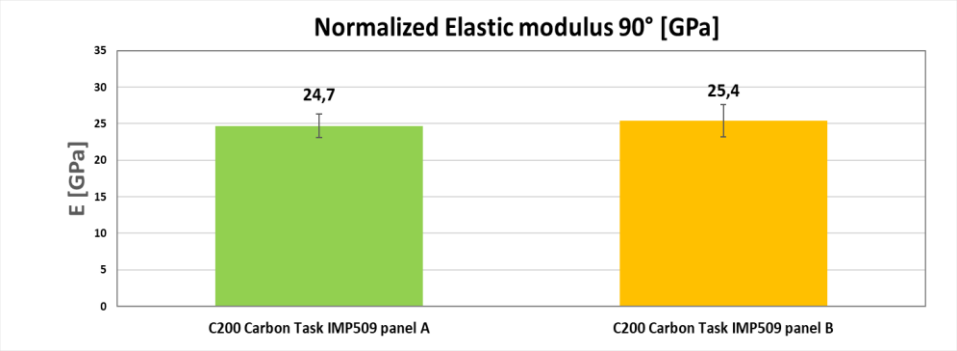

Figure 4.63: C200 Carbon Task IMP509 90° tensile modulus comparison

In this case the values obtained from the samples from the two panels are very close and consistent. Furthermore, the resin loss during processing for this material was large but consistent in the two panels and therefore had a uniform effect on the results obtained from the two panels. All the analyzed figures of merit can be considered equivalent within the experimental error.

4.2.2.2⟶Compression tests of C200 Carbon Task IMP509

Compression tests were performed according to ASTM 695 (SACMA SRM1R-94). The specimens were all obtained from panel A and for their realization 5 layers were laminated with an expected specimen thickness of 2,48 mm. The actual thickness measured was 2,13 mm with an actual resin percentage of 65,75%.

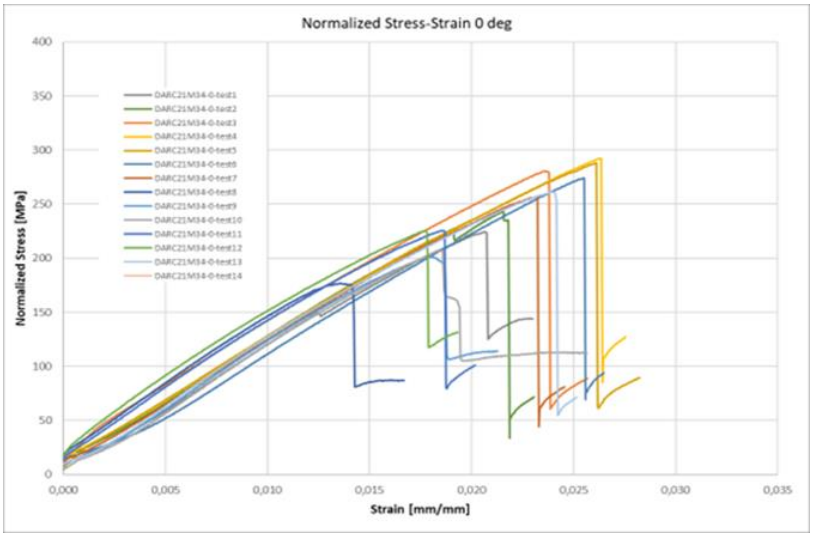

Figure 4.64: C200 Carbon Task IMP509 0° compression test stress-strain curves

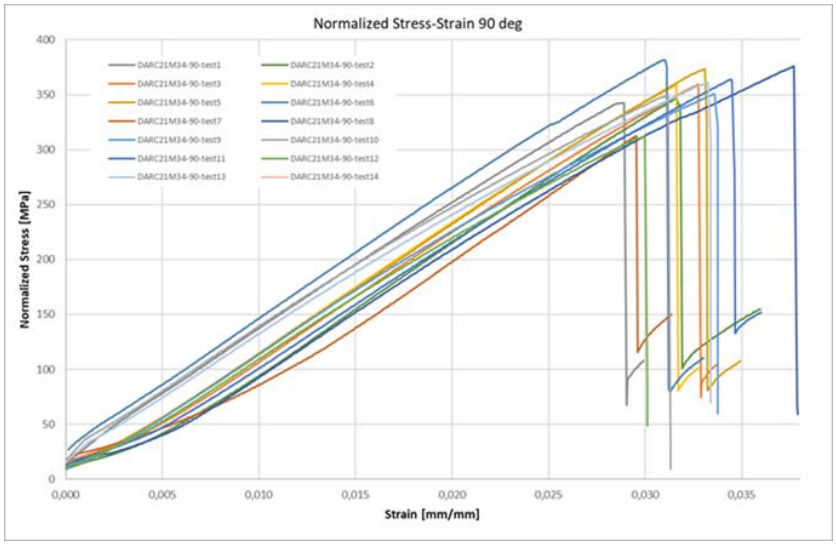

Figure 4.65: C200 Carbon Task IMP509 90° compression test stress-strain curves

Direction	Normalized Compression strength [MPa]	
	Value	Std. deviation
0°	279,4	15,8
90°	353,3	18,2

Table 4.22: C200 Carbon Task IMP509 compression performances

The data obtained confirms that the studied material has better mechanical performances in compression in the direction inclined by 90° compared to the direction considered as the main direction of the material. Also, for the compression specimens it is possible to report a large loss of resin during processing.

The compression specimens are made in two sets on two smaller panels containing 7 specimens each, extracted from different points of panel A. During the compression tests at 0° a large discrepancy was noted between the values obtained for the first set and those obtained for the second. For this reason, micrographs were performed to verify the presence of porosity that may have influenced the results.

Code	DARC21M34-SACMA-00-01	DARC21M34-SACMA-00-02	DARC21M34-SACMA-00-03	DARC21M34-SACMA-00-04	DARC21M34-SACMA-00-05	DARC21M34-SACMA-00-06	DARC21M34-SACMA-00-07	DARC21M34-SACMA-00-08	DARC21M34-SACMA-00-09	DARC21M34-SACMA-00-10	DARC21M34-SACMA-00-11	DARC21M34-SACMA-00-12	DARC21M34-SACMA-00-13	DARC21M34-SACMA-00-14	Avg	Std.Dev	COV %	Norm	FEA
Width [mm]	13,34	13,45	13,15	13	13,08	13,02	13,03	13,01	13,03	13,03	13,13	13,1	13,11	13,06	13,11	0,13	1,00		
Thickness [mm]	2,09	2,09	2,09	2,09	2,09	2,1	2,1	2,23	2,2	2,2	2,22	2,2	2,22	2,19	2,15	0,06	2,83	2,5	
Free Length [mm]	2,9	2,6	2,41	2,84	3,41	3,77	3,63	3,68	3,89	3,6	3,54	3,51	3,61	3,77	3,37	0,47	14,10		
εR [mm/mm]	0,021	0,022	0,024	0,026	0,026	0,026	0,023	0,014	0,018	0,019	0,019	0,018	0,024	#DIV/0!	0,022	0,0037	17,13		0,02
σR [MPa]	266,2	288,6	333,0	346,7	341,6	323,7	303,3	196,4	226,8	233,5	252,0	254,1	291,8	0,0	**286,4**	50,3	17,56		
σ_{norm} [MPa]	224,3	243,2	280,6	292,2	287,9	274,1	256,8	176,6	201,2	207,2	225,6	225,4	261,2	0	**247,1**	36,9	14,94	247,1	207,2
Failure	under tab	under tab	Compression	Compression	Comp.+Shear	Shear	Comp.+Shear	Shear	Compression	Comp.+shear	C+shear	Compression	under tab	not tested					

Uncoherent values

Table 4.23: Second set samples' uncoherent compression strength values

Two specimens from the two different sets were then taken for each direction, polished and observed under the microscope.

Specifically, for the 0° compression tests, specimen DARC21M34-0°-test4 (from the first set) and specimen DARC21M34-0°-test9 (from the second set) were selected and observed.

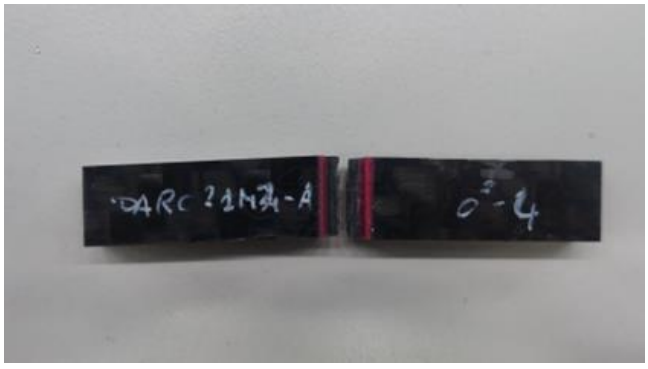

Figure 4.66: DARC21M34-0°-test4

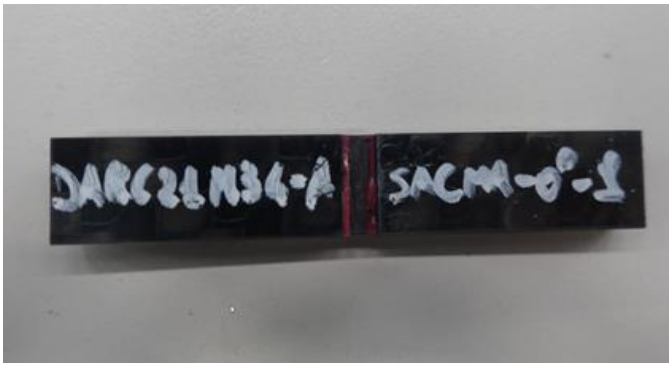

Figure 4.67: DARC21M34-0°-test9

As can be observed from the following micrographs, porosities were found in the second set of specimens.

Figure 4.68: DARC21M34-0°-test4 micrograph

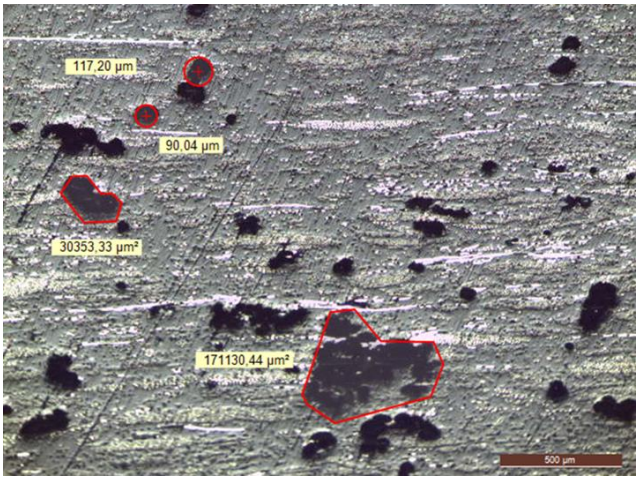

Figure 4.69: DARC21M34-0°-test9 micrograph

The second set of specimens is characterized by large and numerous porosities with an area that can reach a size of even 0.171 mm². This could have had an effect on the measured compression strength values that were much lower than those measured for the first set of specimens. These porosities have a very strong effect on the measured values, invalidating the measurements that were made for the second set of specimens that were, therefore, discarded in the calculation of the compression strength.

The same verification through micrographic analysis was performed for the 90° compression specimens. Specifically, the specimens DARC21M34-90°-test5 (from the first set) and DARC21M34-90°-test8 (from the second set) were selected.

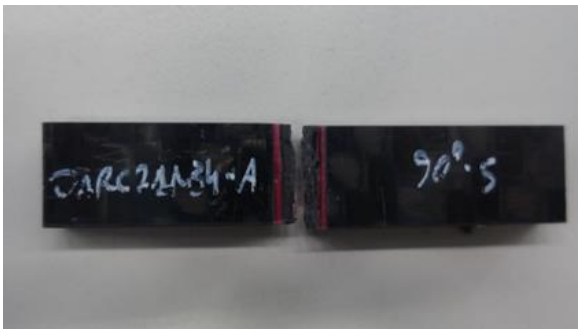

Figure 4.70: DARC21M34-90°-test5

Figure 4.71: DARC21M34-90°-test8

In this case, from the observations, the samples appear to be very homogeneous.

Figure 4.72: DARC21M34-90°-test5 micrograph

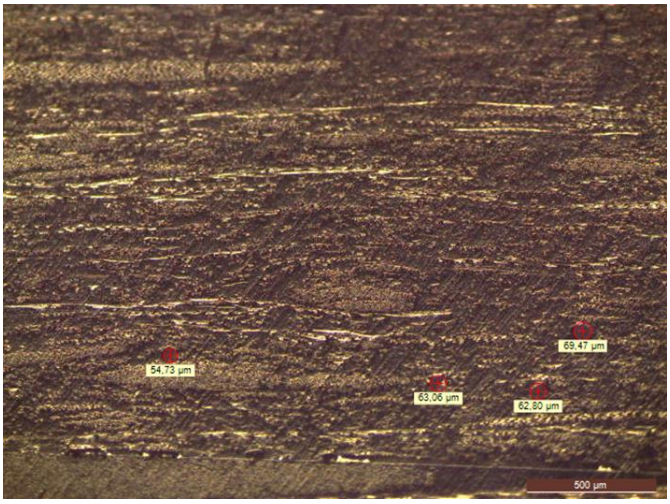

Figure 4.73: DARC21M34-90°-test8 micrograph

The specimens are much more homogeneous than those observed for the second set at 0°. Also in this case, porosities were observed in the second set of specimens, but very rare and small in size (with a diameter of about 60 µm). These do not significantly influence the compression values measured in the second set of specimens at 90°.

What was observed is also confirmed by the coherence of the data obtained for the first and second set. For the calculation of the compression strength, the values of both sets of specimens were therefore considered.

4.2.2.3⟶Three points bending tests of C200 Carbon Task IMP509

The three-point bending tests were carried out according to the ASTM D 790 standard. A series of tests were performed at 0° and 90° with respect to the direction of the material indicated as the main one.

For each direction, 6 repetitions were performed. The specimens were all obtained from panel B and have a standard free length of 150 mm. To make the specimens, 5 plies were laminated for a nominal thickness of 2,49 mm. The average measured thickness value is 2,15 mm with a real percentage of resin of 65,8%. Consistent with that observed for all the other specimens of short-fiber materials, we have a significant reduction in resin during processing, compared to the theoretical 70%.

Below we can observe the stress-strain graphs obtained during the bending tests at 0° and 90°.

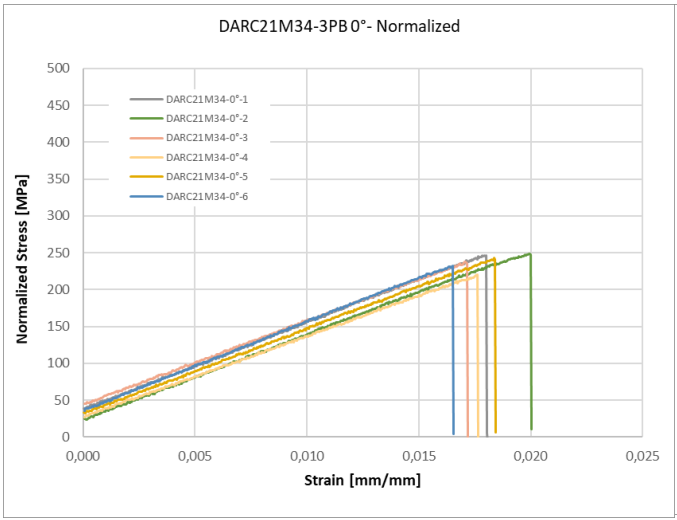

Figure 4.74: C200 Carbon Task IMP509 0° flexural stress-strain curves

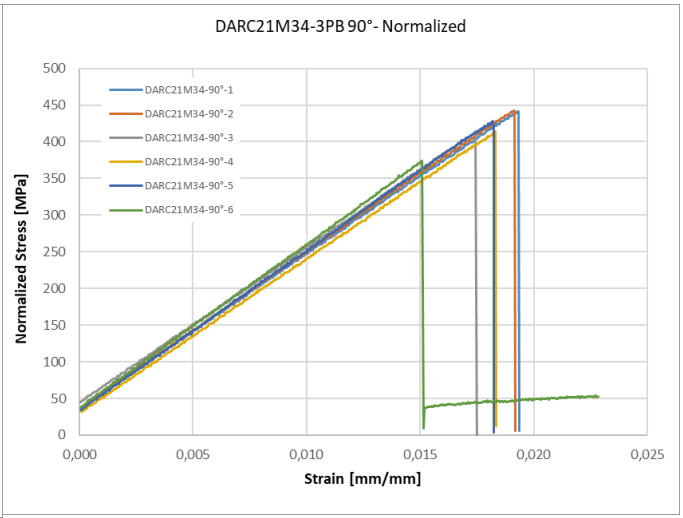

Figure 4.75: C200 Carbon Task IMP509 90° flexural stress-strain curves

Direction	Normalized Flexural strength [MPa]		Normalized Elastic Modulus [GPa]	
	Value	Std. deviation	Value	Std. deviation
0°	238,2	10,5	11,6	0,4
90°	419,3	25,5	21,4	0,5

Table 4.24: C200 Carbon Task IMP509 flexural performances

From the values of flexural strength and flexural elastic modulus obtained in the two directions it is possible to observe, consistently with what has already been observed before, that the material has better performances at 90° compared to the main direction of the material. It was also possible to observe that all the specimens arrived at failure earlier due to the tensile stress.

4.2.2.4⟶Energy absorption tests of C200 Carbon Task IMP509

Let us conclude the mechanical characterization of the C200 Carbon Task IMP509 with the analysis of the energy absorption tests in the event of an impact. For the energy absorption tests in a drop tower, 6 repetitions were carried out. The specimens were made by laminating 5 layers, thus obtaining a thickness of 1,99 mm with a real

percentage of resin of 63,5%, also in this case very low compared to the theoretical percentage of 70%. As can be seen from the following image, the material, in the event of an impact, presents a type of pulverization breakage.

Figure 4.76: Pulverized C200 Carbon Task IMP509's omega samples

In the following graph it is possible to observe the acceleration values measured during the drop tower tests.

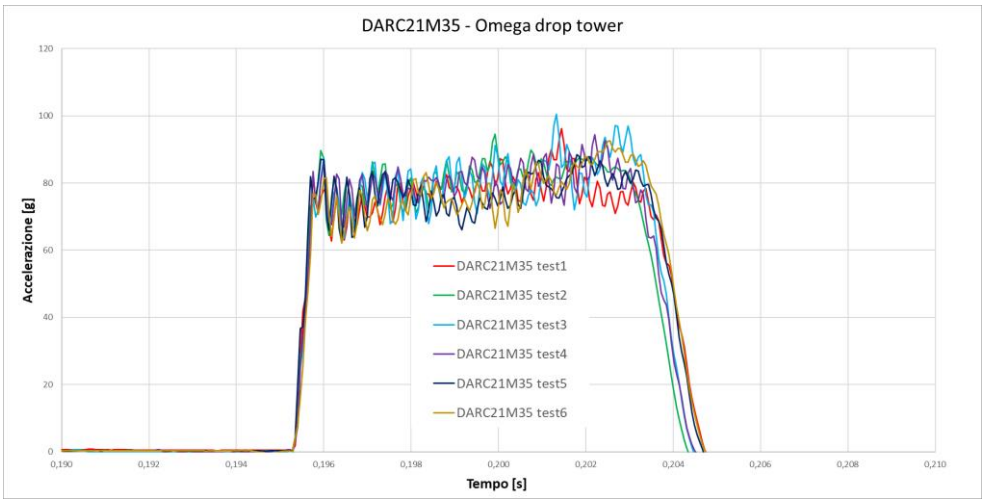

Figure 4.77: Acceleration curves of C200 Carbon Task IMP509's drop tower test

The energy absorbed during impact is measured in SEA [J\g]. The number of Joules absorbed per gram of material can be calculated in two ways that we indicate as calculated SEA and measured SEA. The measured SEA is obtained by considering the difference between the height of the specimen before the test and that after the test.

The measured SEA, instead, is obtained by considering the difference between the mass of the specimen before the test and that after being tested in the drop tower.

Below we indicate the values obtained for the two calculation methods with the corresponding standard deviations.

Property	C200 Carbon Task IMP509 [DARC21M35]	
1) Specific energy absorption		
	Value	Std. deviation
SEA measured [J/g]	**70,6**	**2,7**
SEA calculated [J/g]	**70,5**	**2,5**

Table 4.25: C200 Carbon Task IMP509 SEA values

The two calculated values are very close, and this indicates that the measurement performed is reliable. The material has excellent energy absorption properties.

4.2.2.5⟶C200 Carbon Task IMP509 test overview

To conclude, the analysis of the C200 Carbon Task IMP509 an overview of the values obtained for the different tests is provided.

Property	Standard	Panel A	Panel A NORM	Panel B	Panel B NORM	Average NORM value
1) Tensile properties						
Tensile strength σ 0° [MPa]	ASTM D 638	**223,1**	**191,6**	**231,8**	**186,6**	**189,1**
Tensile modulus E 0° [GPa]		**15,6**	**13,4**	**17,8**	**14,3**	**13,9**
Tensile strength σ 90° [MPa]		**381,5**	**327,7**	**390,3**	**341,1**	**334,4**
Tensile modulus E 90° [GPa]		**28,7**	**24,7**	**31,5**	**25,4**	**25,1**
Tensile strength σ 45° [MPa]	ASTM D 638	**270,6**	**232,4**	-	-	-
Tensile modulus E 45° [GPa]		**19,6**	**16,8**	-	-	-
2) Flexural properties						
3PB strength σ 0° [MPa]	ASTM D 790	-	-	**332,1**	**238,2**	-
3PB modulus E 0° [GPa]		-	-	**16,0**	**11,6**	-
3PB strength σ 90° [MPa]		-	-	**542,3**	**419,3**	-
3PB modulus E 90° [GPa]		-	-	**27,7**	**21,4**	-
3) Compressive properties						
Compressive strength σ 0° [MPa]	Boeing modified ASTM695 (SACMA SRM 1R-94)	**331,2**	**279,4**	-	-	-
Compressive strength σ 90° [MPa]		**413,7**	**353,3**	-	-	-
5) Specific energy absorption						
SEA measured [J/g]	-	**70,6**	-	-	-	-
SEA calculated [J/g]		**70,5**	-	-	-	-

Table 4.26: C200 Carbon Task IMP509 mechanical characterization overview

4.2.3⟶Mechanical characterization of C100 Carbon Task IMP512 BIO

The C100 Carbon Task IMP512 BIO is a short-fiber material impregnated with the IMP512 BIO resin. It differs from other short-fiber materials for its carbon weight. In fact, 100 grams of carbon per square meter can be found in it.

As for the mechanical characterization, we focused on energy absorption properties assuming similar properties for mechanical characteristics.

The only tests that were possible to carry out were those of energy absorption in a drop tower.

For this reason, only the impact tests will be analyzed, and a comparison will be made with other short-fiber materials but with a different carbon weight.

4.2.3.1⟶Energy absorption tests of C100 Carbon Task IMP512 BIO

The energy absorption test was carried out, as for the other short-fiber materials studied, in a drop tower with a series of 6 repetitions.

The C100 Carbon Task IMP512 BIO, characterized by a carbon weight halved compared to that of the other materials studied, requires the lamination of 10 layers to create the specimens. The thickness obtained is 1,97 mm with a real percentage of resin of 63,2%. We can also highlight in this case a non-negligible reduction in the percentage of resin compared to the theoretical one, in line with what was observed for all the other specimens of short-fiber materials.

The material, when subjected to an impact, pulverizes.

Figure 4.78: Pulverized C100 Carbon Task IMP512's omega samples

Below we can see the graph of the acceleration measured during the test.

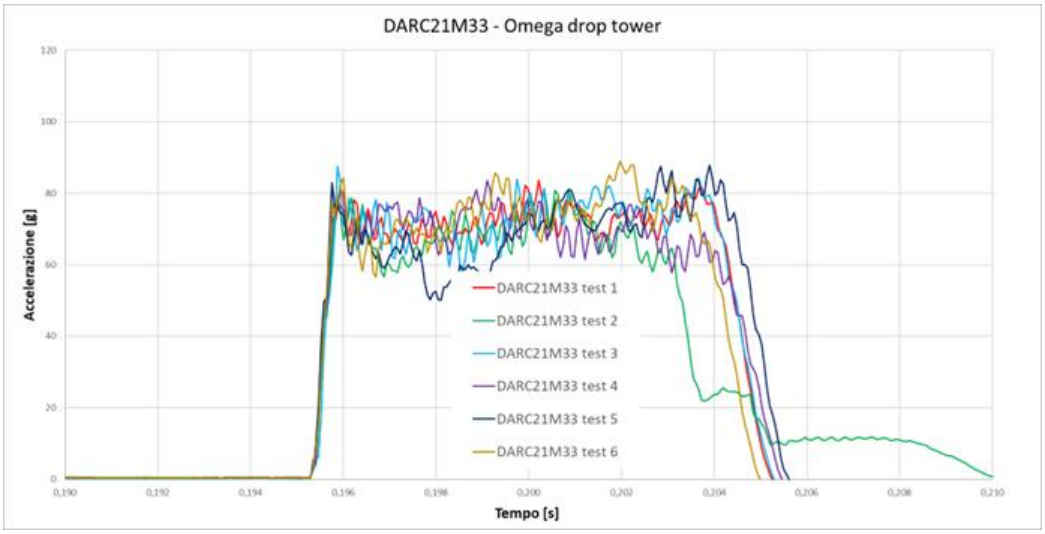

Figure 4.79: Acceleration curves of C100 Carbon Task IMP512's drop tower test

Below, it is possible to see the value of energy absorbed in the impact calculated in two different ways.

Property	C100 Carbon Task IMP512 BIO [DARC21M33]	
1) Specific energy absorption		
	Value	Std. deviation
SEA measured [J/g]	**64,5**	**1,8**
SEA calculated [J/g]	**64,8**	**3,0**

Table 4.27: C100 Carbon Task IMP512 SEA values

The value of energy (Joule) absorbed per gram of material is indicated with the SEA [J/g]. The SEA, as already mentioned for other short-fiber materials, can be measured in two ways, one based on the mass of the specimen, while the other is based on the measurement of its height.

The values measured in the two different ways are very similar and this indicates a good reliability of the data obtained. It can also be stated that the material has good energy absorption performance.

4.2.4⟶Comparison of short-fiber material mechanical performances

To evaluate the behavior of short-fiber materials, it is interesting to make a comparison between the values obtained for the different materials.

Having two short-fiber materials with the same fabric (Carbon Task) and the same areal weight (200 grams per square meter) but one impregnated with bio-resin (IMP512 BIO) and the other with a similar resin but with all the synthetic precursors (IMP509), it is possible to make a comparison between the two materials and understand how much the use of bio-resin influences the mechanical characteristics of the material.

Furthermore, having the data relating to the energy absorption tests of two materials impregnated with the same bio-resin (IMP512 BIO) but with different carbon weights, it is possible to analyze the effect of the different weights on the energy absorption performance of the material.

Let us start by comparing the tensile, compression, bending and energy absorption tests of the C200 Carbon Task IMP512 BIO and the C200 Carbon Task IMP509.

Now it is analyzed the values of tensile strength and elastic modulus obtained for the two materials at 0°, 90° and 45° with respect to the main direction of the material.

Below we can see the stress-strain curves obtained from the tensile tests at 0° for the two materials in the two different panels.

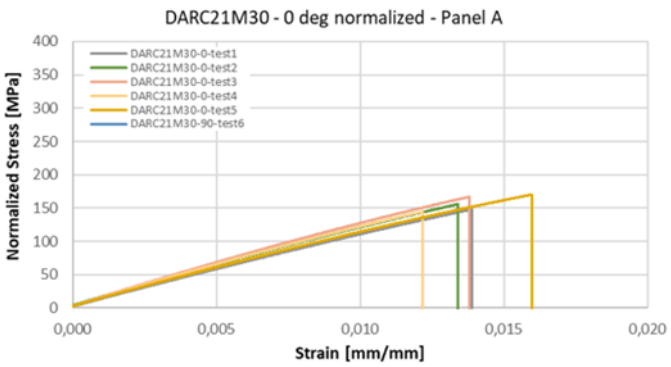

Figure 4.80: C200 Carbon Task IMP512 0°tensile stress-strain curves panel A

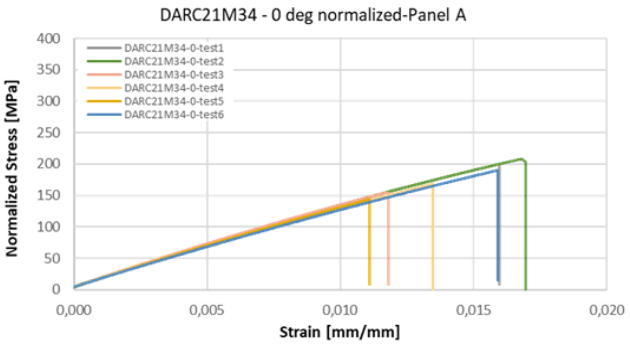

Figure 4.81: C200 Carbon Task IMP509 0°tensile stress-strain curves panel A

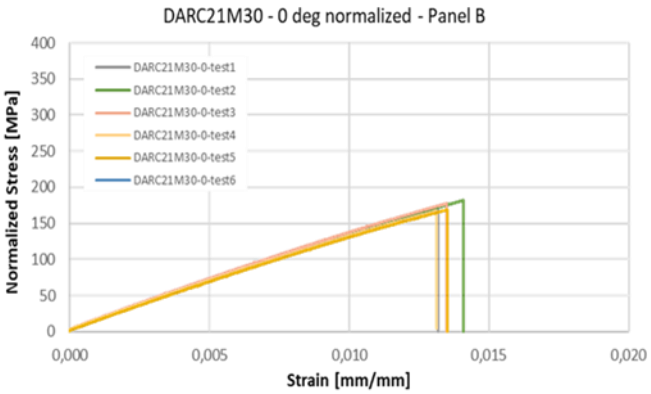

Figure 4.82: C200 Carbon Task IMP512 0°tensile stress-strain curves panel B

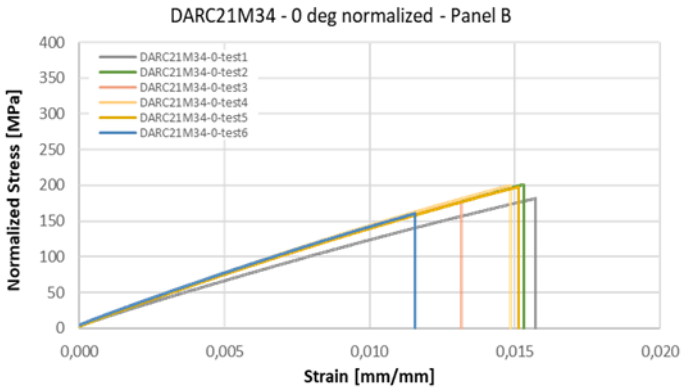

Figure 4.83: C200 Carbon Task IMP509 0°tensile stress-strain curves panel B

Direction 0°				
Material	C200 Carbon Task IMP512 BIO [TCX00259]		C200 Carbon Task IMP509 [TCX00257]	
	Value	Std. deviation	Value	Std. deviation
Average normalized Tensile strength [MPa]	165,3	9,1	189,1	15,6
Average normalized Elastic Modulus [GPa]	13,1	0,6	13,9	0,6

Table 4.28: Short fibers materials 0° tensile performances comparison

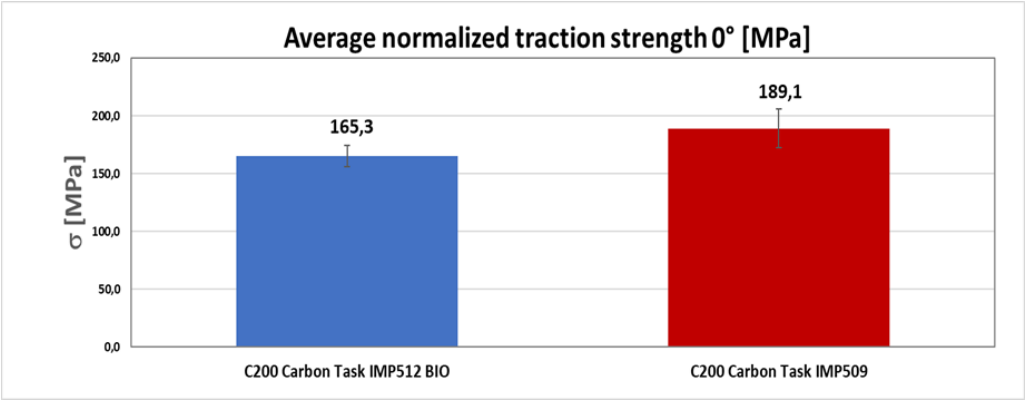

Figure 4.84: Short fibers materials 0° tensile strength comparison

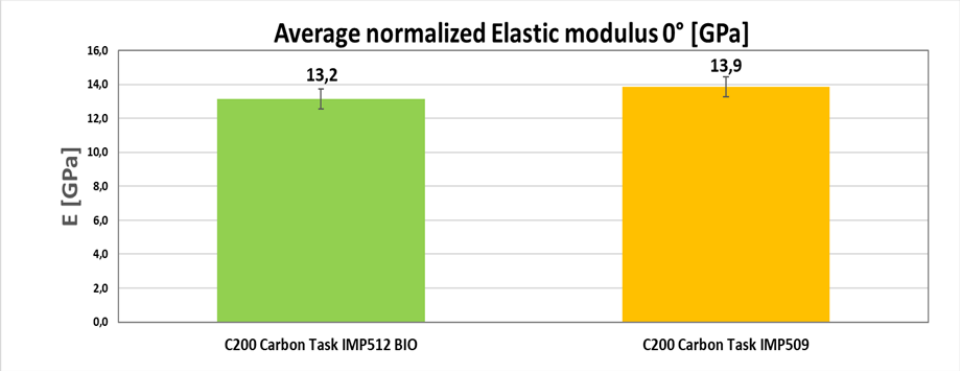

Figure 4.85: Short fibers materials 0° tensile modulus comparison

It is essential to note that the use of bio resin instead of standard resin does not have a significant effect on the 0° tensile performance of the material.

Let us now move on to the analysis of the data obtained through the 90° tensile tests.

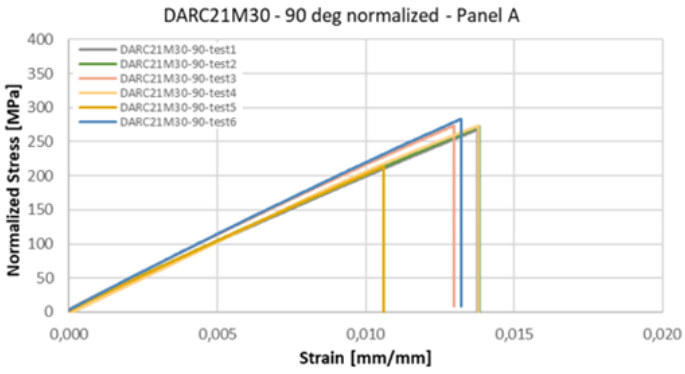

Figure 4.86: C200 Carbon Task IMP512 90°tensile stress-strain curves panel A

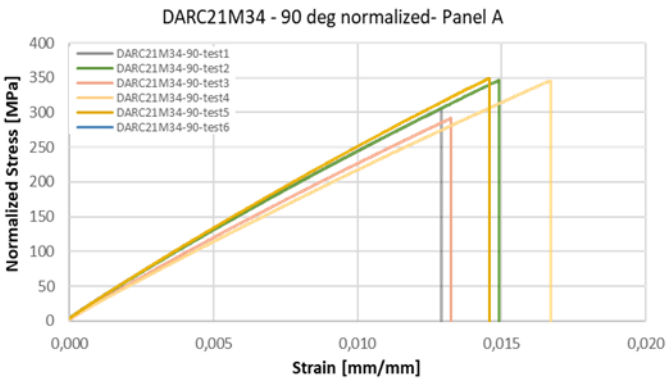

Figure 4.87: C200 Carbon Task IMP512 0°tensile stress-strain curves panel A

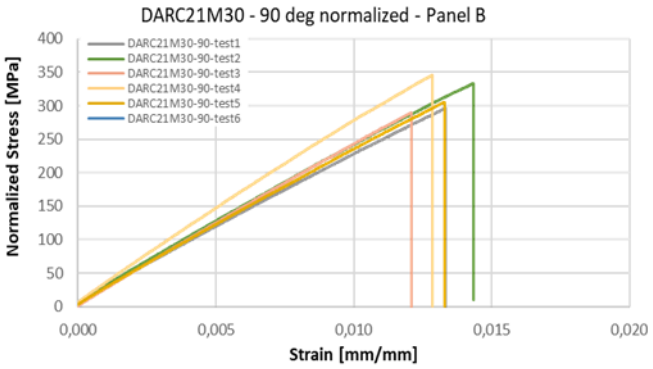

Figure 4.88: C200 Carbon Task IMP512 90°tensile stress-strain curves panel B

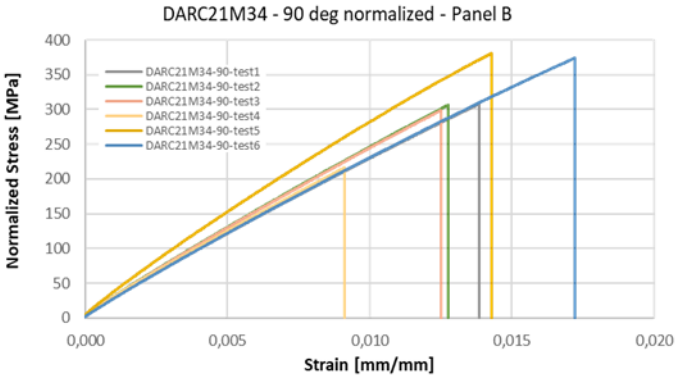

Figure 4.89: C200 Carbon Task IMP509 90°tensile stress-strain curves panel B

Direction 90°				
Material	C200 Carbon Task IMP512 BIO [TCX00259]		C200 Carbon Task IMP509 [TCX00257]	
	Value	Std. deviation	Value	Std. deviation
Average normalized Tensile strength [MPa]	289,1	24,7	334,4	46,5
Average normalized Elastic Modulus [GPa]	22,9	1,6	25,1	1,9

Table 4.29: Short fibers materials 90° tensile performances comparison

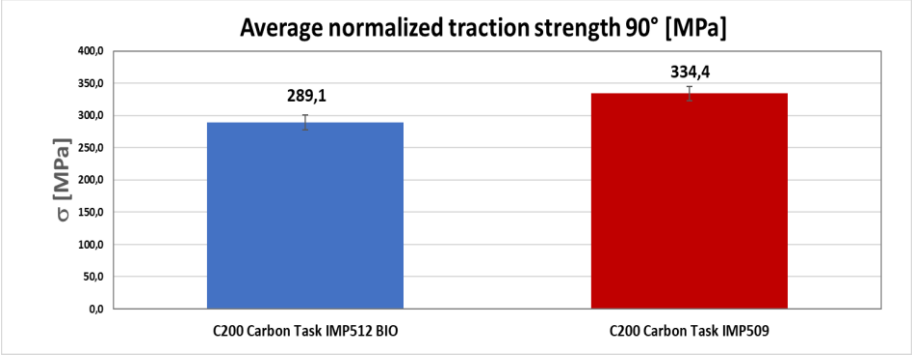

Figure 4.90: Short fibers materials 90° tensile strength comparison

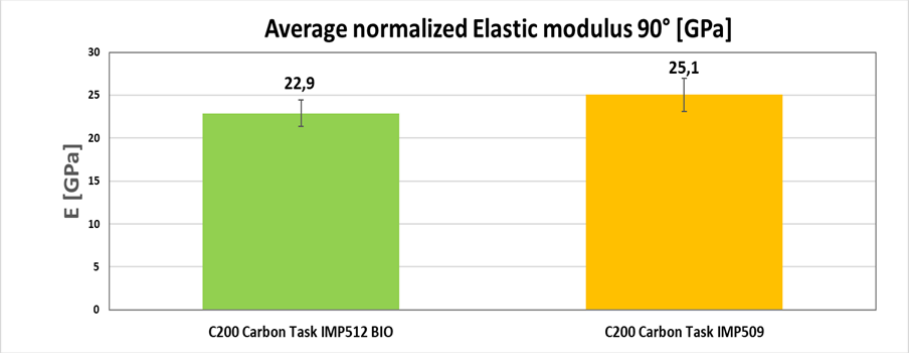

Figure 4.91: Short fibers materials 90° tensile modulus comparison

Even for the values of tensile strength and elastic modulus obtained at 90° it is possible to note that the use of bio resin does not have a significant effect on the mechanical performance of the material. We can also state that the data confirms what was already declared by the manufacturing company, that the material has the best mechanical performance at 90° with respect to the main direction.

Below we analyze the properties of materials subjected to traction at 45°.

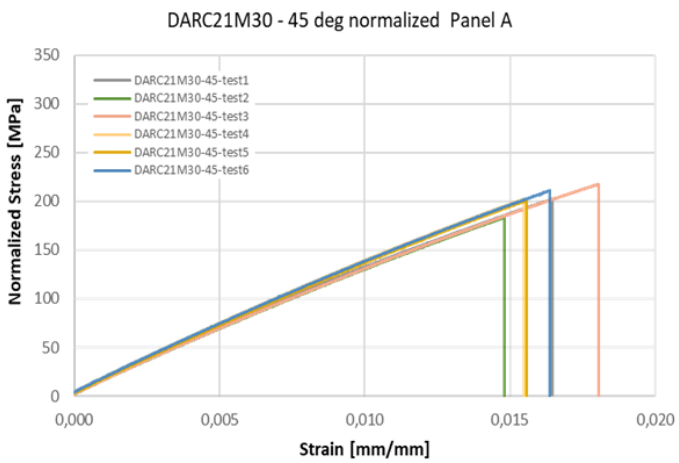

Figure 4.92: C200 Carbon Task IMP512 45°tensile stress-strain curves

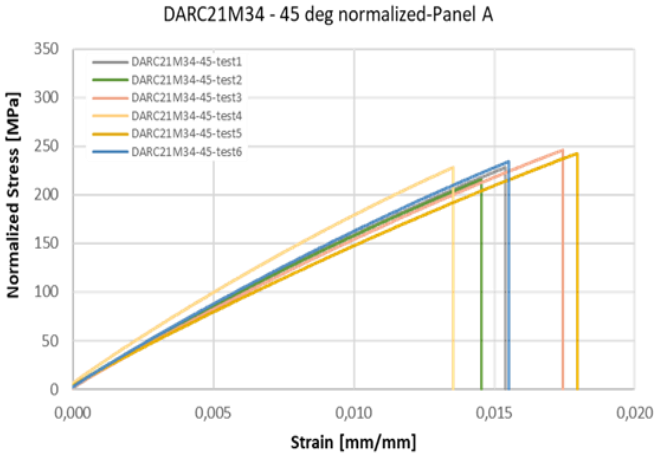

Figure 4.93: C200 Carbon Task IMP509 45°tensile stress-strain curves

Direction 45°				
Material	C200 Carbon Task IMP512 BIO [TCX00259]		C200 Carbon Task IMP509 [TCX00257]	
	Value	Std. deviation	Value	Std. deviation
Average normalized Tensile strength [MPa]	202,8	11,5	232,4	11,0
Average normalized Elastic Modulus [GPa]	13,8	0,3	16,8	1,2

Table 4.30: Short fibers materials 45° tensile performances comparison

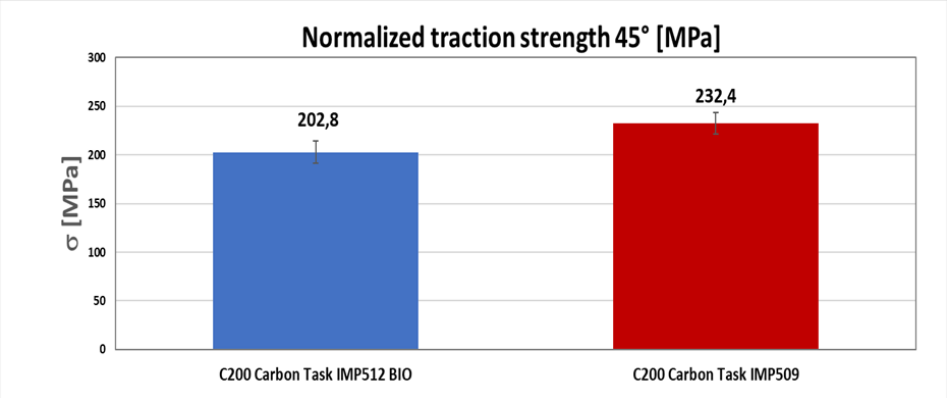

Figure 4.94: Short fibers materials 45° tensile strength comparison

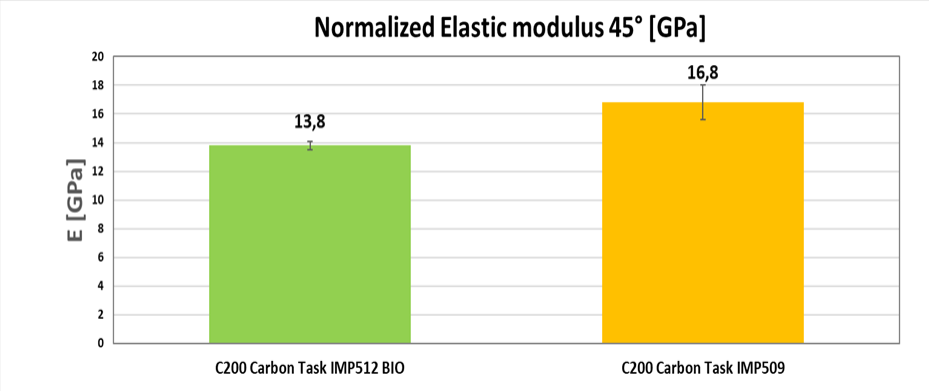

Figure 4.95: Short fibers materials 45° tensile modulus comparison

Observing the values obtained from the 45° traction test, it is possible to state that the use of bio resin causes a slight reduction in the traction strength and a non-negligible reduction in the tensile elastic modulus at 45°.

Let us now move on to the analysis of the compression tests at 0° and 90°. Below we can see the stress-strain data obtained for the two materials in different directions and the histograms representing the values obtained with the corresponding standard deviations.

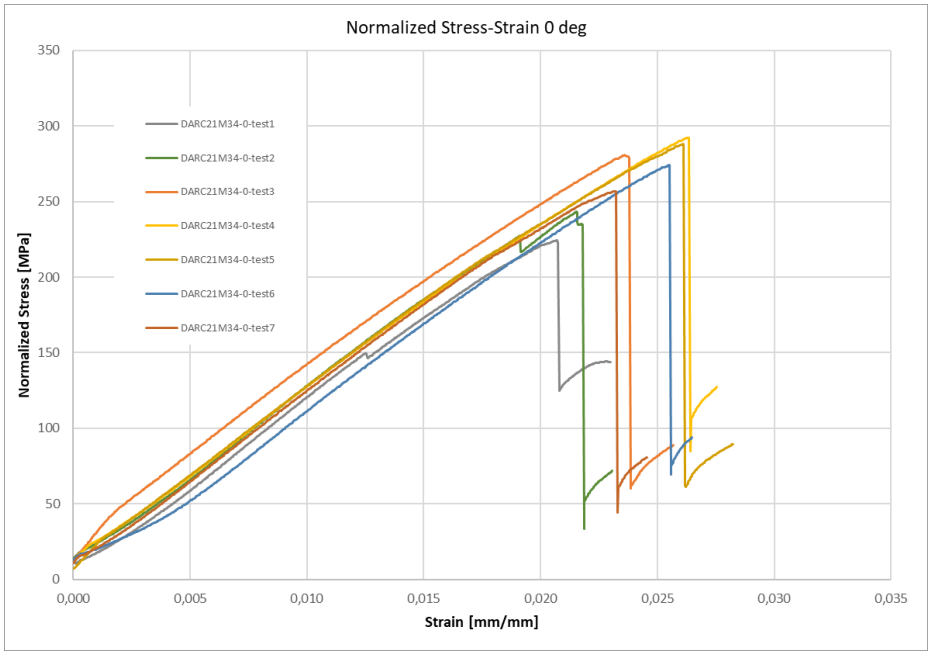

Figure 4.96: C200 Carbon Task IMP509 0°compression stress-strain curves

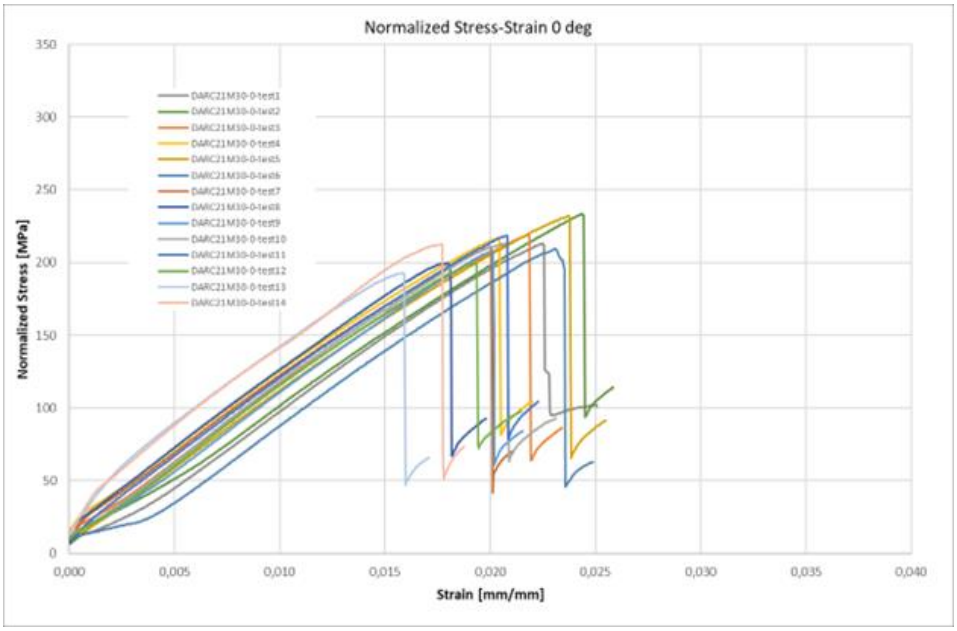

Figure 4.97: C200 Carbon Task IMP512 0°compression stress-strain curves

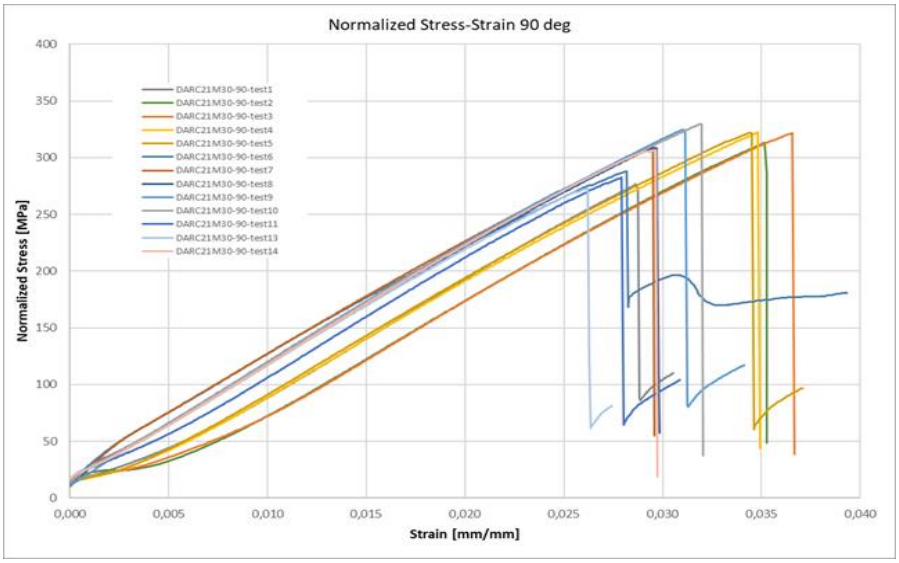

Figure 4.98: C200 Carbon Task IMP512 90°compression stress-strain curves

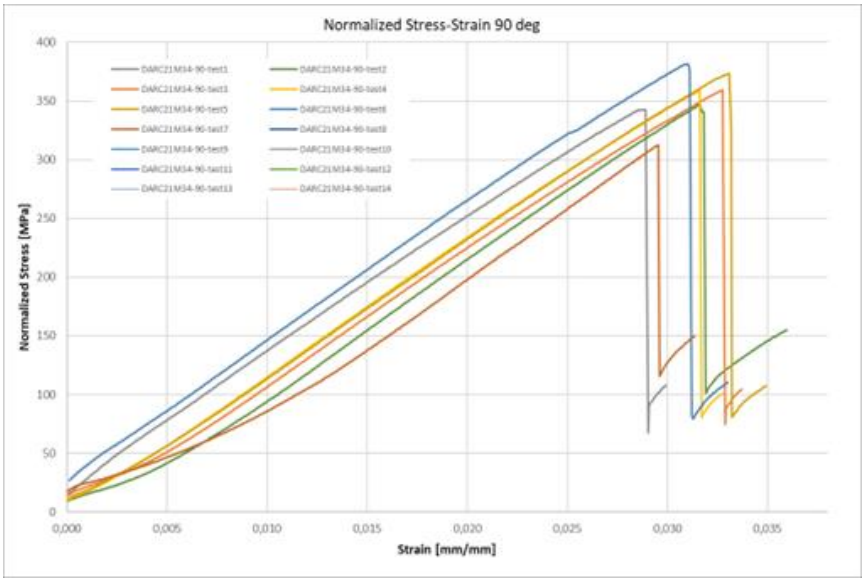

Figure 4.99: C200 Carbon Task IMP509 90°compression stress-strain curves

Material	C200 Carbon Task IMP512 BIO		C200 Carbon Task IMP509	
	Value	Std. deviation	Value	Std. deviation
Norm. Compression strength 0°	211,0	10,0	279,4	15,8
Norm. Compression strength 90°	307,5	19,7	353,3	18,2

Table 4.31: Short fibers materials compression performances comparison

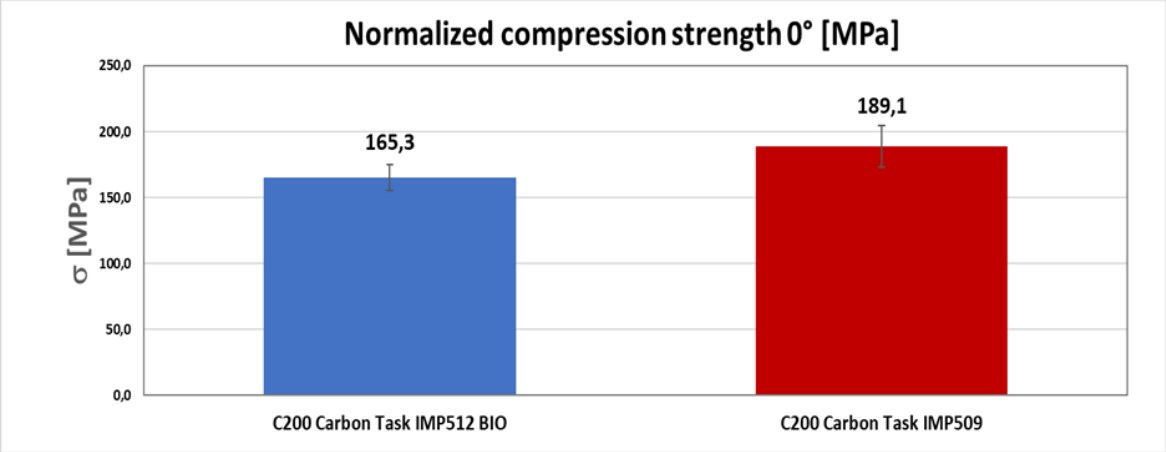

Figure 4.100: Short fiber materials 0° compression strength comparison

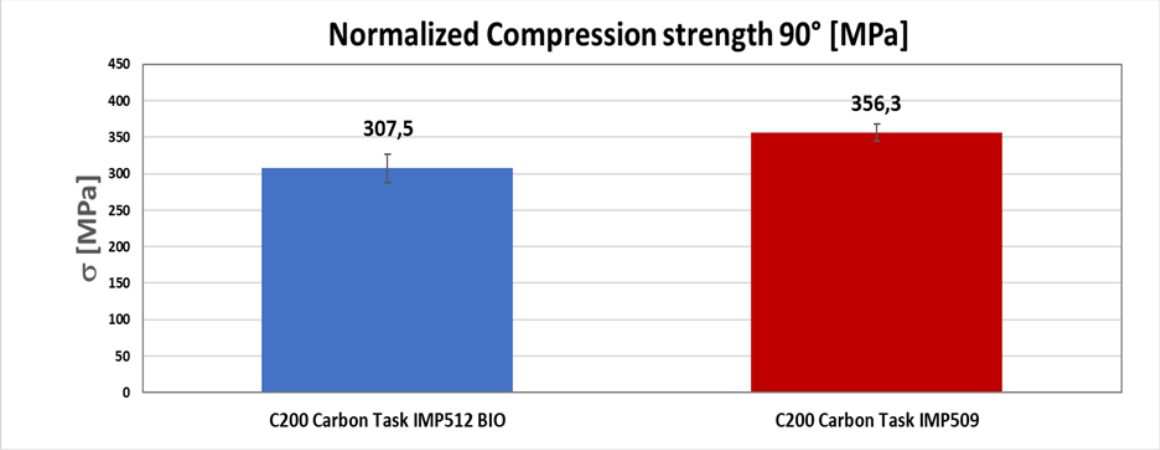

Figure 4.101: Short fiber materials 90° compression strength comparison

From the observation of the data obtained for the compression tests it is possible to state that the use of bio resins slightly reduces the compression performance of the material in both directions considered.

Let us now move on to the analysis of the data obtained from the 0° and 90° bending tests.

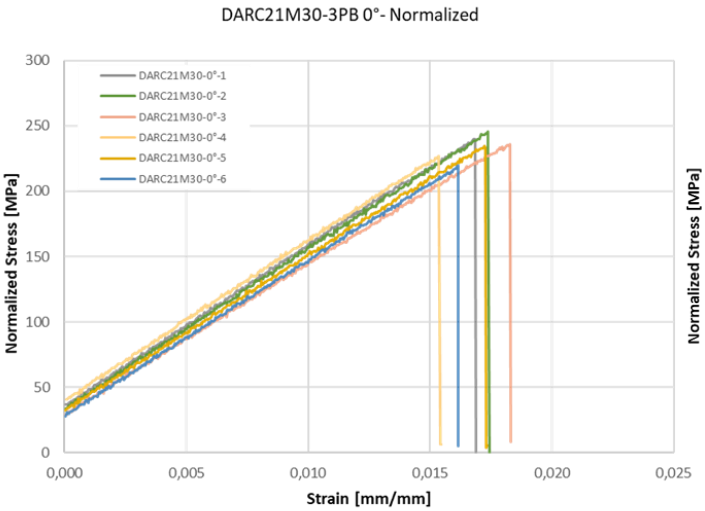

Figure 4.102: C200 Carbon Task IMP512 0°flexural stress-strain curves

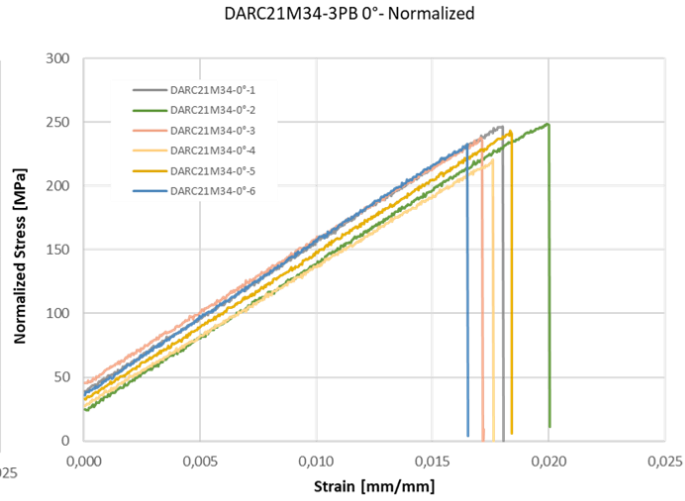

Figure 4.103: C200 Carbon Task IMP509 0°flexural stress-strain curves

Material	Normalized Flexural strength [MPa]		Normalized Elastic Modulus [GPa]	
	Value	Std. deviation	Value	Std. deviation
C200 Carbon Task IMP512 BIO	233,7	9,3	12,0	0,3
C200 Carbon Task IMP509	238,2	10,5	11,6	0,4

Table 4.32: Short fibers materials 0°flexural performances comparison

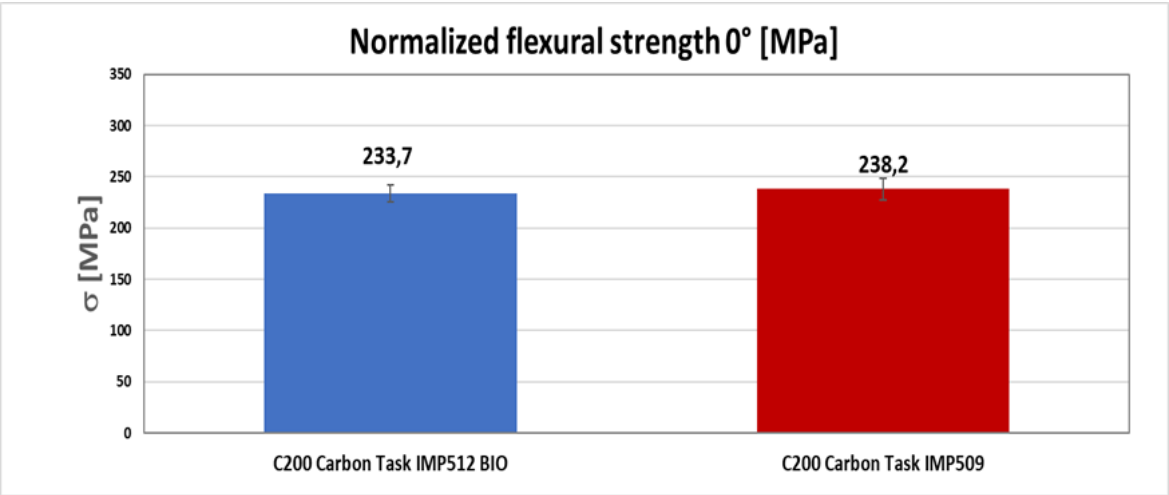

Figure 4.104: Short fibers materials 0° flexural strength comparison

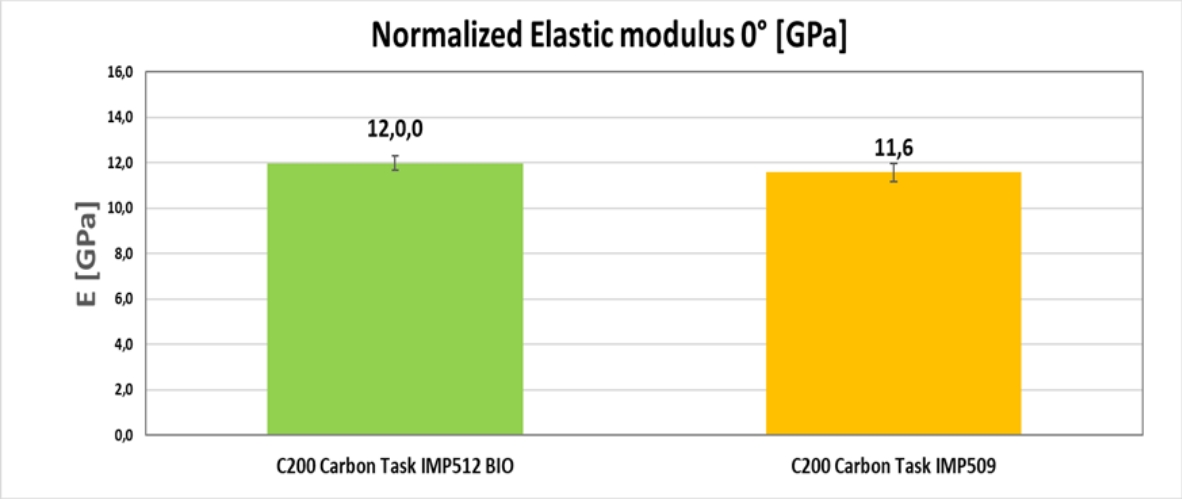

Figure 4.105: Short fibers materials 0° flexural modulus comparison

For the 0° bending tests, the behavior of the two materials both in terms of flexural strength and elastic modulus coincides.

For this reason, we can state that the use of bio resin in the 0° bending tests has no detectable effect on mechanical performance.

Let us now look at the curves and data obtained for the 90° flexural tests.

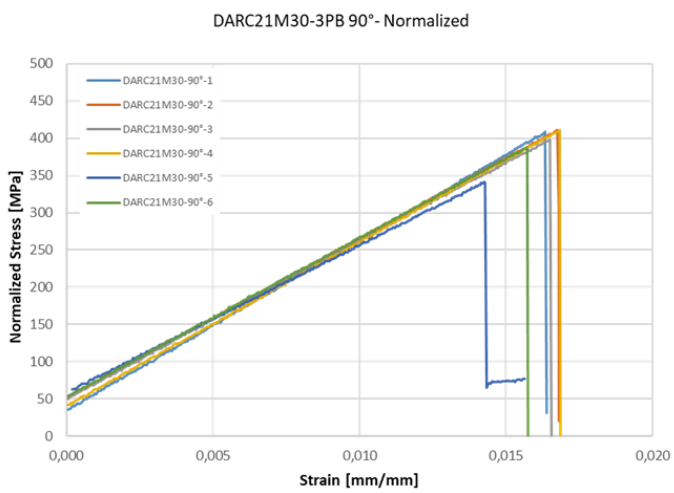

Figure 4.106: C200 Carbon Task IMP512 90°flexural stress-strain curves

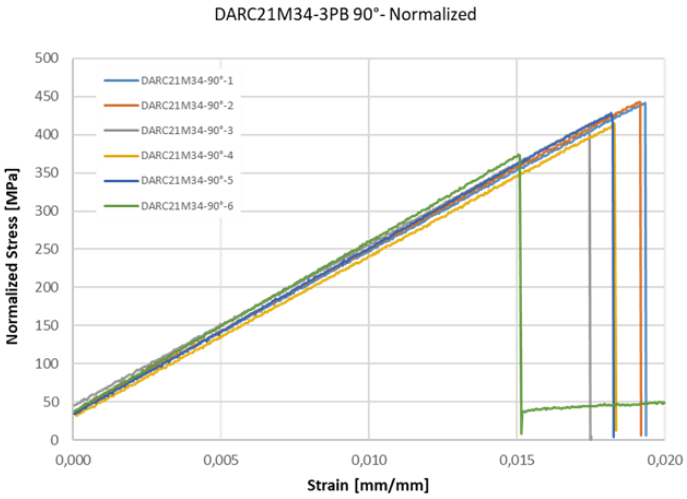

Figure 4.107: C200 Carbon Task IMP509 90°flexural stress-strain curves

Material	Normalized Flexural strength [MPa]		Normalized Elastic Modulus [GPa]	
	Value	Std. deviation	Value	Std. deviation
C200 Carbon Task IMP512 BIO	392,7	27,0	20,2	4,1
C200 Carbon Task IMP509	419,3	25,5	21,4	0,5

Table 4.33: Short fibers materials 90°flexural performances comparison

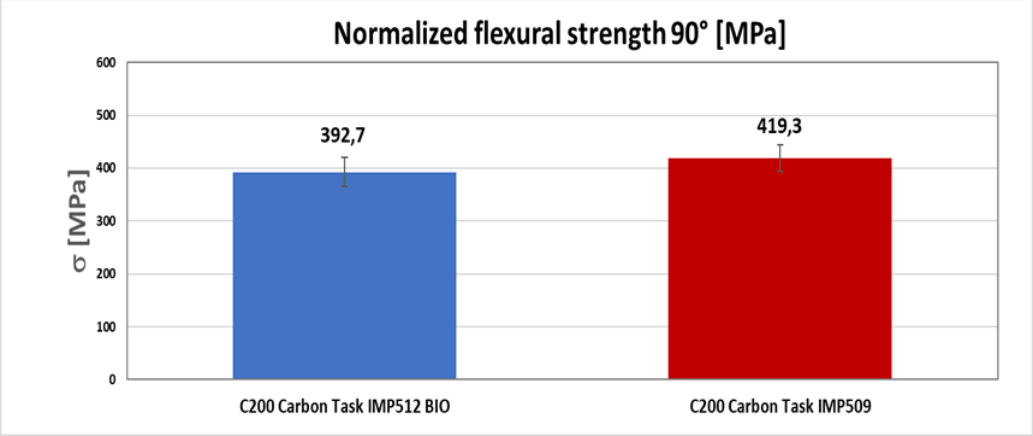

Figure 4.108: Short fibers materials 90° flexural strength comparison

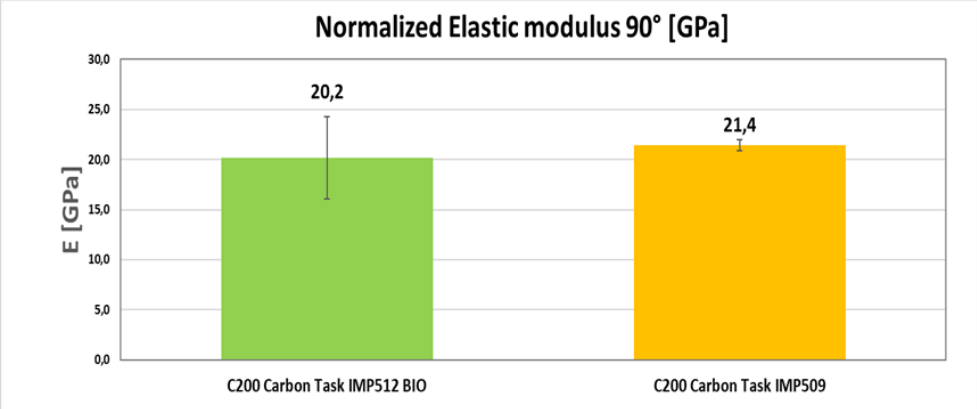

Figure 4.109: Short fibers materials 90° flexural modulus comparison

Also, in this case the behavior of the two materials is perfectly superimposable. It is, therefore, possible to affirm that the use of the bio resin has no significant effects on the performance of the material in bending either at 90° or at 0° with respect to the main direction of the material.

To conclude our analysis, let us make a comparison between the data obtained for the energy absorption tests.

We will start by making a comparison between the data obtained between the two materials with the same carbon weight but impregnated one with the bio resin and the other with the standard resin (C200 Carbon Task IMP512 BIO and C200 Carbon Task IMP509). As we can see from the following images of the tested specimens, both materials show a pulverization impact failure.

Figure 4.110: C200 Carbon Task IMP512 omega sample

Figure 4.111: C200 Carbon Task IMP509 omega sample

Property	C200 Carbon Task IMP512 BIO [DARC21M31]		C200 Carbon Task IMP509 [DARC21M35]	
1) Specific energy absorption				
	Value	Std. deviation	Value	Std. deviation
SEA measured [J/g]	67,7	4,1	70,6	2,7
SEA calculated [J/g]	67,0	4,2	70,5	2,5

Table 4.34: C200 short fiber materials SEA values comparison

The energy absorption values obtained for the two materials are very close, so it can be said that the use of bio resin has a negligible effect on the energy absorption performance of the material.

Let's now move on to a comparison between the two materials impregnated with bio resin (IMP512 BIO), but with a different carbon weight (C200 Carbon Task IMP512 BIO and C100 Carbon Task IMP512 BIO).

Figure 4.112: C200 Carbon Task IMP512 omega sample

Figure 4.113: C100 Carbon Task IMP512 omega sample

Even the C100 Carbon Task IMP512 BIO pulverizes in case of impact. We can therefore affirm that all the studied short-fiber materials in case of impact have a type of pulverization breakage.

Property	C200 Carbon Task IMP512 BIO [DARC21M31]		C100 Carbon Task IMP512 BIO [DARC21M33]	
1) Specific energy absorption				
	Value	Std. deviation	Value	Std. deviation
SEA measured [J/g]	67,7	4,1	64,5	1,8
SEA calculated [J/g]	67,0	4,2	64,8	3,0

Table 4.35: IMP512 impregnated short fiber materials SEA values comparison

The SEA values in this case are also very close and the behavior of the two materials is therefore superimposable.

The following histograms compare SEA values calculated in the two different methods for all three materials.

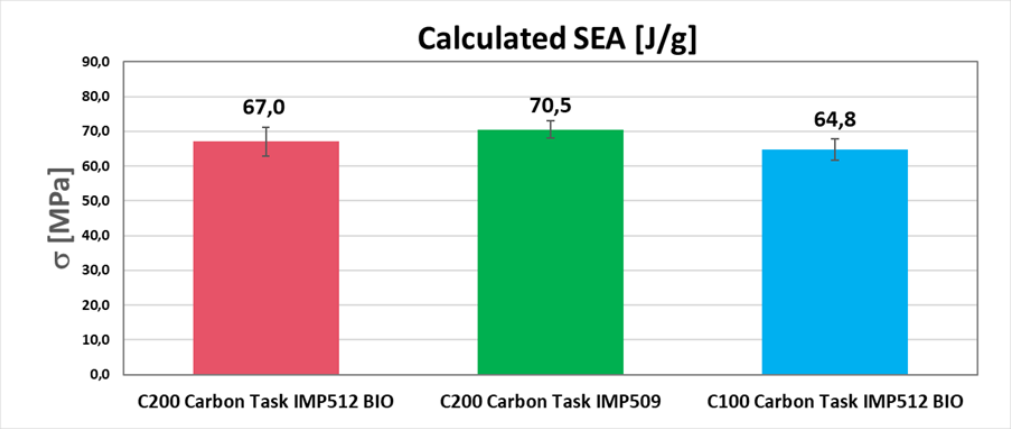

Figure 4.114: Short fibers materials calculated SEA values comparison

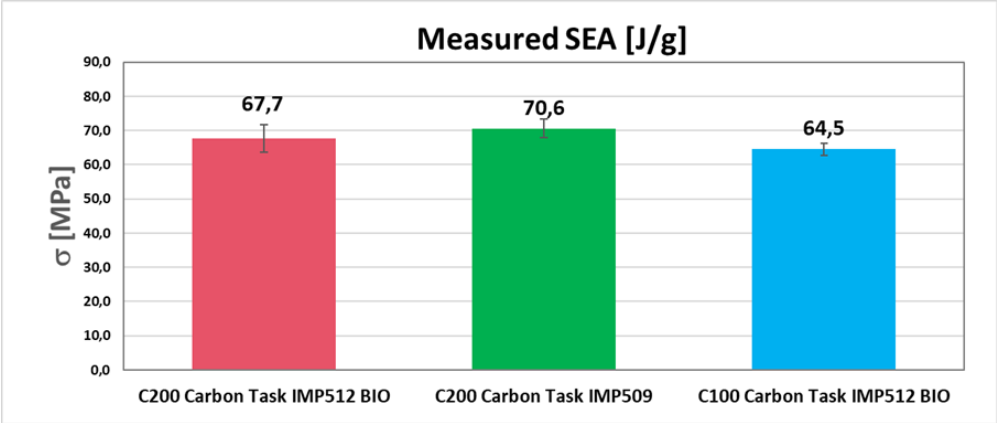

Figure 4.115: Short fibers materials measured SEA values comparison

Considering the two methods of calculating SEA, the considerations that can be made are consistent. It is, in fact, possible to highlight that the behavior of the three materials is superimposable, and it is, therefore, impossible to detect an effect of the use of bio resin on the mechanical impact performances of our material. Furthermore, even the use of a greater or lesser weight of carbon does not affect the energy absorption characteristics.

In general, the SEA values of the three materials, if compared with the performances of other materials with similar characteristics present in the database, are very good.

The above presented analysis, that is considering a throughout mechanical characterization of two materials with the same reinforcement and impregnated by resins belonging to the bio-based epoxy category (IMP512) and standard epoxy one (IMP509) together with the last analysis on the change of areal weight of reinforcement

(C200 Carbon Task IMP512 BIO and C100 Carbon Task IMP512 BIO), demonstrates that:

- The biobased resin has the mechanical properties of the standard epoxy within the experimental errors.
- The process of compression molding that was used to prepare the plates for the mechanical tests as well as the samples for energy absorption characterization is adequate to guarantee good laminate quality, thus opening possible new applications of these non-woven materials.

4.3→Dynamic Mechanical Analysis test

To evaluate the mechanical behavior of the materials studied at different temperatures, identify their glass transition temperatures and evaluate the quality of the production process followed, a Dynamic Mechanical Analysis test was carried out for each material. It is possible, in fact, that the specimens processed in a press or in an autoclave with a shorter curing time than that followed by the supplier, are unable to develop the maximum glass transition temperature declared by the prepreg supplier *Angeloni Group* for the resin with which the materials are impregnated.

The Dynamic Mechanical analysis tests are tests in which the specimens are subjected to an oscillating load or deformation while the temperature of the environment in which the test is performed is varied. During the test, the two components of the elastic modulus of the material (the viscous one and the linear one) are measured. It is, therefore, possible to detect the temperature at which our specimen will pass from an glassy state to a viscous behavior (glass transition).

The tests were performed according to the ASTM D 7028 standard. The specimen is heated at a rate of 5°C/min and the sinusoidal force is applied with a frequency of 1 Hz and the specimens used have a rectangular shape of 60 by 13 mm.

In the following graphs we will see two curves, one relating to the storage modulus (which represents the elastic part of the elastic modulus of the material) and the other called *Tan (Delta)* which is given by the ratio of the loss modulus (*E''*) and the storage modulus (*E'*).

The value of T_g (glass transition temperature) can be calculated in two different ways.

According to the homeset method, the intersection between the straight line representing the first part of the storage modulus curve and the straight-line tangent to the *E'* curve at the point of its maximum curvature must be considered. In this way we have the real value of the glass transition temperature of the tested material.

According to the method based on *Tan(Delta)*, instead, we go to consider the point in which the *Tan(Delta)* curve has its maximum and we go to take the corresponding temperature. The temperature measured in this way, however, is not the glass transition temperature of our material but the temperature at which the studied material will exert the maximum dumping. In DMA tests, the glass transition temperature is calculated based on the mechanical properties of the specimens, while DSC tests calculate it based on the heat absorbed by the specimen during the test, therefore the values we obtain might be different from the one declared by the provider since its value is influenced by the mechanical properties of the fibers.

4.3.1⟶Dynamic Mechanical Analysis of long-fiber materials

Let's now analyze the data obtained from DMA tests for long fiber materials.

This graph was obtained through the DMA test of a sample of C370 MR60 24K IMP512 BIO 38%.

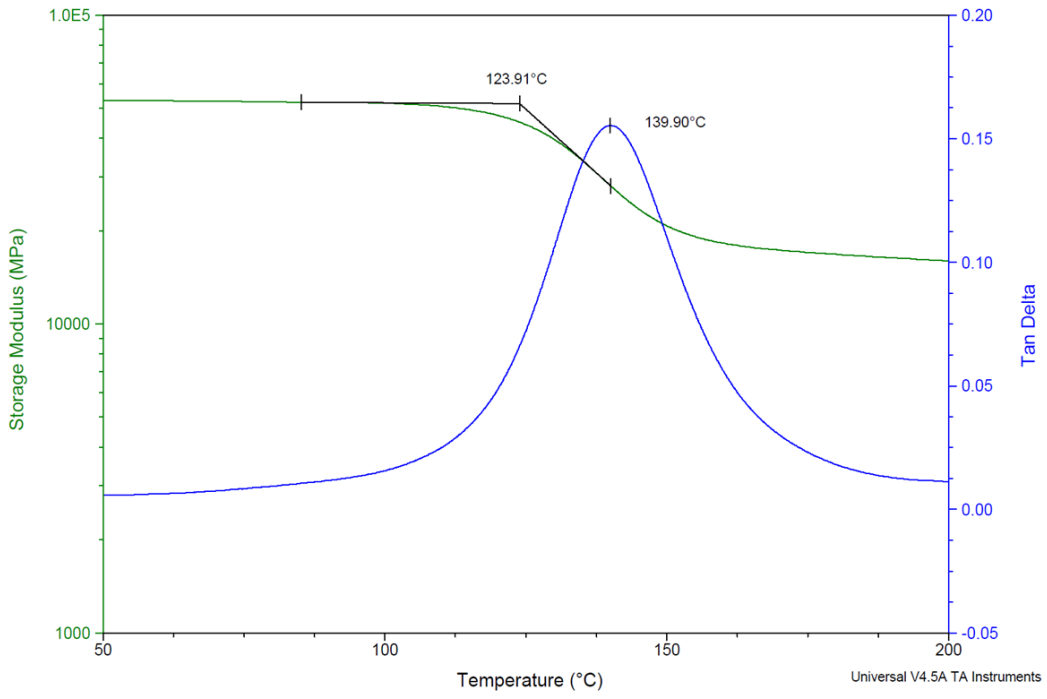

Figure 4.116: C370MR60 24K IMP512 BIO 38% DMA test results

From this graph, it is possible to extract two main pieces of information: the glass transition temperature of the material and the temperature at which the maximum dumping occurs by the material.

The temperature at which the specimen begins its glass transition is the one indicated on the storage modulus curve, with a value of 123,91 °C.

The peak temperature of the material damping, at which the viscous part of the material modulus reaches its maximum value, is instead 139,90 °C.

The maximum glass transition temperature declared by the supplier, achievable with the 90-minute curing cycle at 135 °C, is 140 °C, therefore higher than that obtained.

The cycle used to produce the specimens, in fact, was 90 minutes at 135 °C at a pressure of 6 bar, as prescribed. The T_g value obtained, not being too far from the maximum value indicated, is in line with what was declared by the supplier, in fact the Tg measured by the DMA is influenced also by the mechanical characteristics of the fibers.

Let us now move on to the analysis of the values obtained from the Dynamic Mechanical Analysis tests of the specimens made in C630 TR50 IMP512 BIO 34%.

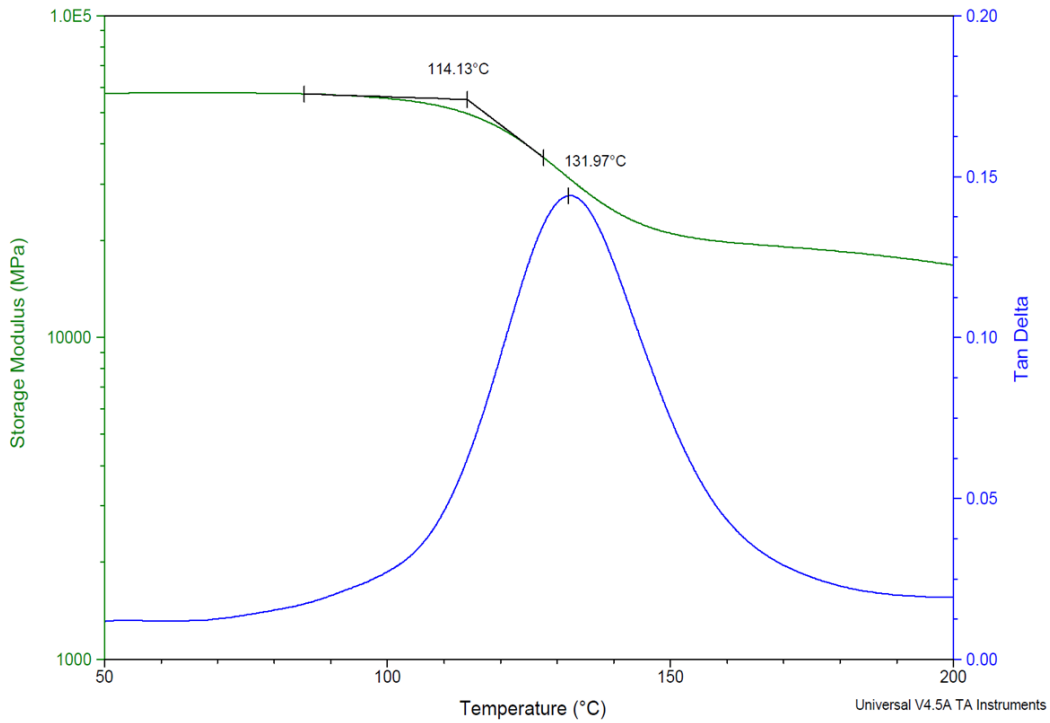

Figure 4.117: C630 TR50 12K IMP512 BIO 34% DMA test results

The glass transition temperature measured in this case is 114.13 °C and in this case, it is lower than that declared by *Angeloni Group*. The peak temperature of *Tan(Delta)* at which the material reaches the maximum value of the loss modulus (*E''*) is instead 131.97 °C. The samples of C630 TR60 IMP 512 BIO 34% were also made according to the prescribed cycle of 90 minutes at 135 °C at a pressure of 6 bar and in this case the material is unable to develop the maximum T_g declared by the supplier of 140 °C. However, since the value obtained is quite close to the declared one, we can say that considering the possible random environmental factors that may have influenced the production process, and the mechanical effect of the fibers on DMA measuring, the T_g value obtained is in line with what was declared by the supplier.

4.3.2⟶Dynamic Mechanical Analysis of short-fiber materials

In this section, we will analyze Dynamic Mechanical Analysis tests related to the specimens obtained from the three short-fiber materials studied.

All the sample, as reported above, were taken from the plates realized for the mechanical characterization and were processed through press.

We begin with the observation of the data obtained for the C200 Carbon Task IMP512 BIO test.

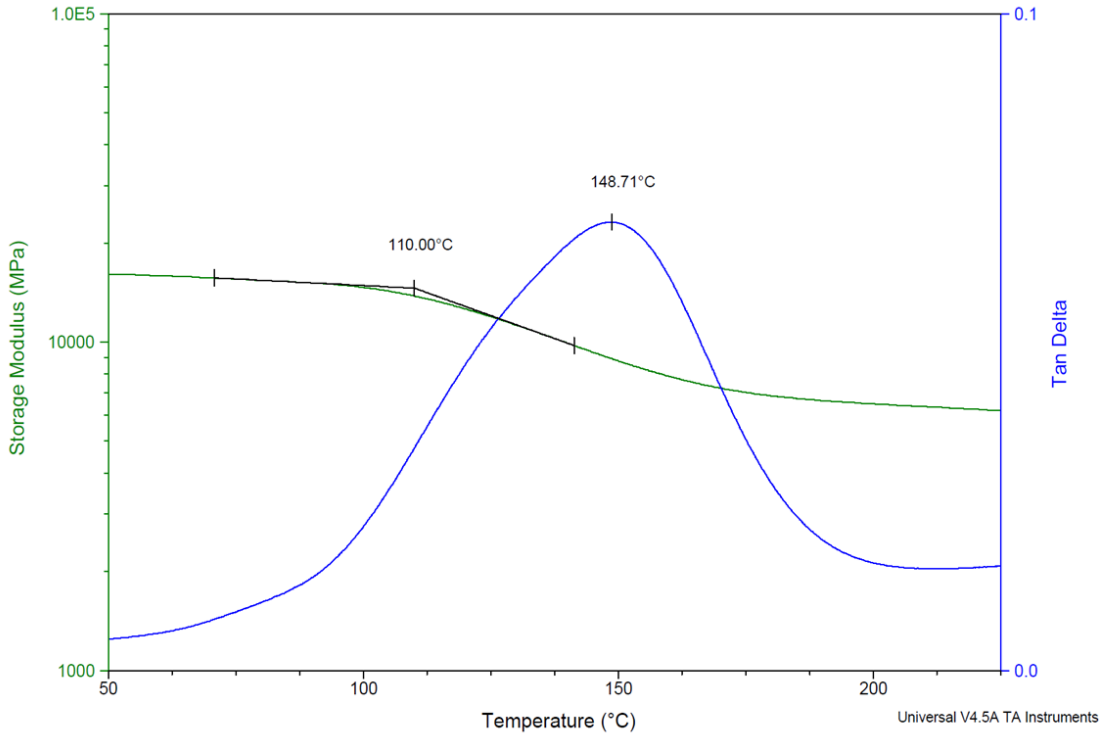

Figure 4.118: C200 Carbon Task IMP512 BIO DMA test results

Also in this case, from the graphs obtained we can obtain the value of the glass transition temperature and the temperature at which the loss modulus of the material is maximum. The T_g obtained is 110,00 °C while the peak *Tan(Delta)* is 148,71 °C. The obtained value of T_g is much lower than the expected value. Therefore, the effect of the mechanical properties of the fibers it not enough to justify this difference.

The glass transition temperature declared by Angeloni is 140 °C for the resin processed in an autoclave at 135 °C for 90 minutes. The short fiber specimens, however, were made in a press with the application of a force of 30 tons, a preheating time of 145 seconds, a curing time of 15 minutes at a temperature of 135 °C. It is, therefore, possible that the bio resin IMP512 BIO processed with the indicated press cycle is not able to develop its maximum glass transition temperature. Again, the graph shows a change in the slope of the *Tan(Delta)* curve before reaching its maximum value and this could be indicative of the lack of total polymerization of the thesis during the test. This hypothesis will then be verified with the help of differential scanning calorimetry tests.

In the following graph, we can observe what was obtained from the DMA test for the material impregnated with the resin in its standard version (C200 Carbon Task IMP509).

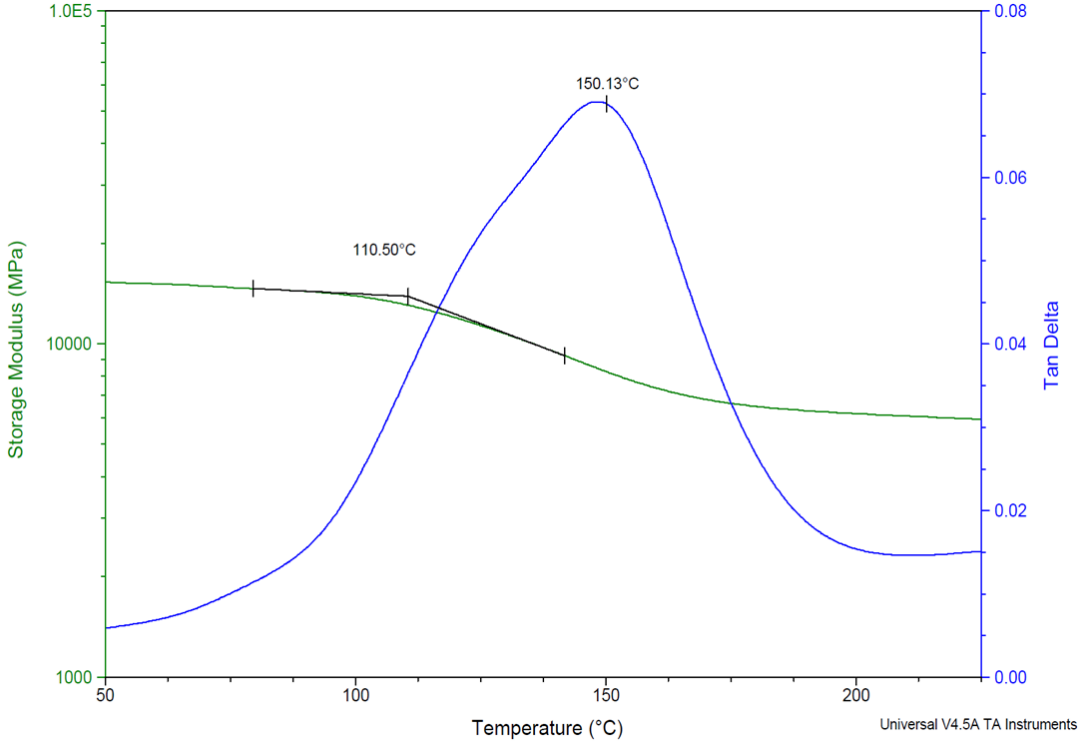

Figure 4.119: C200 Carbon Task IMP509 DMA test results

The temperature at which the glass transition of the material begins recorded is 110,5 °C. Also, in this case the value obtained is significantly lower than that declared by the supplier. The temperature value at which the dissipative behavior of the material is maximum, however, is 150,13 °C.

All the short fiber materials were processed by press with the same cure cycle indicated for the C200 Carbon Task IMP512 BIO. Also in this case, the very low T_g value obtained can be justified by the fact that the press cycle followed does not allow the resin to develop the maximum declared T_g of 140 °C, obtained with a production process in an autoclave at 135 °C for 90 minutes and at a pressure of 6 bar. In line with what was observed for the material impregnated with the bio resin, also in this case it is possible to observe a change in the slope of the *Tan(Delta)* curve before reaching the maximum peak. This may indicate that the material did not fully polymerize during the test and will be verified with a Differential Scanning Calorimetry test.

Finally, let's move on to the analysis of the values obtained for the C100 Carbon Task IMP512 BIO.

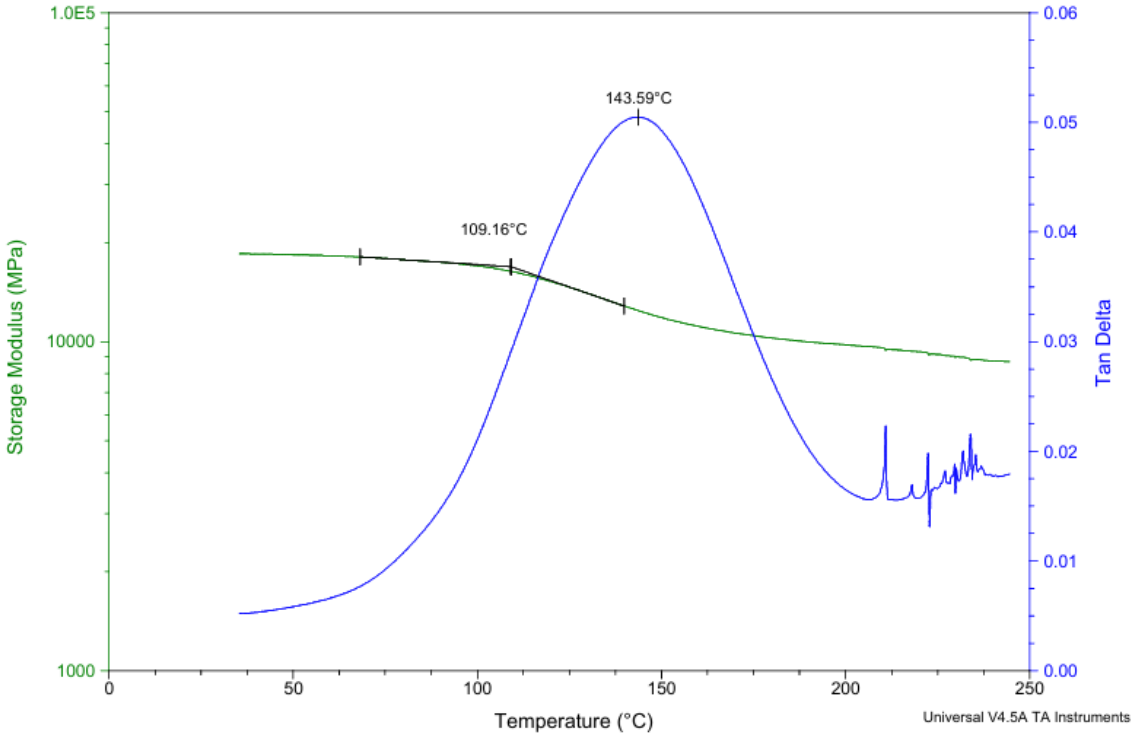

Figure 4.120: C100 Carbon Task IMP512 BIO DMA test results

For the material with the lower carbon weight, the glass transition temperature obtained of 109,16 °C is much lower than the declared 140 °C.

The peak temperature of the *Tan(Delta)* measured is 143,59 °C. Also, in this case it is possible to notice a slight variation of concavity before reaching the maximum of the curve, even if in a much less evident way than for the other two short fiber materials.

All the short fiber materials were processed with the same press cycle, present the change of concavity of the *Tan(Delta)* curve and present very low T_g values compared to the declared one, but at the same time with very coherent values between them.

Having, therefore, obtained very close T_g values both for the materials impregnated with the bio resin and for those impregnated with the standard resin, we can highlight that the use of this bio resin is equivalent to that of the standard resin, as regards the value of the T_g developed.

To evaluate whether the reduction in T_g is due to the lack of total polymerization of the material, Differential Scanning Calorimetry tests will be carried out on all materials.

4.4→Differential Scanning Calorimetry test

The values of glass transition temperature measured with DMA, for the short fiber materials, may be so far from those declared by the supplier, either because the material processed in the press is not able to develop the maximum T_g, due to the chosen cure cycle, or because the process defined by us in the press is not fully optimized. This was a new research activity.

Differential scanning calorimetry tests were carried out to verify these hypotheses.

The differential scanning calorimetry test allows us to measure the maximum value of glass transition temperature that a material can develop when processed in a certain way, as well as the enthalpy of reaction.

This thermal technique measures the T_g of the material considering only the thermodynamic properties of the material and not the mechanical ones as for DMA. The mechanical behavior recorded by DMA, in fact, is also influenced by the characteristics of the fibers. DSC only measures the behavior of the part of the composite material that polymerizes (the resin), because the temperatures reached are insufficient to induce transformations in the fibers of the material being tested.

For this reason, it provides us with a different insight on the thermal properties of the material and in particular is very useful in the case problems with partial polymerization of the specimens.

The DSC measures how much energy it has to be supplied to the specimen to have and increasing of its temperature and this energy will have a maximum or minimum

for reaching the glass transition temperature which corresponds to a transition of the state of the material. The curve of the DSC graph shows on the x-axis the temperature to which the specimen is to be brought, while on the y-axis, it plots the difference between the heat flow supplied to the reference sample and that supplied to the specimen.

To perform the test, we place the specimen of the material to be analyzed in the controlled temperature area where there are a series of thermocouples. The instrument measures the heat flow exchanged in two points of the controlled temperature area. The sample to be tested will be placed in one point while the reference sample will be placed in the other. Two cycles are then performed in which the tempering is increased and then decreased from -25 °C to 250 °C with a temperature increase rate of 10 °C/min (according to ASTM E 2160), in order to evaluate the enthalpy of reaction. The first cycle is used to bring the sample to complete cure, while in the second the sample is completely cured and therefore, we should not notice any maximum or minimum of the curve.

The value of T_g that it is possible to obtain from the first heating cycle, takes into account the processing history of the sample, therefore it represents the temperature of glass transition corresponding to the considered sample processed according to the specific processing cycle followed to obtain it. From the first heating cycle, by evaluating residual enthalpy, it is possible to deduce if the followed curing cycle, allowed to completely cure the sample. If the sample has been completely cured during the processing phase, we should not see any peaks even during the first heating cycle.

The value of T_g obtained from the second heating cycle, instead, it is the maximum value of glass transition temperature that the sample will have processed according to the optimum curing cycle.

The area under the maximum or minimum peaks of the curve that can be found during the first heating cycle represents the residual enthalpy. This represents the amount of energy that we must supply to our sample to complete the cure, and it also represents the energy that the polymer releases during the curing process.

DSCs can be performed on already cured samples to understand their actual thermal state and reached glass transition temperature.

For samples that have not been fully cured, to understand what the missing percentage of polymerization is, it is sufficient to perform a proportion between the enthalpy measured on an a virgin material sample and the one evaluated on the sample.

When our sample is not undergoing any phase transformation, the difference between the two flows will be zero, but when the sample is changing phase, we will have a flow difference other than zero and therefore a change in the curve.

Thermosetting materials, such as those studied, during the curing phase present a peak in the curve, in fact, the polymerization is witnessed by an exothermic transformation that involves the formation of bonds, as the glassy state is a short-range order state. The glass transition temperature, as it is a second order phase transition, it appears as a flex in the curve.

4.4.1⟶Differential Scanning Calorimetry of long-fiber materials

Let us now move on to the analysis of the results obtained for the tests on long-fiber materials.

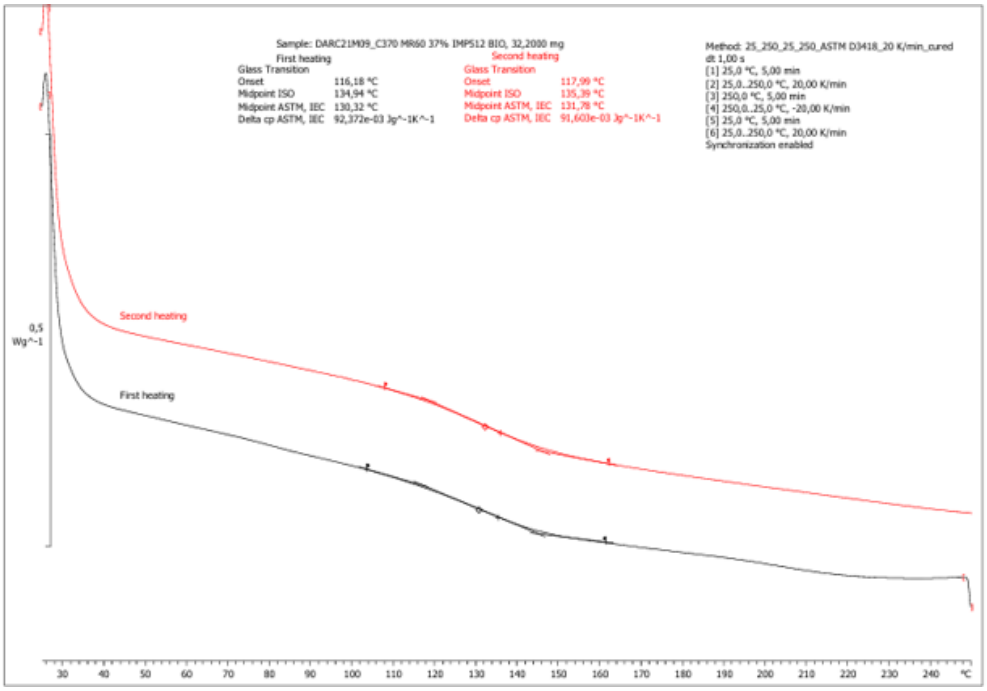

Figure 4.121: C370 MR60 IMP512 BIO 38% DSC test results

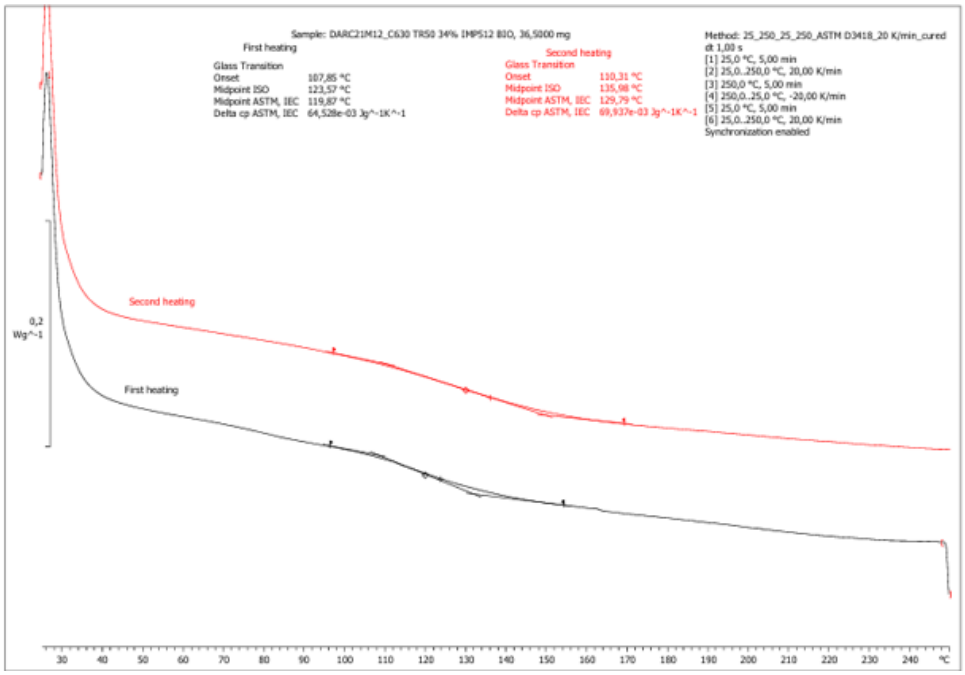

Figure 4.122: C630 TR50 IMP512 BIO 34% DSC test results

For both materials it is possible to note that both curves of the two heating cycles do not present peaks. This allows us to state that the materials have been completely cured during the processing phase. The measured T_g values are for the C370 MR60 IMP512 BIO of 130,32°C, while for the C630 TR50 IMP512 BIO of 119,87 °C. The T_g obtained through the DSC are very similar and therefore consistent with those obtained with the DMA and the samples have been completely polymerized during the processing phase. It is, therefore, possible to say that the curing cycle performed in the autoclave for long-fiber materials is the most appropriate and it allows a complete cure of the laminate. Moreover, it is possible to notice that also the values of T_g obtained from the second heating cycle of the DSC, that should be the maximum obtainable by the material, are slightly lower than the one declared by the producer. This might be caused by the fact that the glass transition temperatures provided have been measured by using a sample only made of resin, instead the sample considered in this study is also made of fibers which might influence the final measurement.

4.4.2⟶Differential Scanning Calorimetry of short-fiber materials

We conclude the chapter concerning the mechanical characterizations of the materials studied with the analysis of the differential scanning calorimetry tests performed on the three short-fiber materials analyzed. All three presented very low T_g values measured through the DMA and *Tan(Delta)* curves with variations in inclination

before reaching the maximum peak. For this reason, it is worth checking the possibility that the specimens, all made according to the same press cycle, were cured completely or not.

Below we find first the graph obtained for the C200 Carbon Task IMP512 BIO specimen, then the one obtained for the C200 Carbon Task IMP509 specimen and finally the one relating to the C100 Carbon Task IMP512 BIO specimen.

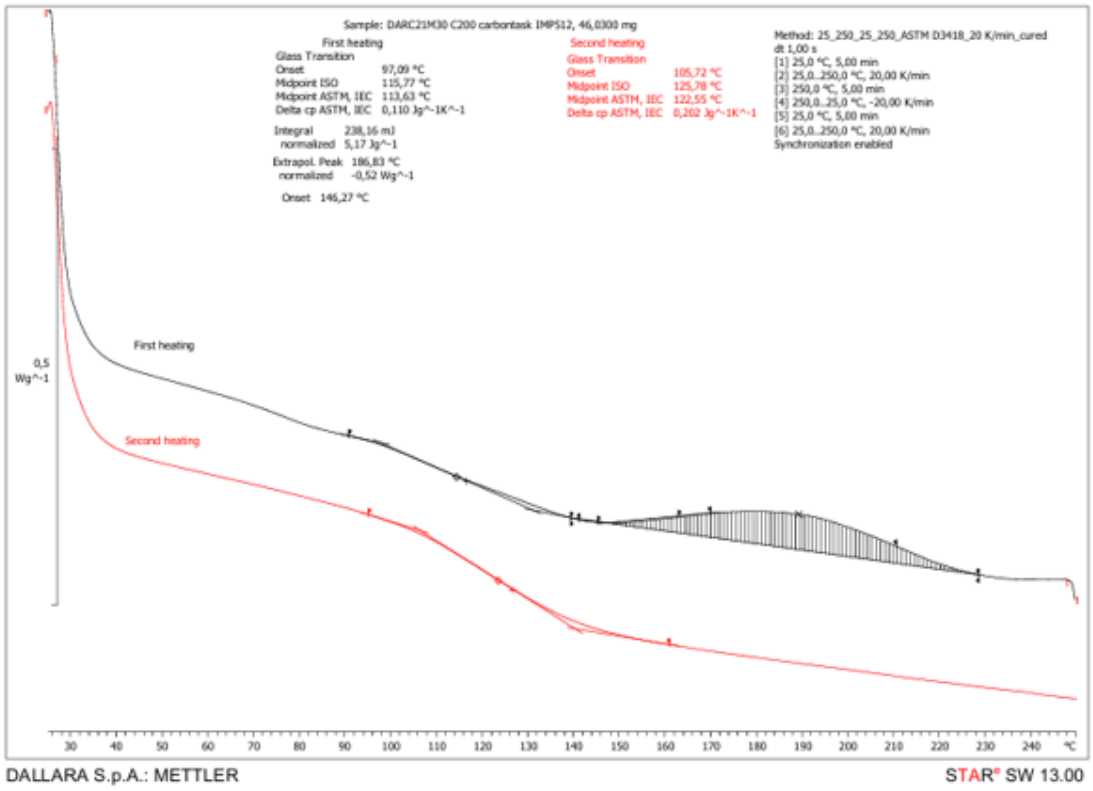

Figure 4.123: C200 Carbon Task IMP512 BIO DSC test results

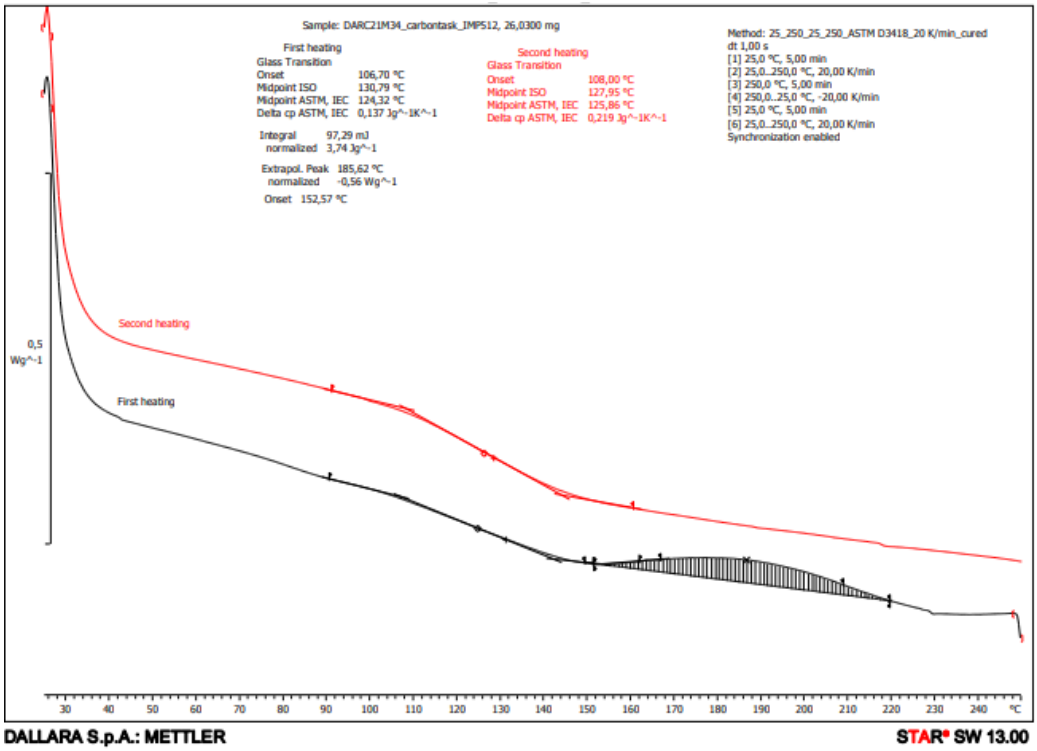

Figure 4.124: C200 Carbon Task IMP509 DSC test results

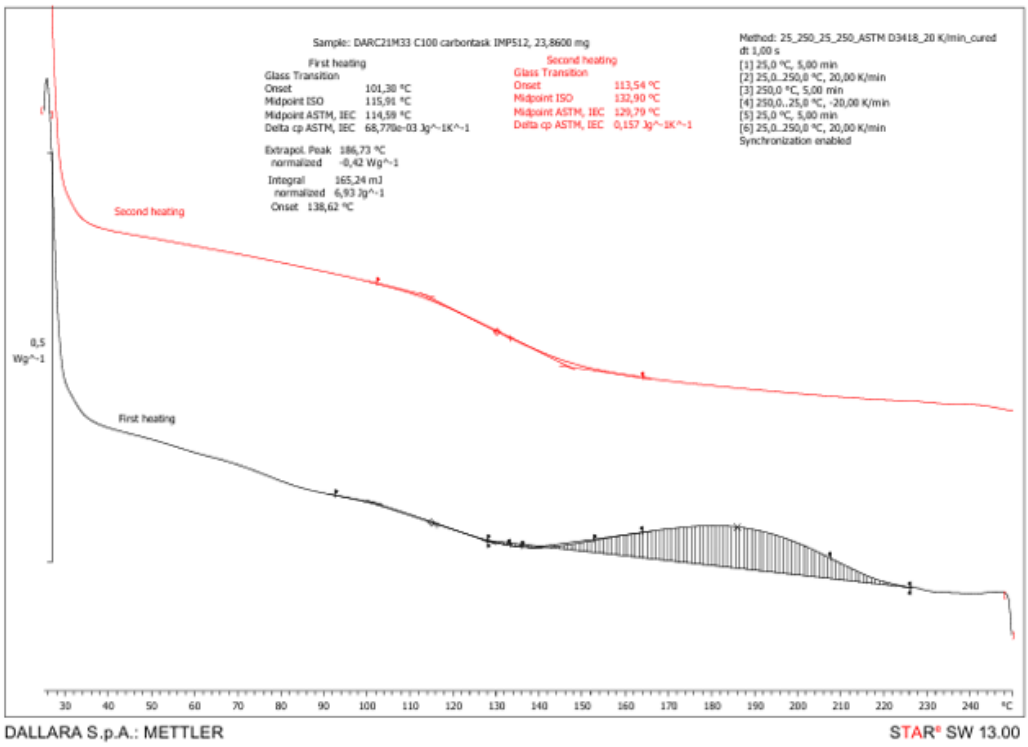

Figure 4.125: C100 Carbon Task IMP512 BIO DSC test results

All three materials tested show a peak residual enthalpy of approximately 5% during the first heating cycle (black curve). This indicates that the specimens were not fully cured during press processing. The T_g values measured with DSC for the three materials are 114°C for the C200 Carbon Task IMP512 BIO, 124°C for the C200 Carbon Task IMP509 and 114°C for the C100 Carbon Task IMP512 BIO. The T_g values obtained with DMA are slightly different from those obtained with DSC, as they are influenced by the mechanical characteristics of the material, but they are very similar with each other. The failure to fully cure the specimens indicates that with a longer curing cycle of 15 or 20 minutes it would have been possible to obtain higher T_g values.

Moreover, all the T_g measured with the second heating cycle, which should be the maximum possible values reachable by the material studied are slightly different from the one declared by *Angeloni Group*. This might be because by the fact that the tested samples are made of both short fibers and resin, while the ones considered for the provided values are made of only resin.

Finally, it is also possible to note from the values obtained by the DSC that the specimen made with the standard resin manages to reach higher glass transition temperatures than those impregnated with the bio resin.

5.→Applications

The current geopolitical situation and the ever-increasing interest in environmental issues has led to a growing interest in reducing CO_2 emissions and energy consumption.

In this context, as we have already described, bio-based composite materials, with fibers and/or resins of natural origin, are gaining ground. The uses of these innovative materials are countless and touch all fields of application.

ESA has collaborated with Côte D'Azur University in France to research bio-derived resins for aerospace applications. [61]

Airbus is committed to leading the decarbonization of the aerospace sector. This involves reducing CO_2 production at all stages of the life cycle of the components it uses. As a result, it has initiated a number of initiatives and research projects that go in this direction, such as research in the area of bio-based composite materials for the production of wings or tanks. Of note is a research project in which bio composites, derived from wood and food waste, were used to make the nose panel of Airbus Helicopters' H145 Pioneer Lab helicopter. [62]

Figure 5.1: Airbus Helicopters' H145 Pioneer Lab

In general, in aerospace, composite materials are already being used even if minimally in cabin and cargo construction due to their high flammability, density and insulation properties and for making primary and secondary structures. [63]

Bio resin composite materials are also attracting great interest in the field of children's toy manufacturing and are pushing studies in this direction as well.

In fact, bisphenol-free bio resins are safer for children's health.

It is possible to mention, among others, the work of researchers at Rajamangala University of Technology Srivijaya in Thailand who made a prototype of a toy boat made of composite material impregnated with bio resin. [64]

Figure 5.2: Toy boat prototype

Moreover, it can be mentioned their use in green energy production. Composite structures such as wind turbines at the end of their life cycle as they are not recyclable are buried in neighboring garments.

This issue has given rise to many research projects. The University of Alberta in Canada has, for example, made a wind turbine out of bio composite materials. [65]

Figure 5.3: Wind turbine wing protype

Among other fields of application, we can also point out the medical field in which the use of bio composite materials finds use in so many ways.

Bio composite materials due to their low toxicity, biodegradability, and biocompatibility have great potential for applications with living tissue.

Indeed, they are used for bone regeneration, in orthopedic and dental implants, wound healing and tissue engineering.

Therefore, they are becoming of fundamental importance in the field of biomedical engineering. [66] [67]

Figure 5.4: Composites prosthetic limbs

Stricter mileage and emissions regulations are driving the trend towards lighter vehicles that consume less fuel. These regulations will continue to become more demanding and increasingly stringent in the coming decades.

The issue of lightness and fuel consumption has been and will be of central importance also in the racing sector. Consequently, the effort to develop polymers used in composite materials will continue because their lightness in turn improves the fuel efficiency of the vehicle.

Compared to traditional reinforcements such as glass fibers, natural fibers offer several environmental advantages. They are renewable, biodegradable and require less energy to be produced.

The use of natural fibers such as those obtained from hemp, wood and flax has already been found widespread use in automotive applications, for non-structural parts such as interior panels. [60]

A polypropylene composite that contains 20% wheat straw and is about 10% lighter than talc-reinforced plastic or slightly more with glass has been developed by A. Schulman.

Ford Motors makes fuel tanks in its 2010 Flex crossover vehicle from a new AgriPlas composite. Ford is considering the composite for other parts of the car, such as center console bins and trays; door trim panel components; and armrest covers.

Royal DSM NV introduced two high-performance bio-based materials for the automotive industry: Palapreg ECO P55-01, a bio-based resin for automotive body parts, including exterior panels, and EcoPaXX, a high-performance bio-based engineering plastic.

DuPont Engineering Polymers introduced a family of high-performance thermoplastic resins and elastomer products made from renewable resources: Sorona polymer and Hytrel. The key ingredient in Sorona is Bio-PDO TM, which is derived from corn sugar using a proprietary, patented fermentation process.[59]

These are just a few examples of the automotive companies that are investing in these renewable materials.

Bio resins are of great interest for the possibility of being recycled. Again, composite materials impregnated with bio resins but reinforced with standard fibers such as carbon, as it was also possible to observe from the following research work, do not have a great decrease in their mechanical properties compared to those impregnated with standard resins.

This type of bio-composite material can be an excellent compromise between mechanical performance and sustainability.

Components made from composite materials with resins of natural origin but reinforced with standard fibers such as carbon can also be used for structural elements such as racing car monocoques or structural beams. [60]

Figure 5.5: Racing car monocoque

Another excellent ally in reducing energy consumption and renewability can be short fiber composites materials.

Short fibers, obtained from weaving waste, reduce the costs of waste and fiber production and are still an excellent alternative to recycled fibers whose recycling process still requires a large amount of energy.

These materials, if also impregnated with bio-based resins that do not have a reducing effect on their mechanical properties, are excellent materials both from an application and sustainability point of view.

Short fiber materials are widely used for the production of lightweight non-structural components for which high mechanical performance is not required such as internal panels, tanks, bands or racing spoilers.

Figure 5.6: Dallara F2 2024 spoiler

To conclude, given the excellent mechanical properties of the green materials studied, and the countless application possibilities that derive from them in the automotive and non-automotive sectors, it is of pivotal importance to increase research projects that aim in this direction.

The interest in achieving ever better performance, with an increasingly urgent attention to respect for the environment and a conscious use of resources, will not die out any time soon and bio composite materials for their versatility and their mechanical performance will be increasingly fundamental over the coming years.

Conclusion

Growing interest in the environment and sustainability issues are pushing researchers to replace conventional synthetic fiber composites with bio-derived composites. Significant progress has been made in this direction in the last decade: industries and research institutions are increasingly developing eco-friendly, reusable and recyclable materials.

Bio composites developed from natural fibers and bio-resin have attracted much attention, as they can provide properties very close to those of standard composites at a reasonable cost. Due to their light weight, versatility and excellent mechanical properties, standard composite materials have become increasingly popular. However, due to their structure and synthetic origin, they are very difficult to decompose while maintaining the properties of the fibers and are not biodegradable. The mixture of fibers and resin is difficult to separate, so many of these products end up in landfill, buried or are reused in low-quality applications.

Bio composite materials, on the other hand, with their resin and reinforcement derived from natural products, are potentially more easily recycled or disposed of once their life cycle is over, with a limited impact on the environment.

The materials supplied studied at *Dallara Automobili* fit perfectly into the current needs of the composite market.

Even in the automotive sector, achieving top-level performance is very important and achieving this is closely linked to the type of materials used to build vehicles.

Composite materials, therefore, with their high performances have already been used for some time, but in this last period, thanks to the ever-increasing interest in sustainability and the push exerted by the regulations of racing championships, even bio composite materials are occupying a pivotal role.

As it was possible to observe from the mechanical characteristics of the materials studied, the use of bio resins does not have a significant impact on the processability and mechanical characteristics of the materials. It is, therefore, possible to have materials with excellent mechanical performances that nevertheless comply with sustainability requirements.

Another type of materials such as short-fiber composites allow the creation of interesting components from an applicative point of view, reducing waste in the carbon fiber weaving phase and therefore reducing the energy demand in the material production phase.

Bio resins reinforced by short fibers allow the creation of materials in which both the production of the matrix and that of the reinforcement comply with sustainability requirements.

With the use of resins of natural origin, it is also possible to reduce the use of bisphenol, one of the main elements of standard resins, whose harmful effects on health are becoming increasingly known to the scientific community and whose use will gradually be reduced.

There are still many steps to take towards the production of biomaterials. In fact, it is necessary to look for new production methods for both fibers and bio resins that make it easier to obtain these materials and from which components with more repeatable and controllable mechanical properties result.

In addition to the search for new production methods, it is also of great importance to standardize and design large-scale processes that allow the simple and economical production of large quantities of green materials, which at the moment are limited to only a few examples and is very expensive.

Only by making bio composite materials competitive also from an economic point of view will it be possible to allow a more pervasive diffusion.

In step with mass production processes, research will have to identify the most convenient ways of recycling these materials to guarantee their sustainability as much as possible.

To conclude, the road to a diffusion of bio composite materials is still very long and requires large investments in research both from an economic point of view and in terms of the use of resources. However, given the importance and the ever-increasing urgency of a green revolution throughout the world of manufacturing and the economic and regulatory efforts introduced by the States, especially in the European Union, the direction taken is the right one.

Bibliography

[1] URL

https://www.infobuildenergia.it/approfondimenti/sostenibili-e-naturali-i-materiali-biocompositi/

[2] URL

https://www.precedenceresearch.com/biocomposites-market

[3] URL

https://www.tecnologiaduepuntozero.it/2020/04/21/fibre-tessili-vegetali-videolezione/

[4]
R. Dinu, U. Lafont, O. Damiano, A. Mija. *Sustainable and recyclable thermosets with performances for high technology sectors. An environmental friendly alternative to toxic derivatives*. as a research art. from Renewable Biosourced Carbon Materials Derived From Biomass and Their Biocomposites Fabrication for Innovative Applications 2023.

[5] URL
https://www.esa.int/Enabling_Support/Preparing_for_the_Future/Discovery_and_Preparation/Boosting_sustainability_with_biobased_resins_composites_for_space_applications#:~:text=To%20tackle%20this%20issue%2C%20ESA,materials%20derived%20from%20sustainable%20sources

[6]

O. Akampumuza, P.M. Wambua, A. Ahmed, W. Li, Xiao-Hong Qin. *Review of applications of biocomposites in the automotive industry*, 2015.

[7]

L.T. Drzal, A.K. Mohanty, M.M. Misra. Bio-composite materials as alternatives to petroleum-based composites for automotive applications. Composite Materials and Structures Center Michigan State University, 2001.

[8]

M.Mohammed, A.J.M. Jawad, A.M. Mohammed, J.K. Oleiwi, T. Adam, A.F. Osman, O.S. Dahham, B.O. Betar, S.C.B. Gopinath, M. Jaafar, *Challenges and advancement in water absorption of natural fiber-reinforced polymer composites*. as an art. Polymer testing. 2023.

[9]

Ezgi Günay. *Natural and Artificial Fiber-Reinforced Composites as Renewable Sources*. Gazi University, Turkey, 2018.

[10]

I. Tivendale1, A. Raheem, T. Haider, S. Mukarram, F. Ahmad, L. Simon, T. Torrezan, A. Kiziltas. *Evaluation of cellulose and glass fiber in recycled-polyamide thermoplastic composites.* University of Waterloo, Suzano Papel e Cellulose, Ford Motors, 2017.

[11] URL

https://www.meccanicanews.com/2021/10/12/reinventare-materiali-con-soluzioni-bio-based/

[12] URL

https://www.bio-sourced.com/flax-materials-in-sports-and-recreation-a-perfect-fit/

[13]

C. I. Idumah, A. Hassan. *Emerging trends in flame retardancy of biofibers, biopolymers, biocomposites, and bionanocomposites* from the journal Reviews in chemical engineering, 2016.

[14] URL

https://lucaalessandrini.com/fibreacoustics

[15] URL

https://www.mordorintelligence.com/fr/industry-reports/composite-material-market

[16] URL

https://cordis.europa.eu/article/id/158628-sugara-and-jute-aeroplane-panels/it

[17] URL

https://cordis.europa.eu/project/id/515769/reporting

[18] URL

https://www.consilium.europa.eu/it/policies/green-deal/#:~:text=Il%20Green%20Deal%20europeo%20%C3%A8%20un%20pacchetto%20di%20iniziative%20strategiche,un'economia%20moderna%20e%20competitiva.

[19]

D. S. Bajwa, S. Bhattacharjee. *Current Progress, Trends and Challenges in the Application of Biofiber Composites by Automotive Industry*, 2016.

[20] URL
https://www.gianeco.com/cn/faq-detail/2/3/chi-ha-inventato-la-plastica-biodegradabile

[21]
URL https://en.wikipedia.org/wiki/Composite_material

[22]
M. Pervaiz, S. Panthapulakkal, M. Sain, J. Tjong. *Emerging Trends in Automotive Lightweighting through Novel Composite Materials*, 2016.

[23]
A. K. Bledzki, A. Jaszkiewicz, M. Urbaniak, D. Walczak. *Biocomposites in the Past and in the Future*, 2012.

[24] URL
https://www.assocompositi.it/wp-content/uploads/2020/11/CETMA.pdf

[25] URL
https://www.toraycma.com/wp-content/uploads/Carbon-Fiber-Selector-Guide.pdf

[26] URL
https://us.mitsubishi-chemical.com/company/carbon-fiber-composites/

[27] URL
https://mccfc.com/pitch-fiber/

[28] URL
https://leadrp.net/it/blog/types-of-carbon-fiber-materials-and-common-applications/

[29] URL

https://www.circularise.com/blogs/composite-waste-understanding-regulations-and-finding-circular-solutions-for-a-growing-problem

[30] URL

https://www.plastmagazine.it/termoplastiche-termoindurenti-compositi/

[31] URL

https://miobook.raffaellodigitale.it/progetti/34/risorse/TECNOLOGIA/ALTALEGGIBILITA/3_1_27.pdf

[32]

J. P. S. Ahmed, K. Satyasree, R. R. Kumar, O. Meenakshisundaram, S. Shanmugavel. *A Comprehensive Review on Recent Developments of Natural Fiber Composites Synthesis, Processing, Properties, And Characterization*, 2023

[33]

M. Zwawi. *A review on Natural Fiber Bio-Composites, Surface Modifications and Applications*. Department of Mechanical Engineering, Faculty of Engineering, King Abdulaziz University, Rabigh, Saudi Arabia, 2019

[34]

M. A. I. Malik, M.A. Kalam, M.A. Mujtaba, F. Almomani. *A review of recent advances in the synthesis of environmentally friendly, sustainable, and nontoxic bio-lubricants: Recommendations for the future implementations*, 2023.

[35]

T. Gurunathan, S. Mohanty, S. K. Nayak. *A review of the recent developments in biocomposites based on natural fibres and their application perspectives*, 2015.

[36]

Nour Mattar. *Matériaux composites biosourcés pour la construction durable*. ICMPE - Institut de Chimie et des Matériaux Paris-Est, 2022.

[37] URL

https://www.tainstruments.com/pdf/brochure/dma.pdf

[38] URL

https://sharedlab.bme.wisc.edu/labs/1002/equipment/mts/mts-insight.pdf

[39] URL

https://anff-qld.org.au/wp-content/uploads/2016/07/Thermal-analysis-characterisation-suite-METTLER-TOLEDO-DSC-1-brochure.pdf

[40] URL

https://it.wikipedia.org/wiki/Prova_di_trazione

[41] URL

https://amse.it/prova-compressione/#:~:text=La%20prova%20compressione%20sui%20materiali,forza%20che%20tende%20a%20comprimerlo

[42] URL

https://www.zwickroell.com/it/settori-industriali/compositi/resistenza-al-taglio-interlaminare-ilss/

[43] URL

https://www.touchstonetesting.com/services/material-testing/dynamic-mechanical-testing/drop-tower-testing/

[44] URL

https://it.wikipedia.org/wiki/Analisi_meccanica_dinamica

[45] URL

https://it.wikipedia.org/wiki/Calorimetria_differenziale_a_scansione

[46] URL

https://online.scuola.zanichelli.it/barbonescienzeintegrate/files/2010/04/V02_06.pdf

[47] URL

https://www.centropiaggio.unipi.it/sites/default/files/course/material/2019-05-21_-_materiali_compositi.pdf

[48] URL

https://www.infobuild.it/approfondimenti/materiali-compositi/

[49] URL

https://www.schmalz.com/it-it/soluzioni/settori-e-applicazioni/fibre-composite/processo-del-preimpregnato/

[50] URL

https://www.fapsteam.it/index.php/it/processo-produttivo/10-schede/11-vacuum-autoclave

[51] URL

https://it.wikipedia.org/wiki/Pre-preg

[52] URL

https://it.wikipedia.org/wiki/Nesting

[53] URL

https://esab.com/it/eur_it/esab-university/blogs/how-does-waterjet-cutting-work/#:~:text=L'effetto%20%C3%A8%20simile%20a,vengono%20spinti%20attraverso%20il%20materiale.

[54] URL

https://headland.au/machining-composites-with-abrasive-waterjet/

[55]

ASTM D3039/D3039M-17 Standard Test Method for Tensile Properties of Polymer Matrix Composite Materials.

[56]

Adams D.O. & Adams, D.F. DOT/FAA/AR-02/106 *Tabbing Guide for Composite Test Specimens*, October 2002.

[57]

BS EN ISO 527-5:2019 Plastics – *Determination of Tensile Properties, Part 5: Test conditions for unidirectional fibre-reinforced plastic composites*.

[58] URL

https://www.linkedin.com/pulse/end-tabbing-composite-test-specimens-theory-geraint-havard/

[59] URL

https://www.plastemart.com/plastic-technical-articles/bio-based-polymers-and-composites-for-automotive-application/1463

[60]

R.H. Martin, S. Giannis, S. Mirza and K. Hansen. *BioComposites in Challenging Automotive Applications Materials*. Engineering Research Laboratory Ltd (MERL) Wilbury Way, Hitchin, Hertfordshire, SG4 0TW, United Kingdom, 2009.

[61] URL
https://www.esa.int/Enabling_Support/Preparing_for_the_Future/Discovery_and_Preparation/Boosting_sustainability_with_biobased_resins_composites_for_space_applications

[62] URL

https://www.airbus.com/en/newsroom/stories/2024-06-developing-bio-based-composites-that-are-fit-to-fly

[63] URL

https://www.aerospacemanufacturinganddesign.com/news/bio-composites-could-transform-aircraft-design/#:~:text=Bio%2Dresins%20are%20made%20of,FST)%2C%20and%20heat%20release

[64]

C. Homkhiew, S. Khamtree, C. Srivabut, T. Petdee *Biocomposite materials from natural rubber/polylactic acid blends reinforced rubberwood sawdust for producing children's toys*, 2024.

[65]

H. Pougnet, E. Lepp, A. Samir Ead, Dr. Jason Carey. *The Application of Bio-based Composites in Wind Turbine Blades*, University of Alberta, Canada, 2021

[66]

Md. Zobair Al Mahmud. *Exploring the versatile applications of biocomposites in the medical field*, 2023.

[67] URL

https://opcenters.com/sustainable-prosthetics-a-green-revolution-in-every-step/

List of figures

List of tables

Acknowledgments

At the end of this paper, I feel it is right to dedicate space to thank all the people who, with their support, helped me and were close to me in my university career and in writing my thesis.

All my gratitude goes to Professor C. Pernechele who not only followed me promptly throughout the internship and writing of the thesis but who with great patience and kindness taught me much of what I know about composite materials. I also want to thank Thomas Martinoni for helping me and explaining many things throughout the duration of my internship.

My thanks then go to Professor A. Toso who, with his availability and his precious advice, guided me during my university career.

I would also like to thank my family, my father, my sister, my grandparents, my uncles and aunts, but in particular I would like to dedicate a special thought to my mother who has always believed in me and has been by my side both in moments of joy and in moments of despair without ever making me feel alone or misunderstood.

Finally, I would like to thank all my friends who, with their closeness and their affection, have been close to me in this experience.